

Gauge-invariant and infrared-improved variational analysis of the Yang-Mills vacuum wave functional

Hilmar Forkel

Institut für Physik, Humboldt-Universität zu Berlin, D-12489 Berlin, Germany

We study a gauge-invariant variational approximation scheme for the Yang-Mills vacuum wave functional. Its foundation is a gauge-projected Gaussian trial-functional family designed to substantially extend previously used trial bases in the infrared. This improvement is achieved by implementing an expansion of the low-momentum covariance which is taken to be analytic at zero momentum. When completed by the perturbative Yang-Mills covariance at high momenta, this leads to a significantly enlarged trial functional space which incorporates both dynamical mass generation and asymptotic freedom. After casting the associated dynamics into a correspondingly generalized effective action for the soft vacuum fields, the leading infrared corrections manifest themselves as four-gradient interactions and turn out to lower the minimum of the vacuum energy density by more than ten percent, indicating a considerable overall improvement of the vacuum description. The dimensional transmutation mechanism and the dynamically generated mass scale remain almost quantitatively robust, however, which ensures that our prediction for the gluon condensate is consistent with standard values. Further results include a finite group velocity of the soft gluonic modes due to the higher-gradient corrections and indications for a negative differential color resistance of the Yang-Mills vacuum.

I. INTRODUCTION

Variational methods were among the first theoretical tools developed to study nonperturbative ground-state properties of quantum systems [1]. Soon after the inception of QCD, variational techniques were similarly brought to bear on the physics of the gluon vacuum [2–5]. Among their most attractive features are the abilities to treat nonperturbative problems analytically, at real time and at strong coupling (in contrast e.g. to semiclassical approximations). As a consequence, variational methods remain applicable even in non-static and curved spacetimes [6, 7] as well as in nonequilibrium [59] situations [9]. Variational problems are naturally formulated in the Schrödinger picture, furthermore, which often invokes quantum-mechanical intuition to shed new light on field-theoretic states, as encoded e.g. in the node number of their wave functionals [10, 11] or in the action of transformation groups [6]. On the other hand, field-theoretic applications have to implement the UV field modes and their dynamics exactly [10], they must deal with the standard renormalization issues in the Schrödinger representation [12, 13], and they require a manageable way of calculating matrix elements by functionally integrating over physical intermediate states. For gauge theories, maintaining gauge invariance becomes an additional mandatory requirement which, in the Hamiltonian formulation, amounts to preserving Gauss’ law. Traditionally, the latter is implemented in combination with (almost) complete gauge fixing to Coulomb gauge [2, 14, 15], although generally without full account of the gauge-group topology and the resulting Gribov copies. In addition, this gauge-fixed approach has to deal with a nonlocal Hamiltonian [16] and must take special precautions to avoid gauge-symmetry breaking approximations [17].

Alternatively, the variational problem can be reformulated in a (residual) gauge-invariant manner which, at least under certain approximations, remains analytically tractable [17]. The mechanism of dimensional transmutation becomes manifestly gauge-invariant and particularly transparent from this perspective [18], and the mass gap (the arguably most fundamental nonperturbative Yang-Mills property [19]) emerges dynamically already from a minimal parametrization of the Gaussian “core” wave functional [17]. The projection onto the gauge-singlet component of this core functional may furthermore generate an area law for spacelike Wilson loops and thereby account for linear quark confinement as well [17, 18, 20]. Another attractive feature of this approach is that it reexpresses the infrared dynamics in terms of gauge-invariant matrix fields (which subsume whole families of gauge-field orbits [21]) and that it preserves traceable links of heuristic value between these soft collective fields and the underlying Yang-Mills fields. Moreover, the gauge-invariant reformulation preserves the global, i.e. topological properties of the gauge fields. The contributions from all vacuum homotopy classes as well as instanton-mediated transitions between them, for example, are explicitly and transparently taken into account without recourse to the semiclassical approximation [6, 17, 21, 22]. Besides such sets of (multi-) instanton and meron orbits, the dynamics contained in the vacuum wave functional sustains a rich variety of additional gauge-invariant infrared modes, including Faddeev-Niemi knots and other topological as well as nontopological solitons [21, 23].

Our main objective in the present article will be to improve the vacuum description provided by the gauge-invariant variational approach. To this end, we develop a trial functional family which accommodates a rather general momentum distribution for the infrared vacuum modes while remaining analytically tractable. Due to the explicit

representation of the ground state, structural aspects of the Yang-Mills dynamics and their impact on the vacuum can then be understood in terms of the resulting gauge-field population. Moreover, our generalized trial basis aids in the full exploration of the gauge-projected Gaussian functional space, e.g. by evaluating and analyzing amplitudes of interest, and thereby in the assessment of both limitations and further improvement potential. In the longer run, this type of analysis should reveal the extent to which Yang-Mills vacuum physics can be captured by infrared-generalized Gaussian core functionals, by their subsequent gauge projection and by the mean-field treatment of the resulting soft-mode action. One may even speculate that these insights will eventually help to find a systematic and manageable approximation to the Yang-Mills vacuum wave functional beyond the Gaussian ansatz.

After having set up our extended trial functional space, the next major task will be to establish the framework for calculating the associated vacuum amplitudes. This will enable us, in particular, to evaluate the vacuum energy density and its reduction in the generalized trial space. The latter provides a quantitative measure for the achieved improvement of the vacuum description. The analysis of the infrared mode distribution encoded in the energetically favored wave functional will furthermore shed new light on the resulting vacuum physics. It will, in particular, reveal the physical significance of the variational parameters and clarify the impact of their optimized values on the soft-mode dynamics. We will also explore the influence of the enlarged trial space on the phase structure and the order-disorder phase transition of the underlying infrared dynamics (which has, like the Yang-Mills dynamics, its origin in the imposition of gauge invariance). In fact, the robustness of this phase transition will turn out to ensure a reliable variational determination of the ground-state energy minimum. Our analysis of the resulting vacuum properties will be further complemented by evaluating the lowest-dimensional gluon condensate. Its value will provide, in particular, a quantitative test of the dynamically generated mass scale and its relation to the underlying trace anomaly. Beyond the evaluation and analysis of specific amplitudes, moreover, we expect the extended variational framework to furnish a transparent theoretical laboratory which is well-suited to build up nonperturbative real-time intuition for the Yang-Mills vacuum [60].

The paper is organized as follows: in Sec. II we introduce and discuss our infrared-generalized, gauge-invariant trial functional family for the Yang-Mills ground state. In Sec. III we rewrite the associated vacuum overlap amplitude in terms of an effective bare action, summarize our strategy for calculating the variational bound on the Yang-Mills vacuum energy and review the perturbative integration of the hard modes which results in a renormalized soft-mode dynamics. In Sec. IV we develop the theoretical framework for calculating relevant amplitudes by functional integration over the soft modes, and in Sec. V we derive explicit expressions for the 2- and 4-point functions. Their quantitative evaluation is prepared in Sec. VI where we set up the saddle-point expansion for the integral over the soft modes. We further derive the corresponding gap equation and find its solutions which provide quantitative information on the phase structure of the soft-mode dynamics. In Sec. VII we calculate the different contributions to the vacuum energy density (both in the ordered and disordered phase) which we minimize in Sec. VIII. In the same section, we further compute the gluon condensate, discuss the physical implications of our results and suggest a few directions for future work. In Sec. IX, finally, we collect our principal results and our main conclusions.

II. VACUUM WAVE FUNCTIONAL

The success of variational estimates depends in large part on the choice of the underlying trial function(al) basis. Ideally, it should be both comprehensive enough to accommodate the relevant physics and concise enough to remain analytically tractable and reasonably transparent. In the following sections we establish the basis of our subsequent analysis by introducing a gauge-invariant trial functional family for the Yang-Mills ground state which is designed to compromise between these conflicting goals. Although our trial functional space expands the minimal one used in Ref. [17] substantially, the ensuing variational analysis will require only moderately larger computational efforts.

Our basis implements Feynman's three requirements for trial wave functionals of gauge theories [10], i.e. the at least approximate calculability of matrix elements, the correct UV asymptotics and gauge invariance. The major methodological advance of Ref. [17] was to show that a trial space of manifestly gauge-invariant wave functionals, namely gauge-projected Gaussians, can still permit an (approximately) analytically manageable variational analysis. In the following sections we first discuss the essential features of the minimal ansatz of Ref. [17], and then generalize it by implementing an in principle general momentum distribution for the infrared vacuum modes.

A. Gauge invariance by projection

Variational analyses are generally carried out in the Hamiltonian formulation of the gauge dynamics and in the "coordinate" Schrödinger picture. In Yang-Mills theories this restricts gauge transformations to a fixed reference time, thereby effectively decoupling them from the dynamical time evolution. In the temporal (or Weyl) gauge

$A_0^a = 0$ which we adopt in the following, the residual gauge transformations are static, furthermore, and problems with negative-norm states (as e.g. in covariant gauges) are avoided from the outset [61]. The gauge invariance of the vacuum wave functional is required by Gauss' law which acts as a subsidiary condition in Fock space. This is particularly crucial for variational treatments of gauge theories because the Yang-Mills Hamiltonian becomes unique only when acting on physical states. Hence, as pointed out in Ref. [17], trying to minimize the vacuum expectation value of the Hamiltonian in the whole space of normalizable functionals could favor contributions from unphysical parts of the Hilbert space which may be almost arbitrarily enhanced by adding products of suitable operators and gauge-group generators to a given Hamiltonian.

Taking ψ_0 as an approximate and hence typically gauge-dependent ‘‘core’’ functional (to be specified in Sec. II B) (which depends on the static gauge fields $\vec{A}(\vec{x})$, i.e. on one half of the canonical variables, as in quantum mechanics), we impose gauge invariance by projecting on its gauge-singlet component, i.e. by averaging over the gauge group [25]. This results in trial vacuum wave functionals of the form

$$\Psi_0[\vec{A}] = \sum_{Q \in \mathbb{Z}} e^{iQ\theta} \int D\mu[U^{(Q)}] \psi_0[\vec{A}^{U^{(Q)}}] =: \int DU \psi_0[\vec{A}^U] \quad (1)$$

where $d\mu$ is the invariant Haar measure of the $SU(N_c)$ gauge group [62], Q is the homotopy degree or winding number of the group element $U^{(Q)}$, and θ is the vacuum angle. The expression (1) acquires the obligatory θ phase under large (i.e. topologically nontrivial) gauge transformations and renders Gauss' law manifest.

Instead of dealing with the gauge-invariant trial functionals (1) from the outset, one may alternatively evaluate the energy density of gauge-*dependent* Gaussian wave functionals and then correct for its lack of gauge invariance before minimizing it. This approach was pursued in Ref. [26] where the spurious kinetic energy due to gauge rotations was subtracted by the Thouless-Valatin projection method (as originally developed for the treatment of deformed nuclei). The main advantages of the technically somewhat more involved gauge-invariant approach are that starting from wave functionals (1) maintains manifest gauge invariance universally in all subsequent calculations and approximations of *all* matrix elements.

B. Gaussian core wave functional

In order to determine the gauge-invariant trial functionals (1) and the related amplitudes completely, it remains to adopt a core functional family ψ_0 . As in any variational calculation, this choice generally remains an uncontrolled approximation without a systematic and analytically tractable improvement strategy. In order to motivate our choice for ψ_0 and to discuss the underlying physics, we start by recalling that the VWF cannot have nodes, i.e. that $\psi_0[A] \geq 0$ for all A [11]. Hence one can write without loss of generality

$$\psi_0[\vec{A}] = \frac{1}{\mathcal{N}} e^{-\Phi[\vec{A}]} \quad (2)$$

where \mathcal{N} is a generally infinite normalization constant and Φ is a real and typically nonlocal functional of the gauge field. (This provides an example for how quantum-mechanical insights remain applicable to field theory in the Schrödinger representation as long as its infinitely many degrees of freedom do not generate qualitatively new effects.) In order to find a viable approximation for Φ , one may think of it as a functional power series in A and determine physically reasonable and analytically tractable truncations. The first two terms of this series are generally discarded: constant terms could be absorbed into the normalization constant \mathcal{N} , while the term linear in the gauge field (by itself) would correspond to a coherent vacuum state which is known to be unstable [27].

The next term in the power series for Φ is quadratic in A and plays several crucial roles. The first one is related to the fact that Φ contains an ambiguity which is due to the invariance of the Haar measure in Eq. (1) under right (or left) multiplication by any given group element. Hence infinitely many choices for $\Phi[A]$ lead up to an unphysical redefinition of the normalization constant to the same $\Psi_0[A]$ [20]. This ambiguity is removed, however, by prescribing the quadratic term in Φ . Furthermore, this term corresponds to a product of exact wave functionals of the Abelian $U(1)$ gauge theory [63] and thus becomes exact in the ultraviolet due to asymptotic freedom. Finally, and from the practical perspective most importantly, the Gaussian functional ψ_0 resulting from a quadratic term can be integrated over A analytically, while any higher-order contribution could at best be treated perturbatively [29]. Hence one generally truncates the series for Φ after the quadratic term, which leads to the ‘‘squeezed’’ approximation for the core functional, i.e. to the Gaussian functional

$$\psi_0^{(G)}[\vec{A}] = \frac{1}{\mathcal{N}_G} \exp\left[-\frac{1}{2} \int d^3x \int d^3y A_i^a(\vec{x}) G_{ij}^{-1ab}(\vec{x} - \vec{y}) A_j^b(\vec{y})\right] \quad (3)$$

with the normalization factor $\mathcal{N}_G^{-1} = [\det(G/2)]^{-1/4}$ and a real kernel or “covariance” G^{-1} which satisfies a normalizability condition (cf. Eq. (8)). Eq. (3) appears to be the “richest” core functional family whose matrix elements can be dealt with by the currently available analytical methods of field theory. (Adding c number sources to the variable A would still allow for an analytical treatment and generate finite vacuum expectation values for A in gauge-fixed approaches, while such local “condensates” are not sustained in our residually gauge-invariant vacuum and would be rendered mute by the gauge projection in Eq. (1).)

The core functional (3) represents an infinite product of Gaussians, one for each Fourier mode of the gauge field with momentum \vec{k} . Hence the elements of the Fourier-transformed covariance

$$\omega_{ij}^{ab}(\vec{k}) := G_{ij}^{-1,ab}(\vec{k}) = g_1^{ab}(k) \delta_{ij} + g_2^{ab}(k) \hat{k}_i \hat{k}_j \quad (4)$$

(where $\hat{k}_i := k_i/k$ with $k := \sqrt{k_i k_i}$) turn after diagonalization into mode frequencies or energies. The squeezed state therefore generalizes the ground state of the quantum-mechanical harmonic oscillator. In our context, it corresponds to a vacuum consisting of color-singlet gauge-field pairs and may therefore be regarded as the protostate for a glueball condensate [30]. (This should be contrasted to the “condensation” of single gluons in a coherent state.)

Since Gaussian functionals transform nontrivially under non-Abelian gauge groups, furthermore, the gauge averaging in Eq. (1) is an integral part of our approximation to the physical vacuum wave functional. Gauge-fixed variational analyses in Coulomb gauge (for references see e.g. [2, 4, 5, 14, 15]), on the other hand, are generally based on Gaussian functionals, too, and were found to generate a mass gap [2, 14] as well as, when multiplied by the inverse square root of the Faddeev-Popov determinant, an approximately linearly rising confinement potential [15].

C. General properties and UV asymptotics of the covariance

We are now going to specify the properties of the covariance (4) which characterizes the members of our core trial functional family (3) and which contains the variational parameters whose values will be adapted below to optimally approximate the Yang-Mills vacuum wave functional. Translational invariance implies $G_{ij}^{-1,ab}(\vec{x}, \vec{y}) = G_{ij}^{-1,ab}(\vec{x} - \vec{y})$ and was already anticipated in Eq. (3). Without loss of generality at the perturbative level (and beyond, since the integration over the gauge group in Eq. (1) averages out longitudinal contributions), we will further specialize to a purely transverse covariance with $g_2 \equiv 0$ [17], i.e.

$$G_{ij}^{-1,ab}(k) = \delta_{ij} G^{-1,ab}(k), \quad (5)$$

which allows for a more direct comparison with the results of Ref. [17] and should be sufficient for our explorative purposes. (The impact of longitudinal contributions $\propto g_2^{ab}$ was discussed in Ref. [18] (cf. also Ref. [31]), and a specific prescription for g_2^{ab} was shown to reproduce the 1-loop Yang-Mills β -function. Due to the ambiguity of the core functional mentioned in Sec. II B, a longitudinal term in the covariance can always be removed from Φ without changing the physical part of the vacuum wave functional, although generally in exchange for terms containing higher powers of the gauge field [20].)

In order to motivate the color structure of our covariance, we note that only the homogeneous part of the gauge transformations keep the exponent Φ of the core functional bilinear in A . Gauge transformations which do not vary significantly over distances for which $G^{-1}(\vec{x} - \vec{y})$ has appreciable support therefore leave the Gaussian part of the exponent with a covariance of the form [17]

$$G^{-1,ab}(k) = \delta^{ab} G^{-1}(k). \quad (6)$$

approximately invariant. This will hold, in particular, for those gauge group elements which determine our soft-mode dynamics (see below). Since the same color structure is appropriate for the hard gauge-field modes, which we will treat perturbatively in the small bare coupling g_b , we adopt Eq. (6) for the remainder of this paper. As a consequence, the core functionals ψ_0 become invariant both under global $U(N_c)$ transformations and under the product of $N_c^2 - 1$ copies of the $U(1)$ gauge group.

Combining the spacial (5) and color (6) structures, our covariance assumes the form

$$G_{ij}^{-1,ab}(\vec{x}, \vec{y}) = \delta^{ab} \delta_{ij} G^{-1}(\vec{x} - \vec{y}) = \delta^{ab} \delta_{ij} \int \frac{d^3 k}{(2\pi)^3} e^{i\vec{k}(\vec{x} - \vec{y})} G^{-1}(k) \quad (7)$$

which is symmetric in each of the 3 “index” pairs. This form of the covariance is further restricted by implementing the requirement that wave functionals of physical states have to be normalizable. Since the norm of the functional

(3) involves an integral over the gauge field's Fourier modes $A(k)$, this implies that the integrand $\psi_0^*(k) \psi_0(k)$ has to damp large gauge fields $A(k)$ for all k . The corresponding localization in field space demands

$$G^{-1}(k) > 0 \quad (8)$$

and ensures vacuum stability and a positive energy spectrum of the associated quantum field theory. The condition (8) will be seen to limit the domain of the variational parameters to be introduced below.

As noted by Feynman, it is furthermore mandatory for trial functionals to reproduce the asymptotically free gauge dynamics in the ultraviolet, i.e. for $k \rightarrow \infty$, exactly [10]. This prevents spurious contributions to the infinitely many UV modes, which are irrelevant for the vacuum physics, from artificially dominating the soft-mode energy density by means of their couplings with the IR modes. In order to implement the correct UV behavior, we factorize the unprojected core functional (3) as

$$\psi_0^{(G)}[\vec{A}] = \psi_0^{(G_{<})}[\vec{A}_{<}] \psi_0^{(G_{>})}[\vec{A}_{>}] \quad (9)$$

by splitting the \vec{k} integration domain in the exponentials into soft/hard momentum regions with $k \gtrless \mu$ relative to a separation scale μ , i.e.

$$\psi_0^{(G_{\lessgtr})}[\vec{A}_{\lessgtr}] = \exp \left\{ -\frac{1}{2} \int \frac{d^3k}{(2\pi)^3} \theta(\pm\mu^2 \mp k^2) A_{\lessgtr,i}^a(k) G_{\lessgtr}^{-1}(k) A_{\lessgtr,i}^a(k) \right\}. \quad (10)$$

This allows to incorporate the asymptotic freedom of Yang-Mills theory (i.e. the Gaussian UV fixed point generated by the negative β function at large momenta) into $G_{>}^{-1}$ by requiring that G approaches the non-interacting, massless static vector field propagator $G_0(k) = 1/k$ for $k \rightarrow \infty$. As long as $\mu \gg \Lambda_{\text{YM}}$ (where Λ_{YM} is the Yang-Mills scale), a natural approximation is therefore [64]

$$G_{>}^{-1}(k) = k \quad (11)$$

which we adopt in the following [65]. More specifically, the value of μ must be chosen large enough for perturbative corrections from the hard modes (with momenta $k > \mu$), or equivalently the RG-improved running coupling $\alpha(\mu) = g^2(\mu)/(4\pi)$, to remain small. (RG-improved perturbative corrections to the leading $k \rightarrow \infty$ behavior will enter when integrating out the hard modes perturbatively, cf. Secs. (VII A) and App. (A 2).) Since μ will be treated as a variational parameter, this has to be checked *a posteriori*, i.e. for the value μ^* which minimizes the vacuum energy. For the infrared momenta $k < \mu$, on the other hand, the nonperturbative Yang-Mills physics induces a qualitatively different IR covariance $G_{<}^{-1}(k)$. In order to better approximate this behavior, we introduce a generalized parametrization for $G_{<}^{-1}$ in the following Sec. II D.

D. Generalized IR (soft-mode) covariance

Due to the logarithmically slow running of the Yang-Mills coupling in the ultraviolet, the high-momentum behavior of our trial functional family is rather accurately implemented by the hard-mode covariance (11). Hence only the IR covariance $G_{<}^{-1}(k)$, which encodes the more complex and less understood nonperturbative vacuum physics, remains to be determined variationally. Our next task is therefore to design a parametrization for $G_{<}^{-1}$ which is sufficiently “rich” to accommodate the relevant physics without impeding an analytically tractable variational analysis. The minimal choice

$$G_{<, \text{KK}}^{-1}(k) = \mu \quad (12)$$

adopted in the pioneering study [17] utilizes the separation scale μ simultaneously as a variational parameter and was shown to generate a mass gap. While it therefore provides an efficient starting point for describing the Yang-Mills vacuum, one may also suspect it to introduce too much bias because it contains just one variational parameter and therefore leaves only one characteristic vacuum scale to be determined by energy minimization. This involves the risk of essentially “building in” the mass gap without gaining much further insight into the underlying vacuum physics.

In the following, we will therefore introduce a more comprehensive parametrization of $G_{<}^{-1}$ which accommodates more of the $k < \mu$ mode dynamics while still allowing for a variational analysis which does not require the solution of a functional differential equation. It is based on the under reasonable analyticity assumptions general gradient expansion [21]

$$G_{<}^{-1}(\vec{x} - \vec{y}) = m_{\text{g}} \left[1 + c_1 \frac{\partial_x^2}{\mu^2} + c_2 \left(\frac{\partial_x^2}{\mu^2} \right)^2 + c_3 \left(\frac{\partial_x^2}{\mu^2} \right)^3 + \dots \right] \delta_{<}^3(\vec{x} - \vec{y}) \quad (13)$$

which can be efficiently truncated to yield a manageable trial function basis for the $k^2 \ll \mu^2$ soft-mode physics. The variational parameters are therefore the IR gluon mass $m_g > 0$ and a few of the low-momentum constants c_n which characterize dispersion properties of the IR modes (cf. Sec. VIII C). (The parameters c_n should be considered as renormalized at μ since they affect just the $k < \mu$ modes and do not receive UV contributions from integrating out the $k > \mu$ modes.) The derivatives of the expansion (13) act on the regularized delta function

$$\delta_{<}^3(\vec{x} - \vec{y}) := \int \frac{d^3k}{(2\pi)^3} \theta(\mu^2 - \vec{k}^2) e^{i\vec{k}(\vec{x} - \vec{y})} \quad (14)$$

which encodes the slow variation $\|\partial A_{<}\| / \|A_{<}\| \leq \mu$ of the soft modes and ensures that the higher-order terms of the above expansion are parametrically suppressed. It further restricts the support of $G_{<}^{-1}$, i.e.

$$G_{<}^{-1}(\vec{x}) \sim 0 \quad \text{for } |\vec{x}| > \frac{1}{\mu}. \quad (15)$$

Together with the hard-mode covariance (11), Eq. (13) provides a rather general parametrization of the core functional (3) which contains the minimal one-parameter ansatz (12) for $c_n = 0$ and $m_g = \mu$.

(Note, incidentally, that the perturbative covariance (11) has a branch point at $k^2 = 0$ and thus cannot be directly expanded as in Eq. (13). Note further that the ansatz (13) could easily be extended beyond the limited spacial tensor structure (5) by writing

$$G_{<,ij}^{-1}(\vec{x} - \vec{y}) = G_{<,ij}^{(L)-1}(\vec{x} - \vec{y}) + G_{<,ij}^{(T)-1}(\vec{x} - \vec{y}) \quad (16)$$

with $(X \equiv L, T)$

$$G_{<,ij}^{(X)-1}(\vec{x} - \vec{y}) = m_g^{(X)} \left[1 + c_1^{(X)} \frac{\partial_x^2}{\mu^2} + c_2^{(X)} \left(\frac{\partial_x^2}{\mu^2} \right)^2 + c_3^{(X)} \left(\frac{\partial_x^2}{\mu^2} \right)^3 \dots \right] \delta_{X,ij}^3(\vec{x} - \vec{y}) \quad (17)$$

where

$$\delta_{X,ij}^3(\vec{x}) = \int \frac{d^3k}{(2\pi)^3} \theta(\mu^2 - \vec{k}^2) \delta_{X,ij}(\hat{k}) e^{i\vec{k}\vec{x}} \quad (18)$$

and $\delta_{T,ij}(\hat{k}) \equiv \delta_{ij} - k_i k_j / \vec{k}^2$ and $\delta_{L,ij}(\hat{k}) \equiv k_i k_j / \vec{k}^2$, which decouples the longitudinal and transverse contributions and implies, in particular,

$$\partial_{x,i} G_{ij}^{(T)-1}(\vec{x} - \vec{y}) = 0. \quad (19)$$

For $m_g^{(T)} = m_g^{(L)}$ and $c_n^{(T)} = c_n^{(L)}$ the general ansatz (16) simplifies to Eq. (13). In the following analysis we adopt the latter, mainly to avoid compromising transparency by additional parameters and to allow for a more direct comparison with Ref. [17].)

In momentum space Eq. (13) becomes

$$G_{<}^{-1}(k) = m_g \left[1 - c_1 \frac{k^2}{\mu^2} + c_2 \left(\frac{k^2}{\mu^2} \right)^2 - c_3 \left(\frac{k^2}{\mu^2} \right)^3 + \dots \right] \theta(\mu^2 - k^2), \quad (20)$$

which renders the relation between the parameters c_n and the dispersion properties of the IR quasiglons (cf. Sec. VIII C) more explicit. It further implies that the effective IR gluon propagator

$$G_{<}(k) = \frac{1}{m_g} \left[1 + c_1 \frac{k^2}{\mu^2} + (c_1^2 - c_2) \frac{k^4}{\mu^4} + (c_1^3 - 2c_1 c_2 + c_3) \frac{k^6}{\mu^6} + \dots \right] \theta(\mu^2 - k^2), \quad (21)$$

resulting from $G_{<}^{-1}(k) G_{<}(k) = 1$, is analytic at $k^2 = 0$. (The finiteness of $G_{<}$ at zero momentum, $G_{<}(0) = m_g^{-1}$, is reminiscent of lattice results for the gluon propagator in Landau gauge [32].) The adjustable parameters m_g , μ and c_n are to be determined variationally (cf. Sec. VIII). Their physically sensible domain is restricted by several constraints, however. As a consequence of the normalizability condition (8), in particular, the low-momentum constants must satisfy the bounds

$$c_1 < 1, \quad c_2 > -1, \dots \quad (22)$$

(for $m_g > 0$). The value of the IR gluon mass $m_g > 0$ is further constrained by requiring continuity of $G^{-1}(k)$ at the matching point $k = \mu$ between soft and hard momenta. This fixes m_g as a function of the other variational parameters. When approximating the series (20) by the truncation $c_{n \geq 2} = 0$, for example, one has

$$m_g(\mu, c_1) = \frac{\mu}{1 - c_1}. \quad (23)$$

Note that the requirement of a non-negative IR gluon mass then restricts the c_1 domain to $c_1 < 1$, in agreement with the bound (22) from normalizability. The singularity of $m_g(\mu, c_1)$ for $c_1 \rightarrow 1$ reflects the onset of vacuum instability for $c_1 \geq 1$ and is inherited by $G_{<}^{-1}(k)$, cf. Eq. (20).

In addition to the minimal approximation (12), our expansion (13) encompasses another previously used ansatz for the IR covariance, namely the inverse of the non-interacting massive vector propagator,

$$G_0^{-1}(\mu; k) = \sqrt{k^2 + \mu^2} \stackrel{k \leq \mu}{=} \mu \left[1 + \frac{1}{2} \frac{k^2}{\mu^2} - \frac{1}{8} \left(\frac{k^2}{\mu^2} \right)^2 + \frac{1}{16} \left(\frac{k^2}{\mu^2} \right)^3 - \dots \right], \quad (24)$$

which obviously corresponds to the parameter choice $m_g = \mu$, $c_1^{(0)} = -1/2$, $c_2^{(0)} = -1/8$ etc.. Its truncation to $c_{n \geq 2} = 0$ was adopted in Ref. [21] as the basis for a gauge-invariant saddle-point expansion of the IR amplitudes and found to reproduce the effective soft-mode action (cf. Sec. III) at its saddle points up to a few percent accuracy. (Lattice simulations similarly found the Landau-gauge gluon propagator to behave like a massive vector propagator at intermediate momenta [33].)

In Fig. 1 we compare the expressions (12) and (24) for the IR covariance with ours for $c_1 = \pm 0.15$ (the positive value is the result of the variational analysis of Sec. VIII A) and $c_{n \geq 2} = 0$. A more detailed discussion of the physics encoded in our IR covariance will be postponed until the variationally optimized values of the low-momentum constants are determined (cf. Sec. VIII C). In summary, the Gaussian ansatz (3) for the core functional encodes the correct UV asymptotics, can be generalized and partly motivated in the IR, and is amenable to existing analytical methods of field theory. As such, it provides the best currently available, analytically manageable and gauge-invariant approximation to the Yang-Mills vacuum wave functional.

III. ENERGY AND SOFT-MODE DYNAMICS OF THE TRIAL FUNCTIONAL FAMILY

A. Computational strategy

Variational analyses à la Rayleigh-Ritz amount to minimizing the expectation value of the Hamiltonian in a trial-state space. In our case, this trial vacuum energy density is

$$\langle \mathcal{H}(A, E) \rangle = \frac{\int D\vec{A} \Psi_0^*[\vec{A}] \mathcal{H}\left(\vec{A}^a, \frac{i\delta}{\delta \vec{A}^a(\vec{x})}\right) \Psi_0[\vec{A}]}{\int D\vec{A} \Psi_0^*[\vec{A}] \Psi_0[\vec{A}]} \quad (25)$$

where \mathcal{H} is the Yang-Mills Hamiltonian (131) in temporal gauge and Ψ_0 the generalized vacuum wave functional family introduced in Sec. II. The calculation of this expectation value is most efficiently performed by means of a generating functional, as summarized in App. A. In the present section we just introduce some of our notation and sketch the formal strategy of calculating the energy density (25) (which straightforwardly generalizes to more general matrix elements, cf. App. A).

After inserting the gauge-projected vacuum wave functional (1) into Eq. (25) and interchanging the order of the integration over gauge fields and gauge groups, the gauge invariance of the \vec{A} integral allows to factor out one gauge group volume. Eq. (25) can be then be rewritten as

$$\langle \mathcal{H}(A, E) \rangle = \frac{\int DU \int D\vec{A} \psi_0[\vec{A}^U] \mathcal{H}\left(\vec{A}^a, \frac{i\delta}{\delta \vec{A}^a(\vec{x})}\right) \psi_0[\vec{A}]}{\int DU \int D\vec{A} \psi_0[\vec{A}^U] \psi_0[\vec{A}]} \quad (26)$$

(where DU is the functional $SU(N_c)$ measure as defined in Eq. (1)). After evaluating the functional derivatives of \mathcal{H} in the integrand, the Gaussian integrations over A can be performed exactly (cf. App. A for more details), resulting in

$$\langle \mathcal{H} \rangle = \frac{\int DU \langle \langle \mathcal{H} \rangle \rangle \exp\{-\Gamma_b[U]\}}{\int DU \exp\{-\Gamma_b[U]\}} \quad (27)$$

where we introduced the abbreviation

$$\langle\langle\langle\vec{A}\dots\vec{A}\dots\vec{E}\dots\vec{E}\rangle\rangle\rangle \exp\{-\Gamma_b[U]\} \equiv \int D\vec{A}\psi_0[\vec{A}^U] \vec{A}\dots\vec{A}\dots\frac{i\delta}{\delta\vec{A}}\dots\frac{i\delta}{\delta\vec{A}}\psi_0[\vec{A}] \quad (28)$$

which also defines the effective bare action $\Gamma_b[U]$ that describes dynamical correlations originating from the gauge projection of the functional ψ_0 . More specifically, from the normalization $\langle\langle\langle 1 \rangle\rangle\rangle = 1$ it follows that

$$\Gamma_b[U] = -\ln \int D\vec{A} \psi_0^*[\vec{A}^U] \psi_0[\vec{A}]. \quad (29)$$

This gauge-invariant, 3-dimensional Euclidean action would become U independent if ψ_0 were gauge invariant by itself. Hence $\Gamma_b[U]$ gathers all those gauge-field contributions to the generating functional whose approximate vacua ψ_0 at $t = \pm\infty$ differ by a relative gauge orientation U . The variable U thus represents the contributions from a specifically weighted ensemble of all gluon field orbits to the vacuum overlap and is gauge invariant by construction.

After splitting $U(\vec{x}) = U_<(\vec{x})U_>(\vec{x})$, $U_>(\vec{x}) = \exp(-ig\phi^a(\vec{x})\lambda^a/2)$ into hard- and soft-mode contributions (with $k^2 \gtrsim \mu^2$) and integrating over the hard UV modes ϕ perturbatively (with the result of Ref. [17], since we use the same UV covariance (11), cf. App. A), one arrives at

$$\langle\mathcal{H}\rangle = \frac{\int DU_< \int D\phi \langle\langle\mathcal{H}\rangle\rangle \exp\{-\Gamma_b[\phi, U_<]\}}{\int DU_< \int D\phi \exp\{-\Gamma_b[\phi, U_<]\}}. \quad (30)$$

After further defining

$$\langle\langle\mathcal{O}\rangle\rangle \exp\{-\Gamma_<[U_<]\} := \int D\phi \langle\langle\mathcal{O}\rangle\rangle \exp\{-\Gamma_b[\phi, U_<]\} \quad (31)$$

in terms of the effective soft-mode action

$$\Gamma_<[U_<] := -\ln \int D\phi \exp\{-\Gamma_b[\phi, U_<]\}, \quad (32)$$

we end up with a reformulation of the matrix element (25) on the basis of the dynamics for the $U_<$ fields, i.e. for the low-momentum components of the integration variable originating from the gauge projection of the vacuum functional (1):

$$\langle\mathcal{H}\rangle = \frac{\int DU_< \langle\langle\mathcal{H}\rangle\rangle \exp\{-\Gamma_<[U_<]\}}{\int DU_< \exp\{-\Gamma_<[U_<]\}}. \quad (33)$$

In other words, the calculation is reduced to an integral over $U_<$ in which the ‘‘reduced’’ (of fixed $U_<$) matrix element $\langle\langle\mathcal{H}\rangle\rangle$ is weighted by a Boltzmann factor containing just the soft-mode action $\Gamma_<[U_<]$. This action is governed by our IR expansion (20) of the covariance $G_<^{-1}$ which produces new interactions to be determined in Sec. III B. Since $\langle\langle\mathcal{H}\rangle\rangle$ consists of nonlocal functionals of the soft modes $U_<$, furthermore, the evaluation of Eq. (33) amounts to calculating specific (equal-time) soft-mode correlation functions. The necessary framework for this calculation will be set up in Sec. IV.

B. Soft-mode action

In this section we derive the low-momentum dynamics (32) which the wave functional (1) based on the Gaussian ansatz (3) with the generalized covariance (11), (13) induces. After specializing the expression (29) for the bare action to the core functional (3), the integral over the gauge fields can be carried out exactly (cf. App. A). The resulting action takes the form of a 3-dimensional, bilocal nonlinear sigma model [17],

$$\Gamma_b[U] = \frac{1}{2g_b^2} \int d^3x \int d^3y L_i^a(\vec{x}) \mathcal{D}^{ab}(\vec{x} - \vec{y}) L_i^b(\vec{y}). \quad (34)$$

(Above we have omitted a term of higher order in the small bare coupling g_b , cf. App. A.) The U fields enter Γ_b both in terms of the left-invariant Maurer-Cartan one-forms

$$L_i(\vec{x}) = U^\dagger(\vec{x}) \partial_i U(\vec{x}) =: L_i^a(\vec{x}) \frac{\lambda^a}{2i} \quad (35)$$

(with real components L_i^a , i.e. the Lie-algebra valued ‘‘currents’’ of the $SU(N_c)$ group) and through higher-order corrections to the bilocal operator

$$\mathcal{D}^{ab} = \left[(G + G^U)^{-1} \right]^{ab} \simeq \frac{1}{2} G^{-1} \delta^{ab} + \dots \quad (36)$$

where $G^U = G^{ab} (\vec{x} - \vec{y}) U^\dagger(\vec{x}) T^a U(\vec{x}) \otimes U(\vec{y}) T^b U^\dagger(\vec{y})$, $T^a = \lambda^a/2$ and $G^{-1ab} = G^{-1} \delta^{ab}$. The above reformulation of the vacuum overlap on the basis of a gauge-invariant Gaussian wave functional [17] can alternatively be obtained from the saddle-point evaluation of the functional integral in Eq. (29) [18].

According to the strategy outlined in Sec. III A, the calculation of infrared amplitudes including the energy density (25) involves an effective action (32) which only retains soft field modes explicitly. After factorizing $U = U_< U_>$, the hard modes $U_>$ or ϕ with $k^2 > \mu^2$ can be integrated out of Eq. (32) perturbatively (cf. App. A) as long as the renormalized coupling [34]

$$g(\mu) = g_b + \frac{g_b^3 N_c}{(2\pi)^2} \ln \frac{\Lambda_{UV}}{\mu} + O(g_b^5) \quad (37)$$

(for $G_>(k) = k^{-1}$) stays sufficiently small. Note that Eq. (37) exhibits asymptotic freedom and differs from the one-loop Yang-Mills coupling only by a small correction factor 1/11 which could be avoided by introducing an anisotropic component for $G_>^{-1}$ [18, 31]. The one-loop integration over the high-momentum modes was found to be reliable down to $\mu \simeq 1.3$ GeV [34]. In this range, the resulting renormalized soft-mode action

$$\Gamma_<[U_<] = \frac{1}{4g^2(\mu)} \int d^3x \int d^3y L_{<,i}^a(\vec{x}) G_<^{-1}(\vec{x} - \vec{y}) L_{<,i}^a(\vec{y}) \quad (38)$$

(cf. Eq. (A48)) is obtained from Eq. (34) by replacing the bare coupling g_b with the running coupling $g(\mu)$. One may further simplify the action (38) by exploiting the strongly local support of the IR covariance (13) (relative to the minimal soft-mode wavelength μ^{-1}) which is manifest in the regularized delta function (14) and its derivatives. It allows to approximately apply the unitarity constraint for the $U_<$ at neighboring points, i.e.

$$G^{-1}(\vec{x} - \vec{y}) U_<^\dagger(\vec{x}) U_<(\vec{y}) \simeq G^{-1}(\vec{x} - \vec{y}), \quad (39)$$

which could be systematically improved by Taylor expansion of the slowly varying soft-mode fields. To leading order, one may therefore replace Eq. (38) by the $2U$ contribution

$$\Gamma_<^{(2U)}[U_<] = \frac{1}{2g^2(\mu)} \int d^3x \int d^3y \text{tr} \left\{ \partial_i U_<(\vec{x}) G^{-1}(\vec{x} - \vec{y}) \partial_i U_<^\dagger(\vec{y}) \right\}. \quad (40)$$

Inserting our expansion (13) of the generalized IR covariance into the low-momentum dynamics (38), on the other hand, yields the full soft-mode action in the form

$$\Gamma_<[U_<] = \int d^3z \left[\mathcal{L}_{<,0}(\vec{z}) + \mathcal{L}_{<,c_1}(\vec{z}) + \mathcal{L}_{<,c_2}(\vec{z}) + \dots \right] \quad (41)$$

where the $\mathcal{L}_{<,n}(\vec{z})$ are (quasi-) local Lagrangians. (A saddle-point expansion of this dynamics, with the c_n determined by the massive vector covariance (24), was employed in Ref. [21] to identify gluonic IR degrees of freedom.) The leading-order, two-derivative Lagrangian

$$\mathcal{L}_{<,0}(\vec{z}) = -\frac{m_g}{2g^2} \text{tr} \left\{ U_<^\dagger(\vec{z}) \partial_i U_<(\vec{z}) U_<^\dagger(\vec{z}) \partial_i U_<(\vec{z}) \right\} = \frac{m_g}{2g^2} \text{tr} \left\{ \partial_i U_<^\dagger \partial_i U_< \right\} \quad (42)$$

(where we used $U_<^\dagger U_< = 1$ and neglected surface terms), in particular, is the standard nonlinear σ model. The $c_n \neq 0$ corrections (with the low-momentum constants c_n restricted by the requirements of a positive static action and a bounded vacuum energy, cf. Sec. II D) generate $2(n+1)$ -derivative interactions which are, relative to the leading term (42), suppressed by n powers of k^2/μ^2 :

$$\mathcal{L}_{<,c_n}(\vec{z}) = \frac{c_n m_g}{2g^2 \mu^{2n}} \text{tr} \left\{ U_<^\dagger(\vec{z}) \partial_i U_<(\vec{z}) \partial^{2n} \left[\partial_i U_<^\dagger(\vec{z}) U_<(\vec{z}) \right] \right\}. \quad (43)$$

The action (41), based on the Lagrangians (42), (43), exhibits the dynamics generated both by the generalized IR covariance (20) and by the gauge projection. It encodes, in particular, information on the vacuum topology which

manifests itself in instanton [35] (through the Atiyah-Manton holonomy [36]), meron [37], monopole [38], Fadeev-Niemi-Cho knot [39, 40] etc. contributions which can be made explicit [21]. The approximation (39) reduces the $c_n \neq 0$ interaction terms to their bilinear (i.e. $2U$) parts

$$\mathcal{L}_{<,c_n}^{(2U)}(\vec{z}) = \frac{c_n m_g}{2g^2 \mu^{2n}} \text{tr} \left\{ \partial_i U_{<}^\dagger(\vec{z}) \partial^{2n} [\partial_i U_{<}(\vec{z})] \right\} \quad (44)$$

which will turn out to generate the most important contributions to the vacuum energy density and other matrix elements.

We close this section by recalling that the soft-mode dynamics (41) follows uniquely from the adopted vacuum wave functional and preserves traceable links between the $U_{<}$ fields and the underlying gauge fields [21]. Nevertheless, it remains reasonably transparent and allows for efficient and controlled truncations resulting e.g. in analytical expressions for the vacuum energy to be derived below. These advantages originate in large part from reexpressing the dynamics in terms of the gauge-invariant fields U which gather collective contributions from whole gauge-field orbits, instead of dealing with the gauge fields individually [21].

IV. SOFT-MODE CORRELATION FUNCTIONS

As outlined in Sec. III A, the calculation of the vacuum energy density requires the evaluation of the reduced matrix element $\langle\langle \mathcal{H} \rangle\rangle$ which contains correlations functions of the soft-mode fields $U_{<}$. In the following section we set up the framework for evaluating these correlators.

A. Generating functional

Soft-mode correlation functions, as they appear in the integrand $\langle\langle \mathcal{H} \rangle\rangle$ of the vacuum expectation value (33) and in the gap equation to be derived below, are efficiently calculated by means of the generating functional

$$Z[j, j^\dagger] = \int DU_{<} \exp \left[-\Gamma_{<}[U_{<}] - \int d^3 z \text{tr} \left\{ j U_{<}^\dagger + j^\dagger U_{<} \right\} \right] \quad (45)$$

where j, j^\dagger are matrix sources. In order to prepare for the (approximate) integration over the soft modes, we first release the unitarity constraint on the $U_{<}$ fields by inserting a delta functional in the usual manner, i.e.

$$Z[j, j^\dagger] = \int DV \delta[V^\dagger V - 1] \exp \left[-\Gamma_{<}[V] - \int d^3 z \text{tr} \left\{ j V^\dagger + j^\dagger V \right\} \right] \quad (46)$$

$$= \int D\Sigma \int DV \exp \left[-\Gamma_{<}[V] - \Gamma_\Sigma[V, \Sigma] - \int d^3 z \text{tr} \left\{ j V^\dagger + j^\dagger V \right\} \right], \quad (47)$$

where the Hermitian matrix fields $\Sigma(\vec{x})$ act as Lagrange multipliers (with a normalization chosen for later convenience) and the additional action $\Gamma_\Sigma[V, \Sigma]$ contains the interactions between the Σ and V fields,

$$\Gamma_\Sigma[V, \Sigma] = \int d^3 x \mathcal{L}_\Sigma(\vec{z}) = \frac{m_g}{2g^2} \int d^3 x \text{tr} [\Sigma (V^\dagger V - 1)]. \quad (48)$$

The integral over the unconstrained, complex matrices V has a linear, Euclidean measure DV . Hence it can be performed analytically after pulling out the subleading (cf. Sec. III B), non-Gaussian $4U$ interactions as functional derivatives with respect to the sources. This results in

$$Z[j, j^\dagger] = \int D\Sigma DV \exp \left\{ - \int d^3 z \left[\mathcal{L}_{<,0} + \mathcal{L}_\Sigma + \mathcal{L}_{<,c_1} + \mathcal{L}_{<,c_2} + \dots + \text{tr} \left\{ j V^\dagger + j^\dagger V \right\} \right] \right\} \quad (49)$$

$$= \int D\Sigma DV \exp \left[- \int d^3 z \left(\mathcal{L}_{<,c_1}^{(4U)} + \mathcal{L}_{<,c_2}^{(4U)} + \dots \right) \right] \exp \left[- \int d^3 z \left(\mathcal{L}^{(2U)} + \text{tr} \left\{ j V^\dagger + j^\dagger V \right\} \right) \right] \quad (50)$$

$$= \mathcal{V}^{(4U)} \left[\frac{\delta}{\delta j}, \frac{\delta}{\delta j^\dagger} \right] Z^{(2U)}[j, j^\dagger], \quad (51)$$

where we have extracted the part of the generating functional which originates from the bilinear Lagrangian

$$\mathcal{L}^{(2U)} := \mathcal{L}_{<,0} + \mathcal{L}_{<,c_1}^{(2U)} + \mathcal{L}_{<,c_2}^{(2U)} + \dots + \mathcal{L}_\Sigma =: \text{tr} \left\{ V_{<}^\dagger \Delta V_{<} \right\} - \frac{m_g}{2g^2} \text{tr} \left\{ \Sigma \right\} \quad (52)$$

with the kernel

$$\Delta(\vec{x} - \vec{y}; \{c_n\}, \Sigma) := -\frac{m_g}{2g^2} \left(\partial_x^2 + \frac{c_1}{\mu^2} \partial_x^4 + \frac{c_2}{\mu^4} \partial_x^6 + \dots - \Sigma \right) \delta_{<}^3(\vec{x} - \vec{y}) \quad (53)$$

(which defines the inverse soft-mode propagator) as

$$Z^{(2U)}[j, j^\dagger] = \int D\Sigma DV \exp \left[- \int d^3z \left(\mathcal{L}^{(2U)} + \text{tr} \{jV^\dagger + j^\dagger V\} \right) \right]. \quad (54)$$

All contributions from the $4U$ vertices, on the other hand, are collected in the functional potential

$$\mathcal{V}^{(4U)}[U^\dagger, U] = \exp \left[- \int d^3z \left(\mathcal{L}_{<,c_1}^{(4U)} + \mathcal{L}_{<,c_2}^{(4U)} + \dots \right) \right]. \quad (55)$$

The Gaussian integral over the V fields in Eq. (54) can then be performed analytically, with the result

$$\frac{Z^{(2U)}[j, j^\dagger]}{Z^{(2U)}[0, 0]} = \int D\Sigma \exp \left[\int d^3x \int d^3y \text{tr} \{j^\dagger(\vec{x}) \Delta^{-1}(\vec{x} - \vec{y}; \{c_n\}, \Sigma) j(\vec{y})\} \right]. \quad (56)$$

The whole Σ dependence of the correlators, as well as the c_n dependence originating from the $2U$ interactions, is now concentrated in the gauge-invariant soft-mode propagator Δ^{-1} which we will analyze in Sec. IV C. The perturbative treatment of the $4U$ vertices for $|c_n| \ll 1$, on the other hand, starts from the expansion

$$\mathcal{V}^{(4U)} \left[\frac{\delta}{\delta j}, \frac{\delta}{\delta j^\dagger} \right] \equiv \exp \left[- \int d^3z \mathcal{L}_{<,c_1}^{(4U)} \left(\frac{\delta}{\delta j}, \frac{\delta}{\delta j^\dagger} \right) - \dots \right] \quad (57)$$

$$= 1 - \int d^3z \mathcal{L}_{<,c_1}^{(4U)} \left(\frac{\delta}{\delta j}, \frac{\delta}{\delta j^\dagger} \right) + O(c_1^2, c_{n \geq 2}) \quad (58)$$

of the functional potential which contains the remaining c_n dependence induced by the $4U$ interactions.

B. Mean-field approximation and vacuum phases

After having rewritten the generating functional as an integral over the auxiliary field Σ , we now evaluate this integral in the saddle-point or mean-field approximation (cf. App. A 3). When the integrand in Eq. (47) is expressed as a Boltzmann factor

$$\exp \left\{ -\tilde{\Gamma}[\Sigma] \right\} := \int DV \exp \{ -\Gamma_{<}[V] - \Gamma_\Sigma[V, \Sigma] \} \quad (59)$$

(in the present section we are interested only in the vacuum overlap amplitude and therefore set the sources to zero), the saddle-point or mean-field equation takes the form

$$\frac{\delta \tilde{\Gamma}[\Sigma]}{\delta \Sigma(\vec{x})} = \exp \tilde{\Gamma}[\Sigma] \int DV \frac{\delta \Gamma_\Sigma[V, \Sigma]}{\delta \Sigma(\vec{x})} \exp \{ -\Gamma_{<}[V] - \Gamma_\Sigma[V, \Sigma] \} \quad (60)$$

$$= \frac{m_g}{2g^2} \exp \tilde{\Gamma}[\Sigma] \int DV [V^\dagger(\vec{x}) V(\vec{x}) - 1] \exp \{ -\Gamma_{<}[V] - \Gamma_\Sigma[V, \Sigma] \} = 0 \quad (61)$$

which ensures that its solutions extremize the effective action $\tilde{\Gamma}$. To leading order in the saddle-point expansion, integrals over Σ are then approximated by their integrands, with Σ replaced by a solution $\Sigma^{(\text{mf})}$ of Eq. (61). This turns Eq. (61) into

$$\langle U^\dagger(\vec{x}) U(\vec{x}) \rangle = 1, \quad (62)$$

in particular, and thereby restores the unitarity constraint at the mean-field level. In a homogeneous vacuum one expects the solution of Eq. (62) to be a constant mean field. Then the interaction (48) becomes a mass term for V which triggers dimensional transmutation (as in $O(n)$ models) and generates a mass gap. Hence Eq. (62) plays the role of a gap equation. Since for $\Sigma > 0$ the ‘‘chiral’’ $SU_L(N_c) \times SU_R(N_c)$ symmetry of the soft-mode action (41) is unbroken, the mean-field solution should further be proportional to the unit matrix, i.e.

$$\Sigma^{(\text{mf})} = \bar{\Sigma} \times 1, \quad (63)$$

where $\bar{\Sigma}$ is a real constant.

In order to exhibit the vacuum phase structure encoded in the wave functional (1) more fully, an analogous mean-field treatment of the V integral in Eq. (47) (which reproduces its Gaussian part exactly) turns out to be useful. Defining the effective action (again for vanishing sources) as

$$\exp \left\{ -\tilde{\Gamma} [V] \right\} := \int D\Sigma \exp \left\{ -\Gamma_{<} [V] - \Gamma_{\Sigma} [V, \Sigma] \right\} \quad (64)$$

one obtains the corresponding saddle-point equation

$$\frac{\delta \tilde{\Gamma} [V]}{\delta V^{\dagger}(\vec{x})} = \exp \tilde{\Gamma} [V] \int D\Sigma \frac{\delta \left\{ \Gamma_{<} [V] + \Gamma_{\Sigma} [V, \Sigma] \right\}}{\delta V^{\dagger}(\vec{x})} \exp \left\{ -\Gamma_{<} [V] - \Gamma_{\Sigma} [V, \Sigma] \right\} \quad (65)$$

$$\rightarrow \frac{m_g}{2g^2} \exp \tilde{\Gamma} [\bar{V}] [\bar{\Sigma} \bar{V}] \exp \left\{ -\Gamma_{\Sigma} [\bar{V}, \bar{\Sigma}] \right\} = 0. \quad (66)$$

In the second line we have saturated the Σ integral with the constant (i.e. vacuum) mean fields \bar{V} and $\bar{\Sigma}$. This implies $\Gamma_{<} [\bar{V}] = 0$, in particular, since $\Gamma_{<}$ consists only of derivative interactions. Hence Eq. (66) reduces to

$$\langle \Sigma U(\vec{x}) \rangle = 0. \quad (67)$$

(The ‘‘chiral’’ symmetry of Γ (under which V transforms as $V \rightarrow RVL^{\dagger}$) turns a nonzero mean field \bar{V} into a continuous family of degenerate saddle points. The associated Goldstone zero-mode contributions are therefore not suppressed by the Gaussian weight and have to be integrated exactly.)

The solutions of the mean-field equations (62) and (67) approximately characterize the vacuum phases of the effective σ model (41). The gap equation (62) determines the auxiliary mean field $\bar{\Sigma}$ and will be solved in Sec. VI. The saddle-point equation (67) shows that the vacuum can exist in two phases, as expected on general grounds and confirmed by lattice simulations [41, 42] and the ε -expansion [43]. More specifically, with increasing ‘‘analog temperature’’ $g^2(\mu)$ or decreasing μ one expects the vacuum to pass through an disorder-order phase transition, as in the analogous statistical spin model. In the ordered low-temperature (i.e. weakly coupled) phase, one has

$$\langle U \rangle \neq 0, \quad \langle \Sigma \rangle = 0, \quad (68)$$

i.e. the ‘‘chiral’’ symmetry is broken to its diagonal subgroup and $N_c^2 - 1$ massless Goldstone bosons are generated. In the disordered high-temperature (strong-coupling) phase with

$$\langle U \rangle = 0, \quad \langle \Sigma \rangle \neq 0, \quad (69)$$

on the other hand, the ‘‘chiral’’ symmetry is restored [66]. The order-disorder transition thus occurs when $\langle \Sigma \rangle$ reaches zero in the disordered phase and is, as usual, the result of a competition between the ordering tendency of the energy and the disordering propensity of the entropy. Our above arguments imply, furthermore, that the *qualitative* phase structure is independent of the detailed interactions (43) as long as the soft-mode dynamics contains only derivative interactions, which is guaranteed by the unitarity of the $U_{<}$ fields. As a consequence of $\Gamma_{<} [\bar{V}] = 0$, in particular, the mean-field equations and hence the qualitative phase structure have no *explicit* dependence on the low-momentum constants c_n .

C. Soft-mode propagator

The static soft-mode propagator Δ^{-1} determines the Gaussian part (56) of the generating functional and thereby encapsulates most of the impact of the higher-derivative interactions on the vacuum dynamics and amplitudes. From the Fourier transform

$$\Delta(\vec{x} - \vec{y}) = \frac{m_g}{2g^2} \int \frac{d^3 k}{(2\pi)^3} \theta(\mu^2 - k^2) \left(k^2 - \frac{c_1}{\mu^2} k^4 + \frac{c_2}{\mu^4} k^6 - \dots + \bar{\Sigma} \right) e^{i\vec{k}(\vec{x} - \vec{y})} \quad (70)$$

of its inverse (53), which we have specialized to the constant mean field (63), the propagator is obtained as the solution of

$$\int d^3 z \Delta^{-1}(\vec{x} - \vec{z}) \Delta(\vec{z} - \vec{y}) = \delta_{<}^3(\vec{x} - \vec{y}) \quad (71)$$

where δ_{ζ}^3 is the regularized delta function (14). In terms of the dimensionless variables

$$\vec{\kappa} \equiv \frac{\vec{k}}{\mu}, \quad \xi \equiv \frac{\sqrt{\Sigma}}{\mu} \quad (72)$$

one therefore has

$$\Delta^{-1}(\vec{x} - \vec{y}) = \int \frac{d^3\kappa}{(2\pi)^3} e^{i\mu\vec{\kappa}(\vec{x}-\vec{y})} \Delta^{-1}(\kappa) \quad (73)$$

with

$$\Delta^{-1}(\kappa) = \frac{2g^2\mu}{m_g} \frac{\theta(1-\kappa^2)}{\kappa^2 + \xi^2 + \mathcal{M}^2(\kappa^2)}. \quad (74)$$

The Fourier representation (73) of the soft-mode propagator can be simplified by performing the angular integrals analytically,

$$\Delta^{-1}(\vec{x} - \vec{y}) = \frac{g^2}{\pi^2 m_g} \frac{1}{|x-y|} \int_0^1 d\kappa \frac{\kappa \sin(\kappa\mu|x-y|)}{\kappa^2 + \xi^2 + \mathcal{M}^2(\kappa^2)}, \quad (75)$$

which is useful for numerical implementations and demonstrates that the isotropic regularization (i.e. $\kappa \leq 1$) preserves

$$\Delta^{-1}(\vec{x} - \vec{y}) = \Delta^{-1}(\vec{y} - \vec{x}). \quad (76)$$

Equation (74) reveals that the higher-derivative interactions generate a momentum-dependent selfenergy

$$\mathcal{M}^2(\kappa^2) = -c_1\kappa^4 + c_2\kappa^6 - c_3\kappa^8 + \dots \quad (77)$$

for the soft modes. Hence the propagator (74) may be regarded as the resummation of a static self-energy (i.e. \mathcal{M}^2) insertion. This geometric series converges for $|\mathcal{M}^2(\kappa^2)/(\kappa^2 + \xi^2)| < 1$. Expecting the c_1 contribution to dominate at small momenta $k \ll \mu$ and therefore truncating to $c_{n \geq 2} = 0$ (see below), this implies

$$|c_1| < \frac{\kappa^2 + \xi^2}{\kappa^4}. \quad (78)$$

For $\kappa \in [0, 1]$ and $\xi \geq 0$, the above inequality is satisfied if $|c_1| < 1$. This does not additionally constrain the parameter space, however, since $c_1 < 1$ guarantees the normalizability of the vacuum wave functional (cf. Eq. (22)) and $|c_1| \ll 1$ ensures the validity of our perturbative $O(c_1)$ treatment (58) of the residual $4U$ interactions.

In order to analyze the singularity structure of the soft-mode propagator, we rewrite Eq. (74) for $c_{n \geq 2} = 0$ as

$$\Delta^{-1}(\kappa) = \frac{2g^2\mu}{m_g} \frac{\theta(1-\kappa^2)}{\kappa^2(1-c_1\kappa^2) + \xi^2} = \frac{2g^2\mu}{m_g} \frac{\theta(1-\kappa^2)}{\sqrt{1+4c_1\xi^2}} \left(\frac{1}{\kappa^2 - \kappa_2^2} - \frac{1}{\kappa^2 - \kappa_1^2} \right) \quad (79)$$

which reveals two poles at the momenta

$$\kappa_{1,2}^2(\xi, c_1) = \frac{1}{2c_1} \left(1 \pm \sqrt{1 + 4c_1\xi^2} \right). \quad (80)$$

The pole position κ_1^2 (with the positive sign in Eq. (80)) diverges for $c_1 \rightarrow 0$ but decreases monotonically for $c \rightarrow 1$ to reach $\kappa_1^2(\xi, c_1 = 1) \geq 1$. Hence the pole at κ_1^2 lies outside of the integration range $\kappa \in [0, 1]$ for all $c_1 \in [-\infty, 1]$ (and even for $\xi \rightarrow 0$). The second pole at κ_2^2 lies inside the integration range for $c_1 > -\infty$ and $\xi = 0$. For $c_1 = 0$, in particular, it turns into the standard infrared pole of the $c_n = 0$ propagator, showing that the momentum-dependent selfenergy does not create singularities beyond the $\xi \rightarrow 0$ pole of the uncorrected soft-mode propagator.

V. EVALUATION OF THE 2- AND 4-POINT CORRELATORS FOR $c_{n \geq 2} = 0$

After having established our calculational framework for the generating functional, we now derive explicit expressions for the soft modes' two- and four-point functions. Those will underlie our subsequent evaluation of the matrix elements

$\langle U_{<}^\dagger(\vec{x}) U_{<}(\vec{x}) \rangle$ in the gap equation (62) and $\langle L_{<,i}^a(\vec{x}_1) L_{<,i}^a(\vec{x}_2) \rangle$ in the chromo-electric contribution (142) to the vacuum energy density.

As stated previously, among the contributions from the higher-derivative interactions (43) those associated with c_1 are expected to dominate at small momenta $k^2 \ll \mu^2$. This expectation is further supported by evidence from Ref. [21] where relevant infrared physics was found to be captured by the truncation of the covariance expansion (13) to $c_{n \geq 2} = 0$. (More specifically, the first correction term $\mathcal{L}_{<,c_1}$ turned out to reproduce the full (nonlocal) IR action (38) at its saddle points with better than 10% accuracy.) Although the $c_{n \geq 2}$ corrections are straightforward to implement, they would furthermore obscure the (e.g. graphical) analysis of the vacuum energy density and the interpretation of other amplitudes. Hence we will restrict the remainder of our investigation to the c_1 corrections, associated with the four-gradient interactions

$$\mathcal{L}_{<,c_1}(\vec{z}) = \frac{c_1 m_g}{2g^2 \mu^2} \text{tr} \left\{ U_{<}^\dagger(\vec{z}) \partial_i U_{<}(\vec{z}) \partial^2 \left[\partial_i U_{<}^\dagger(\vec{z}) U_{<}(\vec{z}) \right] \right\} \quad (81)$$

$$= \mathcal{L}_{<,c_1}^{(2U)}(\vec{z}) + \mathcal{L}_{<,c_1}^{(4U)}(\vec{z}) \quad (82)$$

(where derivatives are implied to act on the nearest field only) which we have split as in Sec. III B into the dominant $2U$ interaction term $\mathcal{L}_{<,c_1}^{(2U)}$ given by Eq. (44) for $n = 1$, and the $4U$ contribution

$$\mathcal{L}_{<,c_1}^{(4U)}(\vec{z}) = \frac{c_1 m_g}{2g^2 \mu^2} \text{tr} \left\{ U_{<}^\dagger \partial_i U_{<} \left[2 \partial_i \partial_k U_{<}^\dagger \partial_k U_{<} + \partial_i U_{<}^\dagger \partial^2 U_{<} \right] \right\}. \quad (83)$$

As discussed in Sec. IV A, the $2U$ contributions to the relevant n -point functions will be evaluated exactly while the residual contributions from the $4U$ vertices will be treated perturbatively [67] to $O(c_1)$. The latter has to be justified *a posteriori*, by showing that the variational results favor small enough coupling values $|c_1^*| \ll 1$ (cf. Sec. VIII A).

A. The 2-point function

In this section we evaluate the 2-point soft-mode correlator (for $c_{i \geq 2} = 0$) which simultaneously provides the basis for the calculation of the 4-point correlator in the next section. Since we are working to $O(c_1)$ in the $4U$ interactions, we will only keep one insertion of the $\mathcal{L}_{<,c_1}^{(4U)}$ vertex in the functional potential operator (58), which thus reduces to

$$\mathcal{V}^{(4U,c_1)} \left[\frac{\delta}{\delta j}, \frac{\delta}{\delta j^\dagger} \right] = 1 - \frac{c_1 m_g}{2g^2 \mu^2} \int d^3 z \partial^2 \left[\frac{\partial_i \delta}{\delta j_{MN}(\vec{z})} \frac{\delta}{\delta j_{PM}^\dagger(\vec{z})} \right] \frac{\delta}{\delta j_{QP}(\vec{z})} \frac{\partial_i \delta}{\delta j_{NQ}^\dagger(\vec{z})} \quad (84)$$

(where the notation $(\partial_i \delta) / \delta j(\vec{z})$ implies that the partial derivative is acting *only* on the result of the associated functional derivation). The 2-point function is then obtained by taking derivatives of the generating functional (51) with respect to the matrix sources j and j^\dagger , i.e.

$$\left\langle U_{<,AB}^\dagger(\vec{x}) U_{<,CD}(\vec{y}) \right\rangle = \frac{-\delta}{\delta j_{BA}(\vec{x})} \frac{-\delta}{\delta j_{DC}^\dagger(\vec{y})} \mathcal{V}^{(4U,c_1)} \left[\frac{\delta}{\delta j}, \frac{\delta}{\delta j^\dagger} \right] \frac{Z^{(2U)}[j, j^\dagger]}{Z^{(2U)}[0, 0]} \Bigg|_{j, j^\dagger=0}, \quad (85)$$

where the superscript $(2U)$ indicates as in Eq. (54) that the corresponding quantity is evaluated by using the $2U$ approximation to the full soft-mode action. Eq. (85) can thus be rewritten as

$$\begin{aligned} \left\langle U_{<,AB}^\dagger(\vec{x}) U_{<,CD}(\vec{y}) \right\rangle &= \left\langle U_{<,AB}^\dagger(\vec{x}) U_{<,CD}(\vec{y}) \right\rangle^{(2U)} \\ &\quad - \left\langle U_{<,AB}^\dagger(\vec{x}) \int d^3 z \mathcal{L}_{<,c_1}^{(4U)} \left[U_{<}^\dagger(\vec{z}), U_{<}(\vec{z}) \right] U_{<,CD}(\vec{y}) \right\rangle^{(2U)} \end{aligned} \quad (86)$$

where

$$\left\langle U_{<,AB}^\dagger(\vec{x}) U_{<,CD}(\vec{y}) \right\rangle^{(2U)} = \frac{\delta^2}{\delta j_{BA}(\vec{x}) \delta j_{DC}^\dagger(\vec{y})} \frac{Z^{(2U)}[j, j^\dagger]}{Z^{(2U)}[0, 0]} \Bigg|_{j, j^\dagger=0} = \delta_{AD} \delta_{BC} \Delta^{-1}(\vec{y}, \vec{x}) \quad (87)$$

is determined by the $2U$ part of the higher-derivative interactions only, while the $4U$ dynamics generates the perturbative $O(c_1)$ correction

$$\left\langle U_{<,AB}^\dagger(\vec{x}) \int d^3 z \mathcal{L}_{<,c_1}^{(4U)}(\vec{z}) U_{<,CD}(\vec{y}) \right\rangle^{(2U)} = \frac{c_1 m_g}{2g^2 \mu^2} \frac{\delta^2}{\delta j_{BA}(\vec{x}) \delta j_{DC}^\dagger(\vec{y})} v[j, j^\dagger] \Bigg|_{j, j^\dagger=0} \quad (88)$$

which is due to the insertion of the vertex

$$v [j, j^\dagger] := \frac{2g^2\mu^2}{c_1 m_g} \int d^3 z \mathcal{L}_{<, c_1}^{(4U)} \left(\frac{\delta}{\delta j}, \frac{\delta}{\delta j^\dagger} \right) \frac{Z^{(2U)} [j, j^\dagger]}{Z^{(2U)} [0, 0]} \quad (89)$$

$$= \int d^3 z \partial^2 \left[\frac{\partial_i \delta}{\delta j_{MN}(\vec{z})} \frac{\delta}{\delta j_{PM}^\dagger(\vec{z})} \right] \frac{\delta}{\delta j_{QP}(\vec{z})} \frac{\partial_i \delta}{\delta j_{NQ}^\dagger(\vec{z})} \frac{Z^{(2U)} [j, j^\dagger]}{Z^{(2U)} [0, 0]} \quad (90)$$

(where ∂^2 acts only on the square bracket).

After evaluating the functional derivatives in Eq. (90), the contributions to the vertex v can be grouped according to the number of source fields which they contain as

$$v [j, j^\dagger] = \frac{Z^{(2U)} [j, j^\dagger]}{Z^{(2U)} [0, 0]} (v_d + v_{jj^\dagger} [j, j^\dagger] + v_{jj^\dagger jj^\dagger} [j, j^\dagger]). \quad (91)$$

The constant $v_d = v [0, 0]$ is the IR-divergent, disconnected part which originates from the “8” vacuum-bubble diagram, with all four legs of the vertex $v [j, j^\dagger]$ closed among themselves, and reads

$$v_d = -N^3 \mu^6 \left(\frac{g^2}{\pi^2 m_g} \right)^2 \tilde{v}_2^2 (\xi, c_1) (2\pi)^3 \delta^3 (0) \quad (92)$$

(the integral $\tilde{v}_2 (\xi, c_1)$ is defined in App. B). More generally, disconnected contributions to the n -point functions arise when all functional derivatives associated with external lines hit the $Z^{(2U)} [j, j^\dagger] v_d$ part of $v [j, j^\dagger]$. The resulting products of free Green functions with v_d will play no role in our following discussion. All remaining terms require one (two) pair(s) $(\delta/\delta j) (\delta/\delta j^\dagger)$ to hit v_{jj^\dagger} ($v_{jj^\dagger jj^\dagger}$) and thus contribute exclusively to the *connected* 2-(4-)point function. The 2-line connected part of the vertex thus becomes

$$v_{jj^\dagger} [j, j^\dagger] = -\frac{g^2 N \mu^3}{\pi^2 m_g} \tilde{v}_2 (\xi, c_1) \int d^3 z \left[-j_{MN}^\dagger \Delta^{-1} \partial^2 \Delta^{-1} j_{NM} + (\partial_i \Delta^{-1} j_{MN}) j_{NM}^\dagger \overleftarrow{\partial}_i \right] \quad (93)$$

(where the ∂_i ($\overleftarrow{\partial}_i$) act on the first (second) argument of Δ^{-1} and integrals over the arguments of Δ^{-1} folded with a source are implied but not written explicitly). The 4-line connected part, finally, is

$$v_{jj^\dagger jj^\dagger} [j, j^\dagger] = \int d^3 z (\partial_i \Delta^{-1} j_{QN}) j_{PQ}^\dagger \Delta^{-1} \times \\ \times \left[2 (\partial_j \Delta^{-1} j_{MP}) (j_{NM}^\dagger \Delta^{-1} \overleftarrow{\partial}_i \overleftarrow{\partial}_j) + (\partial^2 \Delta^{-1} j_{MP}) (j_{NM}^\dagger \Delta^{-1} \overleftarrow{\partial}_i) \right] \quad (94)$$

and contributes only to $n \geq 4$ point functions. (In both of the above expressions the “open” arguments (i.e. those not integrated over) are always the vertex coordinates \vec{z} with $\partial_i \equiv \partial/\partial z_i$.)

We now proceed with the calculation of the 2-point (and $2n$ -point) functions by evaluating the $4U$ -vertex-induced functional

$$\Pi_{ABCD}^{(2)} [j, j^\dagger] (\vec{x}, \vec{y}) := \frac{-\delta}{\delta j_{BA}(\vec{x})} \frac{-\delta}{\delta j_{DC}^\dagger(\vec{y})} v [j, j^\dagger] =: \frac{Z^{(2U)} [j, j^\dagger]}{Z^{(2U)} [0, 0]} \bar{\Pi}_{ABCD}^{(2)} [j, j^\dagger] (\vec{x}, \vec{y}) \quad (95)$$

which yields

$$\bar{\Pi}_{ABCD}^{(2)} [j, j^\dagger] (\vec{x}, \vec{y}) = \delta_{AD} \Delta_{CB}^{-1} (\vec{y} - \vec{x}) (v_{jj^\dagger} + v_{jj^\dagger jj^\dagger}) \\ + \int d^3 z'' j_{AB}^\dagger(\vec{z}'') \Delta^{-1} (\vec{z}'' - \vec{x}) \int d^3 z' \Delta^{-1} (\vec{y} - \vec{z}') j_{CD}(\vec{z}') (v_{jj^\dagger} + v_{jj^\dagger jj^\dagger}) \\ + \int d^3 z' \Delta^{-1} (\vec{y} - \vec{z}') j_{CD}(\vec{z}') \frac{\delta (v_{jj^\dagger} [j, j^\dagger] + v_{jj^\dagger jj^\dagger} [j, j^\dagger])}{\delta j_{BA}(\vec{x})} \\ + \int d^3 z'' j_{AB}^\dagger(\vec{z}'') \Delta^{-1} (\vec{z}'' - \vec{x}) \frac{\delta (v_{jj^\dagger} [j, j^\dagger] + v_{jj^\dagger jj^\dagger} [j, j^\dagger])}{\delta j_{DC}^\dagger(\vec{y})} \\ + \frac{\delta^2 (v_{jj^\dagger} [j, j^\dagger] + v_{jj^\dagger jj^\dagger} [j, j^\dagger])}{\delta j_{BA}(\vec{x}) \delta j_{DC}^\dagger(\vec{y})}. \quad (96)$$

The 2-point function is obtained from $\Pi^{(2)}$ by setting the sources j, j^\dagger to zero. Since then $v_{jj^\dagger}[0, 0] = v_{jj^\dagger jj^\dagger}[0, 0] = 0$ and also the one-derivative terms as well as the term with two derivatives on $v_{jj^\dagger jj^\dagger}$ vanish, one is left with

$$\Pi_{ABCD}^{(2)}[0, 0](\vec{x}, \vec{y}) = \frac{\delta^2 v_{jj^\dagger}[j, j^\dagger]}{\delta j_{BA}(\vec{x}) \delta j_{DC}^\dagger(\vec{y})} \quad (97)$$

(the right-hand side is independent of j, j^\dagger – hence one does not have to impose $j, j^\dagger = 0$ explicitly). It thus remains to calculate

$$\frac{\delta^2 v_{jj^\dagger}[j, j^\dagger]}{\delta j_{BA}(\vec{x}) \delta j_{DC}^\dagger(\vec{y})} = \delta_{AD} \delta_{CB} \frac{4Ng^4}{\pi^2} \frac{\mu}{m_g^2} \tilde{v}_2(\xi, c_1) \partial_x^2 \frac{-\partial}{\partial \xi^2} \Delta^{-1}(\vec{y} - \vec{x}) \quad (98)$$

$$= -\delta_{AD} \delta_{BC} \frac{2g^2}{m_g} \frac{\gamma}{\zeta \mu} \bar{\Delta}^{-1}(\vec{x} - \vec{y}), \quad (99)$$

where we used the symmetry property (76) and defined the “vertex-inserted” soft-mode propagator

$$\bar{\Delta}^{-1}(\vec{x}) := 2\tilde{v}_2 \mu \partial_x^2 \frac{\partial}{\partial \xi^2} \Delta^{-1}(\vec{x}) = \frac{4g^2 \mu^4}{m_g} \tilde{v}_2(\xi, c_1) \int \frac{d^3 \kappa}{(2\pi)^3} \frac{\kappa^2 \theta(1 - \kappa^2) e^{i\vec{\kappa} \mu \vec{x}}}{[\kappa^2(1 - c_1 \kappa^2) + \xi^2]^2} \quad (100)$$

as well as the dimensionless parameters

$$\xi = \frac{\sqrt{\Sigma}}{\mu}, \quad \gamma \equiv \frac{g^2 N_c}{\pi^2} = 4N_c \frac{\alpha}{\pi}, \quad \zeta \equiv \frac{m_g}{\mu}. \quad (101)$$

Hence the c_1 correction (88) to the connected 2-point function, which originates from the perturbative insertion of the $4U$ part (83) of the four-derivative interactions, becomes

$$\left\langle U_{<,AB}^\dagger(\vec{x}) \int d^3 z \mathcal{L}_{<,c_1}^{(4U)}(\vec{z}) U_{<,CD}(\vec{y}) \right\rangle^{(2U)} = \frac{c_1 m_g}{2g^2 \mu^2} \Pi_{ABCD}^{(2)}[0, 0](\vec{x}, \vec{y}) = -\delta_{AD} \delta_{BC} \frac{c_1 \gamma}{\zeta \mu^3} \bar{\Delta}^{-1}(\vec{x} - \vec{y}). \quad (102)$$

Our final result for the 2-point function is therefore

$$\left\langle U_{<,AB}^\dagger(\vec{x}) U_{<,CD}(\vec{y}) \right\rangle = \delta_{AD} \delta_{BC} \left[\Delta^{-1}(\vec{x} - \vec{y}) + \frac{c_1 \gamma}{\zeta \mu^3} \bar{\Delta}^{-1}(\vec{x} - \vec{y}) \right]. \quad (103)$$

Its diagonal dependence on the group indices reflects the $SU_L(N_c) \times SU_R(N_c)$ symmetry of the soft-mode dynamics (42) and (81).

B. The 4-point function

In this section we sketch the analogous evaluation of the 4-point function. Although our main goal of computing c_n corrections to the vacuum energy density involves (in our approximation) only the 2-point function, the explicit expression for the 4-point function

$$\delta_4 \equiv \left\langle U_{<,AB}^\dagger(\vec{z}_1) U_{<,CD}(\vec{z}_2) U_{<,EF}^\dagger(\vec{z}_3) U_{<,GH}(\vec{z}_4) \right\rangle \quad (104)$$

$$= \frac{-\delta}{\delta j_{BA}(\vec{z}_1)} \frac{-\delta}{\delta j_{DC}^\dagger(\vec{z}_2)} \frac{-\delta}{\delta j_{FE}(\vec{z}_3)} \frac{-\delta}{\delta j_{HG}^\dagger(\vec{z}_4)} \mathcal{V}^{(4U, c_1)} \left[\frac{\delta}{\delta j}, \frac{\delta}{\delta j^\dagger} \right] \frac{Z^{(2U)}[j, j^\dagger]}{Z^{(2U)}[0, 0]} \Bigg|_{j, j^\dagger=0} \quad (105)$$

$$=: \delta_4^{(2U)} - \delta_4^{(4U, O(c_1))} + \dots \quad (106)$$

will be useful because it allows for consistency checks and an alternative estimate of parts of the energy density. Above, we have defined

$$\delta_4^{(2U)} \equiv \left\langle U_{<,AB}^\dagger(\vec{z}_1) U_{<,CD}(\vec{z}_2) U_{<,EF}^\dagger(\vec{z}_3) U_{<,GH}(\vec{z}_4) \right\rangle^{(2U)} \quad (107)$$

$$= \frac{\delta^4}{\delta j_{FE}(\vec{z}_3) \delta j_{HG}^\dagger(\vec{z}_4) \delta j_{BA}(\vec{z}_1) \delta j_{DC}^\dagger(\vec{z}_2)} \frac{Z^{(2U)}[j, j^\dagger]}{Z^{(2U)}[0, 0]} \Bigg|_{j, j^\dagger=0} \quad (108)$$

$$= \delta_{AD} \delta_{CB} \Delta^{-1}(\vec{z}_2, \vec{z}_1) \delta_{EH} \delta_{GF} \Delta^{-1}(\vec{z}_4, \vec{z}_3) + \delta_{AH} \delta_{GB} \Delta^{-1}(\vec{z}_4, \vec{z}_1) \delta_{ED} \delta_{CF} \Delta^{-1}(\vec{z}_2, \vec{z}_3) \quad (109)$$

which shows that in the absence of the $4U$ interactions the 4-point function factorizes as

$$\begin{aligned} \left\langle U_{LAB}^\dagger(\vec{z}_1) U_{LCD}(\vec{z}_2) U_{LEF}^\dagger(\vec{z}_3) U_{LGH}(\vec{z}_4) \right\rangle &= \left\langle U_{LAB}^\dagger(\vec{z}_1) U_{LCD}(\vec{z}_2) \right\rangle \left\langle U_{LEF}^\dagger(\vec{z}_3) U_{LGH}(\vec{z}_4) \right\rangle \\ &+ \left\langle U_{LAB}^\dagger(\vec{z}_1) U_{LGH}(\vec{z}_4) \right\rangle \left\langle U_{LEF}^\dagger(\vec{z}_3) U_{LCD}(\vec{z}_2) \right\rangle, \end{aligned} \quad (110)$$

and

$$\delta_4^{(4U, O(c_1))} \equiv \left\langle U_{<,AB}^\dagger(\vec{z}_1) U_{<,CD}(\vec{z}_2) \int d^3z \mathcal{L}_{<,c_1}^{(4U)}(\vec{z}) U_{<,EF}^\dagger(\vec{z}_3) U_{<,GH}(\vec{z}_4) \right\rangle^{(2U)} \quad (111)$$

$$= \frac{c_1 m_g}{2g^2 \mu^2} \frac{\delta^4 v [j, j^\dagger]}{\delta j_{FE}(\vec{z}_3) \delta j_{HG}^\dagger(\vec{z}_4) \delta j_{BA}(\vec{z}_1) \delta j_{DC}^\dagger(\vec{z}_2)} \Big|_{j, j^\dagger=0} \quad (112)$$

$$=: -\frac{c_1 m_g}{2g^2 \mu^2} \Pi_{ABCDEFGH}^{(4)}(\vec{z}_1, \vec{z}_2, \vec{z}_3, \vec{z}_4). \quad (113)$$

The above reordering of the functional derivatives furthermore implies that the intermediate result (95) from the calculation of the 2-point function (with $\vec{x} \rightarrow \vec{z}_1$ and $\vec{y} \rightarrow \vec{z}_2$) can be used. Indeed, to $O(c_1)$ the correction due to the $4U$ interaction becomes

$$\Pi_{ABCDEFGH}^{(4)}(\vec{z}_1, \vec{z}_2, \vec{z}_3, \vec{z}_4) := \frac{\delta}{\delta j_{FE}(\vec{z}_3)} \frac{\delta}{\delta j_{HG}^\dagger(\vec{z}_4)} \Pi_{ABCD}^{(2)}[j, j^\dagger](\vec{z}_1, \vec{z}_2) \Big|_{j, j^\dagger=0} \quad (114)$$

which can be further simplified in the zero-distance limit for some of its arguments (as it occurs in applications in our context) and then renders, together with Eq. (109), the coordinate dependence of the 4-point function explicit.

VI. SOLUTION OF THE GAP EQUATION AND PHASE DIAGRAM

As discussed in Sec. IV B, the above expressions for the 2- and 4-point functions have to be evaluated at the saddle point (63) of the integral over the auxiliary Σ field in the generating functional (56). This saddle point, $\bar{\Sigma} =: (\mu\bar{\xi})^2$, is the (minimal-action) solution of the gap equation (62) or, more explicitly,

$$\left\langle U_{<,AB}^\dagger(\vec{x}) U_{<,BC}(\vec{x}) \right\rangle = \delta_{AC}. \quad (115)$$

After inserting the result (103) for the connected 2-point function (and recalling $\delta_{AA} = N_c$), Eq. (115) turns into

$$N_c \left[\Delta^{-1}(0) + \frac{c_1 \gamma}{\zeta \mu^3} \bar{\Delta}^{-1}(0) \right] = 1. \quad (116)$$

Expressing the zero-distance limits of the propagator (73) with Fourier transform (74) and the correction (100) in terms of the integrals \tilde{i}_n, \tilde{j}_n defined in App. B,

$$\Delta^{-1}(0) = \frac{\gamma}{\zeta N_c} \tilde{i}_1(\xi, c_1), \quad (117)$$

$$\bar{\Delta}^{-1}(0) = \frac{2\gamma}{\zeta N_c} \mu^3 \tilde{i}_2(\xi, c_1) \tilde{j}_2(\xi, c_1) \quad (118)$$

(both are of $O(g^2/\zeta)$), then yields the gap equation in its final form

$$\frac{\gamma}{\zeta} \left[\tilde{i}_1(\xi, c_1) + 2c_1 \frac{\gamma}{\zeta} \tilde{i}_2(\xi, c_1) \tilde{j}_2(\xi, c_1) \right] = 1. \quad (119)$$

(For $c_1 = 0$ and $\zeta = 1$, Eq. (119) reduces as expected [17] to $\gamma \tilde{i}_1(\xi) = 1$ (except for diverging γ , see below).) Together with the explicit ξ dependence of the integrals (B1) and (B2), this equation exhibits the nonperturbative character of its solution(s) $\xi(\mu, c_1, \zeta)$ which arise by resummation of the infinitely many diagrams required to generate a finite dynamical mass gap.

Before determining the solutions of Eq. (119) as a function of the variational parameters, we specialize ζ to the form required by the continuity of $G^{-1}(k)$ at $k = \mu$ (cf. Eq. (23), i.e. to

$$\zeta_{\text{ct}}(c_1) = \frac{m_g}{\mu} = \frac{1}{1 - c_1}. \quad (120)$$

To render the μ dependence of the running coupling $g(\mu)$ explicit, furthermore, we will adopt the one-loop Yang-Mills coupling. Although it is by a factor of 11/10 [31, 34] larger than the coupling (37) obtained by integrating out the high-momentum modes [34] governed by the UV covariance (11), we use the Yang-Mills coupling

$$\gamma(\mu) = \frac{g_{\text{YM}}^2(\mu) N_c}{\pi^2} = \frac{g_{\text{YM}}^2(\mu) N_c}{\pi^2} \stackrel{N_c=3}{=} \frac{3g_{\text{YM}}^2(\mu)}{\pi^2} \simeq \frac{24}{11 \ln \frac{\mu}{\Lambda_{\text{YM}}}} \quad (121)$$

because the discrepancy can be mended by admitting non-transverse modes to the UV covariance [18] and because it facilitates direct comparison with the numerical results of Ref. [17].

Hence the solutions of Eq. (119) depend on just two variational parameters, the RG scale μ which enters through the coupling (121) and c_1 which controls the leading momentum dependence of the infrared covariance $G_{<}^{-1}(k)$. Before finding the solutions $\bar{\xi}(\mu, c_1)$ numerically, we determine the critical line $\mu_c(c_1)$ in the parameter space (i.e. for $\mu \geq 0$ and $c_1 < 1$) which joins the points where the phase transition takes place, i.e. where

$$\bar{\xi}(\mu_c(c_1), c_1) = 0. \quad (122)$$

This one-dimensional subspace can be found analytically since the integrals \tilde{i}_1 , \tilde{i}_2 and \tilde{j}_2 in the gap equation (119) simplify for $\xi = 0$ to (cf. App. B2)

$$\tilde{i}(c_1) := \tilde{i}_1(0, c_1) = \frac{\text{arctanh} \sqrt{c_1}}{\sqrt{c_1}}, \quad \tilde{i}_2(0, c_1) = \frac{\tilde{i}(c_1) - 1}{c_1} \quad (123)$$

and

$$\tilde{j}_2(0, c_1) = \frac{1}{2} \left[\frac{1}{1 - c_1} + \tilde{i}(c_1) \right]. \quad (124)$$

In order to exhibit the μ dependence of the critical line, we resolve the gap equation at $\xi = 0$ for $\gamma(\mu)$, which yields

$$\frac{1}{\zeta_{\text{ct}}^2} \left(\frac{\tilde{i} - 1}{1 - c_1} + \tilde{i}(\tilde{i} - 1) \right) \gamma^2 + \frac{\tilde{i}}{\zeta_{\text{ct}}} \gamma - 1 = 0. \quad (125)$$

The two solutions of this equation combine into the critical line $\mu_c(c_1)$. With $\gamma(\mu)$ from Eq. (121) it takes the explicit form

$$\frac{\mu_{c,1,2}(c_1)}{\Lambda_{\text{YM}}} = \exp \left[\frac{48}{11} \frac{(1 - c_1) [1 - \tilde{i}(c_1)] [1 + (1 - c_1) \tilde{i}(c_1)]}{(1 - c_1) \tilde{i}(c_1) \pm \sqrt{5\tilde{i}^2(c_1) (1 - c_1)^2 - 4(1 - c_1) [1 - c_1 \tilde{i}(c_1)]}} \right]. \quad (126)$$

The plot of Eq. (126) is shown in Fig. 3. For each c_1 for which a solution exists, Eq. (122) is satisfied by two values of μ_c , except for the maximal and minimal values where μ_c becomes unique. Vice versa, for each μ_c there are thus two c_1 for which Eq. (122) holds. Furthermore, solutions (126) exist only in the limited parameter ranges

$$0.5 \lesssim \frac{\mu_c}{\Lambda_{\text{YM}}} \lesssim 8.86 \quad (127)$$

and

$$-0.48 \lesssim c_1 < 1. \quad (128)$$

This prevents the minimal-energy solution (to be determined in Sec. VIII A) from attaining unacceptably large values of μ and $|c_1|$. In particular, the normalizability condition $c_1 < 1$ is automatically satisfied in the existence range of gap-equation solutions. Equation (126) further shows that nontrivial (i.e. nonzero) solutions of the gap equation exist only for couplings beyond a critical value, i.e. for

$$g^2(\mu) > g_c^2(c_1), \quad (129)$$

as expected on physical grounds. The maximal critical coupling is attained at $c_1 = 0$ and therefore identical to that of Ref. [17], i.e.

$$g_c^2(c_1) \leq g_c^2(c_1 = 0) = \frac{\pi^2}{N_c}. \quad (130)$$

Only part of the critical line (126) is physical, however. Its validity range is limited to $|c_1| \ll 1$ for which the $O(c_1)$ evaluation of the $4U$ correction included in Eq. (126) is reliable, and to $\mu/\Lambda_{\text{YM}} \gtrsim 5 - 6$ which justifies the $O(g)$ approximation. In fact, these two restrictions eliminate most of the $\mu_{c,1}$ branch and the lower- μ part of the $\mu_{c,2}$ branch. (The $c_1 = 0$ solution with $\mu_c/\Lambda_{\text{YM}} \rightarrow 1$ and thus $g^2(\mu_c) \rightarrow \infty$, in particular, invalidates the $O(g)$ treatment but nevertheless demonstrates that the gap equation does not reduce to $\gamma_{\tilde{t}_1}(\xi) = 1$ for $c_1 \rightarrow 0$ if $\gamma(\mu_c)$ simultaneously diverges.)

In Fig. 2 we plot the full, numerically generated solution $\bar{\xi}(\mu, c_1)$ of the gap equation (119) in the physically reliable parameter domain. As expected, the $\bar{\xi} \geq 0$ region is surrounded by the critical line (126) and exist for $0.5 \lesssim \mu/\Lambda_{\text{YM}} \lesssim 8.86$. Moreover, Fig. 2 shows that even for our infrared-generalized vacuum wave functionals the transition from the disordered to the ordered phase remains of second order (as for $c_1 \equiv 0$) [68].

VII. VACUUM ENERGY DENSITY

We have now assembled all the necessary infrared information to evaluate the expectation value (25) of the Yang-Mills Hamiltonian density

$$\mathcal{H}_{\text{YM}} = \frac{1}{2} (E_i^a E_i^a + B_i^a B_i^a) \quad (131)$$

(in $A_0 = 0$ gauge and with the chromoelectric and -magnetic fields $E_i^a = F_{0i}^a$ and $B_i^a = \frac{1}{2}\varepsilon_{ijk}F_{jk}^a$) in the generalized trial vacuum state (1), with the IR covariance expansion (20) truncated to $c_{n \geq 2} = 0$ as discussed above. Of course, the Hamiltonian (131) is formal and needs renormalization. Since we are interested in its matrix elements between the Poincaré-invariant vacuum trial states with perturbative one-loop corrections only, however, a regularization of the vacuum matrix elements by a momentum cutoff Λ_{UV} will be sufficient [17]. In fact, the Λ_{UV} dependence of the vacuum energy density (25) can then be completely removed by normal-ordering the Hamiltonian (131) with respect to the noninteracting vacuum. This amounts to subtracting the ultraviolet-divergent energy density

$$\langle \mathcal{H}_{\text{YM}} \rangle_0 = 2(N_c^2 - 1) \frac{G_0^{-1}(\vec{x}, \vec{x})}{2} = 2(N_c^2 - 1) \int \frac{d^3k}{(2\pi)^3} \frac{\hbar\omega_k}{2} = \frac{N_c^2 - 1}{8\pi^2} \Lambda_{\text{UV}}^4 \quad (132)$$

(where we wrote $\omega_k = k$ for the free gluon energy and reinstated \hbar) of the noninteracting vacuum, i.e. the sum over the zero-point energies of two transverse, massless vector modes, from $\langle \mathcal{H}_{\text{YM}} \rangle$. (Recall that momentum cutoffs are imposed on integrals over the gauge-invariant U modes and therefore do not compromise (residual) gauge invariance.)

A. Hard-mode contribution

According to the strategy outlined in Sec. III A, the calculation of the trial energy density $\langle \mathcal{H}_{\text{YM}} \rangle$ given by Eq. (25) starts with integrating over the static gauge fields and the hard modes $U_{>}$. This will be done for the chromoelectric $\langle E^2 \rangle$ and -magnetic $\langle B^2 \rangle$ contributions separately. We start with the intermediate matrix element

$$\begin{aligned} \langle \langle \langle E_i^a(\vec{x}) E_j^b(\vec{y}) \rangle \rangle \rangle &= \frac{\int D\vec{A} \psi_0[\vec{A}^U] \frac{i\delta}{\delta A_i^a(\vec{x})} \frac{i\delta}{\delta A_j^b(\vec{y})} \psi_0[\vec{A}]}{\int D\vec{A} \psi[\vec{A}^U] \psi[\vec{A}]} = \delta_{ij} \delta^{ab} G^{-1}(\vec{x}, \vec{y}) \\ &\quad - \int d^3z_1 \int d^3z_2 G^{-1}(\vec{x} - \vec{z}_1) G^{-1}(\vec{y} - \vec{z}_2) \langle \langle \langle A_i^a(\vec{z}_1) A_j^b(\vec{z}_2) \rangle \rangle \rangle \end{aligned} \quad (133)$$

($E_i^a = i\delta/\delta A_i^a$, cf. App. A) for the chromoelectric 2-point function. With the expression (A21) for the gauge-field matrix element in terms of functionals $a[U]$ and $\mathcal{M}[U]$ as defined in Eq. (A14), this specializes to

$$\begin{aligned} \langle \langle \langle E^2 \rangle \rangle \rangle &:= \langle \langle \langle E_i^a(\vec{x}) E_i^a(\vec{x}) \rangle \rangle \rangle = 3(N_c^2 - 1) G^{-1}(\vec{x}, \vec{x}) \\ &\quad - \int d^3z_1 d^3z_2 G^{-1}(\vec{x} - \vec{z}_1) G^{-1}(\vec{x} - \vec{z}_2) [\mathcal{M}_{ii}^{-1aa}(\vec{z}_1, \vec{z}_2) + a_i^a(\vec{z}_1) a_i^a(\vec{z}_2)]. \end{aligned} \quad (134)$$

The expression for the chromomagnetic contribution involves 2-, 3- and 4-point functions of the gauge field. After rewriting them with $B_i^a = \varepsilon_{ijk} (\partial_j A_k^a + \frac{g}{2} f^{abc} A_j^b A_k^c)$ as well as Eqs. (A21), (A22) and (A23), the analogous result is

$$\begin{aligned} \langle\langle\langle B^2 \rangle\rangle\rangle &:= \langle\langle\langle B_i^a(\vec{x}) B_i^a(\vec{x}) \rangle\rangle\rangle = \varepsilon_{ijk} \varepsilon_{ilm} \partial_{z_{1j}} \partial_{z_{2l}} \mathcal{M}_{km}^{-1aa}(\vec{z}_1, \vec{z}_2) \Big|_{\vec{z}_i = \vec{x}} + \varepsilon_{ijk} \varepsilon_{ilm} \partial_j a_k^a \partial_l a_m^a \\ &+ g \varepsilon_{ijk} \varepsilon_{ilm} f^{abc} \left[\mathcal{M}^{-1}(\vec{x}, \vec{x})_{lm}^{bc} \partial_j a_k^a + \partial_{z_{1,j}} \mathcal{M}^{-1}(\vec{z}_1, \vec{x})_{km}^{ac} a_l^b \right. \\ &+ \left. \partial_{z_{1,j}} \mathcal{M}^{-1}(\vec{z}_1, \vec{x})_{kl}^{ab} a_m^c + \partial_j a_k^a a_l^b a_m^c \right]_{z_i \rightarrow x} \\ &+ \frac{g^2}{4} f^{abc} f^{ade} \left[12 \mathcal{M}^{-1bd} \mathcal{M}^{-1ce} + 8 \mathcal{M}^{-1bd} a_i^c a_i^e + 2 a_i^b a_j^c a_i^d a_j^e \right] \end{aligned} \quad (135)$$

(where all spacial arguments are set to \vec{x} after taking the derivatives).

The next step is the computation of the hard-mode contributions to the chromoelectric and -magnetic vacuum energies, as outlined in Sec. III A and App. A. This amounts to calculating the intermediate matrix elements (31) for E^2 and B^2 to leading order in g , i.e.

$$\langle\langle E^2, B^2 \rangle\rangle := \frac{\int D\phi [\langle\langle\langle E^2, B^2 \rangle\rangle\rangle + O(g)] \exp\{-\Gamma_{b,>}[\phi]\}}{\int D\phi \exp\{-\Gamma_{b,>}[\phi]\}}. \quad (136)$$

The hard-mode action $\Gamma_{b,>}[\phi]$ is defined in Eq. (A42). Since it is bilinear in ϕ , the integrals in Eq. (136) are Gaussian and can be calculated analytically as outlined in App. A. The results are

$$\begin{aligned} \langle\langle E^2 \rangle\rangle &= (N_c^2 - 1) \int \frac{d^3 k}{(2\pi)^3} \theta(\Lambda_{UV}^2 - k^2) G^{-1}(k) \\ &+ \frac{1}{2} (N_c^2 - 1) \int \frac{d^3 k}{(2\pi)^3} \theta(\mu^2 - k^2) G^{-1}(k) + \langle\langle E^2 \rangle\rangle_{U_<} + O(g), \end{aligned} \quad (137)$$

which includes the contribution

$$\langle\langle E^2 \rangle\rangle_{U_<} := -\frac{1}{4g^2} \int d^3 z_1 \int d^3 z_2 G_{<}^{-1}(\vec{x} - \vec{z}_1) G_{<}^{-1}(\vec{x} - \vec{z}_2) \langle\langle L_{<,i}^a(\vec{z}_1) L_{<,i}^a(\vec{z}_2) \rangle\rangle \quad (138)$$

from the soft modes $U_<$, and

$$\langle\langle B^2 \rangle\rangle = (N_c^2 - 1) \int \frac{d^3 k}{(2\pi)^3} \theta(\Lambda_{UV}^2 - k^2) k^2 G(k) + O(g). \quad (139)$$

With $\theta(k^2 - \mu^2) G(k) = \theta(k^2 - \mu^2) k^{-1}$ (cf. Eq. (11)) one thus finds the Λ_{UV} dependence of $\langle\langle E^2 \rangle\rangle$ and $\langle\langle B^2 \rangle\rangle$ to be identical. Hence the lowest-dimensional gluon condensate $\langle F^2 \rangle = 2[\langle B^2 \rangle - \langle E^2 \rangle]$ (to be discussed in Sec. VIII B) is Λ_{UV} -independent by itself while the Λ_{UV} dependence of $\langle\langle \mathcal{H}_{YM} \rangle\rangle$ has to be removed by renormalization. As noted above, at our level of approximation this simply amounts to normal-ordering the Hamiltonian, i.e. to subtracting the non-interacting vacuum expectation values $\langle E^2 \rangle_0 = \langle B^2 \rangle_0 = (N_c^2 - 1) G_{m=0}^{-1}(\vec{x}, \vec{x})$ from $\langle\langle \mathcal{H}_{YM} \rangle\rangle$. This yields

$$\langle\langle :E^2: \rangle\rangle = (N_c^2 - 1) \int \frac{d^3 k}{(2\pi)^3} \theta(\mu^2 - k^2) \left[\frac{3}{2} G^{-1}(k) - k \right] + \langle\langle E^2 \rangle\rangle_{U_<} + O(g) \quad (140)$$

and

$$\langle\langle :B^2: \rangle\rangle = (N_c^2 - 1) \int \frac{d^3 k}{(2\pi)^3} \theta(\mu^2 - k^2) [k^2 G(k) - k] + O(g). \quad (141)$$

These expressions are indeed Λ_{UV} -independent and receive only soft-mode contributions with momenta $k < \mu$. (Both properties have to become manifest already at this stage because they remain unaffected by the subsequent integration over the $U_<$.) Furthermore, the above results provide a nontrivial check of the fact that by restoring residual gauge invariance the integration over ϕ has removed the longitudinal hard-mode contributions.

B. Soft-mode contribution in the disordered phase

Our next step is to calculate the chromoelectric soft-mode contribution to the vacuum energy density. Here the impact of the generalized IR covariance (13) becomes fully nonperturbative and the dependence on the variational parameters enters through the solution of the gap equation (119). From Eq. (138) one obtains after performing the remaining part of the $U_<$ integration (cf. Eq. (33)), i.e. after integrating over Σ ,

$$\langle E^2 \rangle_{U_<} = -\frac{1}{4g^2} \int d^3 z_1 \int d^3 z_2 G_<^{-1}(\vec{x} - \vec{z}_1) G_<^{-1}(\vec{x} - \vec{z}_2) \langle L_{<,i}^a(\vec{z}_1) L_{<,i}^a(\vec{z}_2) \rangle, \quad (142)$$

In the mean-field approximation of Sec. IV B, the Σ integration amounts to evaluating $\langle\langle L_{<,i}^a(\vec{z}_1) L_{<,i}^a(\vec{z}_2) \rangle\rangle$ at the saddle-point solution $\bar{\Sigma}(\mu, c_1) = [\mu \bar{\xi}(\mu, c_1)]^2$ of the gap equation (119). Since the integrals over $G^{-1}(\vec{x} - \vec{z}_1) G^{-1}(\vec{x} - \vec{z}_2)$ in Eq. (142) have most of their support at $|\vec{z}_1 - \vec{z}_2| < \mu^{-1}$ where $U_<(\vec{z}_2) U_<^\dagger(\vec{z}_1) \simeq 1$, we will approximate

$$\langle L_{<,i}^a(\vec{z}_1) L_{<,i}^a(\vec{z}_2) \rangle = 2 \left\langle \text{tr} \left\{ \partial_i U_<^\dagger(\vec{z}_2) U_<(\vec{z}_2) U_<^\dagger(\vec{z}_1) \partial_i U_<(\vec{z}_1) \right\} \right\rangle \quad (143)$$

$$\stackrel{|\vec{z}_1 - \vec{z}_2| < \mu^{-1}}{\simeq} 2 \left\langle \text{tr} \left\{ \partial_i U_<^\dagger(\vec{z}_2) \partial_i U_<(\vec{z}_1) \right\} \right\rangle \quad (144)$$

(as in the $2U$ approximation (44) to the Lagrangian (43)). From Eq. (103) one then has

$$\langle L_{<,i}^a(\vec{z}_1) L_{<,i}^a(\vec{z}_2) \rangle \simeq 2N_c^2 \partial_{z_2,i} \left[\Delta^{-1}(\vec{z}_2 - \vec{z}_1) + \frac{c_1 \gamma}{\zeta \mu^3} \bar{\Delta}^{-1}(\vec{z}_2 - \vec{z}_1) \right] \overleftarrow{\partial}_{z_1,i} \quad (145)$$

and with Eqs. (73), (74) (specialized to $c_{n \geq 2} = 0$) and (100) further

$$\begin{aligned} \langle L_{<,i}^a(\vec{z}_1) L_{<,i}^a(\vec{z}_2) \rangle &\simeq 4N_c \pi^2 \frac{\gamma}{\zeta} \mu^2 \int \frac{d^3 \kappa}{(2\pi)^3} \kappa^2 \theta(1 - \kappa^2) e^{i\vec{\kappa}\mu(\vec{z}_2 - \vec{z}_1)} \\ &\times \left[\frac{1}{\kappa^2(1 - c_1 \kappa^2) + \xi^2} + \frac{2c_1 \gamma \zeta^{-1} \tilde{i}_2(\bar{\xi}, c_1) \kappa^2}{[\kappa^2(1 - c_1 \kappa^2) + \xi^2]^2} \right] \end{aligned} \quad (146)$$

which attains the coincidence limit

$$\langle L_{<,i}^a(\vec{z}) L_{<,i}^a(\vec{z}) \rangle \simeq 2N_c \frac{\gamma}{\zeta} \mu^2 \left[\tilde{i}_2(\bar{\xi}, c_1) + 2c_1 \frac{\gamma}{\zeta} \tilde{i}_2(\bar{\xi}, c_1) \tilde{j}_3(\bar{\xi}, c_1) \right]. \quad (147)$$

Hence Eq. (142) becomes with Eq. (13) (for $c_{i \geq 2} = 0$)

$$\begin{aligned} \langle E^2 \rangle_{U_<} &= -\frac{m_g^2}{4g^2} \int \frac{d^3 k}{(2\pi)^3} \theta(\mu^2 - \vec{k}^2) \left(1 - c_1 \frac{k^2}{\mu^2}\right) \int \frac{d^3 p}{(2\pi)^3} \theta(\mu^2 - \vec{p}^2) \left(1 - c_1 \frac{p^2}{\mu^2}\right) \\ &\times \int d^3 z_1 \int d^3 z_2 e^{i\vec{k}(\vec{x} - \vec{z}_1)} e^{i\vec{p}(\vec{x} - \vec{z}_2)} \langle L_{<,i}^a(\vec{z}_1) L_{<,i}^a(\vec{z}_2) \rangle \end{aligned} \quad (148)$$

which yields

$$\langle E^2 \rangle_{U_<} = -\frac{N_c^2 \zeta}{2\pi^2} \mu^4 \left[\tilde{i}_2 - 2c_1 \tilde{i}_3 + c_1^2 \tilde{i}_4 + 2c_1 \frac{\gamma}{\zeta} \tilde{i}_2 (\tilde{j}_3 - 2c_1 \tilde{j}_4 + c_1^2 \tilde{j}_5) \right]. \quad (149)$$

(Note that the integrals $\tilde{i}_n(\xi, c_1)$ and $\tilde{j}_n(\xi, c_1)$ receive most of their contributions from vacuum modes with momenta $k \sim \mu$ (cf. App. A).)

It will furthermore be useful to consider the $c_1 \rightarrow 0$ limit of Eq. (149). After specializing the IR mass parameter ζ to $\zeta_{\text{ct}}(c_1) := (1 - c_1)^{-1} = 1 + c_1 + O(c_1^2)$, which ensures a continuous covariance (cf. Eq. (120)), and using the small- c_1 expansions (B66), (B67) of the integrals \tilde{i}_n and \tilde{j}_n , the soft-mode contribution $\varepsilon_{U_<} = \langle E^2 \rangle_{U_<} / 2$ to the energy density becomes

$$\varepsilon_{U_<}(\mu, c_1, \zeta_{\text{ct}}; \bar{\xi}) = -\frac{N_c^2}{4\pi^2} \mu^4 \left\{ \tilde{i}_2(\bar{\xi}) + c_1 [\tilde{i}_2(\bar{\xi}) - 2\tilde{i}_3(\bar{\xi}) + \tilde{j}_4(\bar{\xi}) + 2\gamma \tilde{i}_2(\bar{\xi}) \tilde{j}_3(\bar{\xi})] \right\} + O(c_1^2) \quad (150)$$

$$\simeq -\frac{N_c^2}{4\pi^2} \mu^4 (1 + c_1) \tilde{i}_2(\bar{\xi}) \quad (151)$$

for $|c_1| \ll 1$. (The last expression provides a very reasonable approximation for $|c_1| \lesssim 0.1$.) Moreover, with $c_1 = 0$ and $m_g = \mu$ (and approximating $N_c^2 - 1 \sim N_c^2$) the above expression reduces to the result

$$\varepsilon_{U<}(\mu, c_1 = 0, \zeta = 1; \bar{\xi}) = -\frac{N_c^2}{4\pi^2} \mu^4 \tilde{\nu}_2(\bar{\xi}) = -\frac{N_c^2}{4\pi^2} \mu^4 \left[\frac{1}{3} - \bar{\xi}^2 \left(1 - \bar{\xi} \arctan \frac{1}{\bar{\xi}} \right) \right] \quad (152)$$

of Ref. [17], as it should.

C. Energy density in the disordered phase (i.e. for $\mu \ll \Lambda_{UV}$)

The remaining (normalized) integral over the auxiliary field Σ turns the matrix element $\langle\langle \mathcal{H}_{YM} \rangle\rangle$ into the trial vacuum energy density $\langle \mathcal{H}_{YM} \rangle$ (cf. Eq. (33)). This integral is nontrivial only for the $U<$ and hence ξ dependent part (138) of the integrand (137). Its evaluation in the previous section yielded Eq. (149). Combining the above results and separating the complete vacuum energy density $\varepsilon = E/V = \langle \mathcal{H}_{YM} \rangle$ into hard and soft contributions ε_{\geq} ,

$$\varepsilon(\mu, c_1, \zeta; \bar{\xi}) = \langle \mathcal{H}_{YM} \rangle = \varepsilon_{>}(\mu) + \varepsilon_{<}(\mu, c_1, \zeta; \bar{\xi}) \quad (153)$$

(with ζ still unspecified), one finds

$$\varepsilon_{>}(\mu) = \frac{1}{2} (N_c^2 - 1) \int \frac{d^3 k}{(2\pi)^3} [\theta(\Lambda_{UV}^2 - k^2) - \theta(\mu^2 - k^2)] [G_{>}^{-1}(k) + k^2 G_{>}(k)] \quad (154)$$

and

$$\varepsilon_{<}(\mu, c_1, \zeta; \bar{\xi}) = \frac{1}{2} (N^2 - 1) \int \frac{d^3 k}{(2\pi)^3} \theta(\mu^2 - k^2) \left[\frac{3}{2} G_{<}^{-1}(k) + k^2 G_{<}(k) \right] + \frac{1}{2} \langle E^2 \rangle_{U<}(\mu, c_1, \zeta; \bar{\xi}). \quad (155)$$

The energy density $\varepsilon_{>}$ of the hard modes involves only $G_{>}^{-1}(k) = k = k^2 G_{>}(k)$ and evaluates further to

$$\varepsilon_{>}(\mu) = 2 (N_c^2 - 1) \int \frac{d^3 k}{(2\pi)^3} [\theta(\Lambda_{UV}^2 - k^2) - \theta(\mu^2 - k^2)] \frac{\hbar k}{2} = \frac{N_c^2 - 1}{8\pi^2} (\Lambda_{UV}^4 - \mu^4), \quad (156)$$

which is just the (regularized) zero-point energy density of two transverse, *massless* modes with energy $\omega(k) = k$ (recall that the integration over ϕ has removed the longitudinal mode contribution) and reflects the built-in asymptotic freedom of the $k > \mu$ modes. As anticipated, the subtraction of the free vacuum energy density (132) in the course of normal-ordering cancels its Λ_{UV} dependence.

The soft-mode contribution is mainly of nonperturbative origin, on the other hand, and therefore structurally more complex. Inserting the covariance (20) and its inverse (21) (for $c_{n \geq 2} = 0$, as before, and $\zeta = m_g/\mu$) into Eq. (155) yields

$$\varepsilon_{<} = \frac{N_c^2 - 1}{4\pi^2} \left[\frac{\zeta}{2} \left(1 - \frac{3c_1}{5} \right) - \frac{1}{\zeta c_1^2} \left(1 + \frac{c_1}{3} - \frac{\operatorname{arctanh} \sqrt{c_1}}{\sqrt{c_1}} \right) \right] \mu^4 + \frac{\langle E^2 \rangle_{U<}}{2}, \quad (157)$$

so that the total energy density (153), after dropping the constant zero-point contribution $(N_c^2 - 1) \Lambda_{UV}^4 / (8\pi^2)$, becomes

$$\varepsilon = \frac{N_c^2 - 1}{4\pi^2} \frac{\mu^4}{\zeta c_1^2} \left[-\frac{3(3\zeta c_1 - 5\zeta + 5)\zeta c_1^2 + 10c_1 + 30}{30} + \frac{\operatorname{arctanh} \sqrt{c_1}}{\sqrt{c_1}} \right] + \frac{\langle E^2 \rangle_{U<}}{2}. \quad (158)$$

After further approximating $N_c^2 - 1 \simeq N_c^2$, ensuring the continuity of $G_{<}(k)$ by imposing Eq. (120) and using Eq. (149), we obtain our final expression for the energy density in the disordered phase,

$$\begin{aligned} \bar{\varepsilon}(\mu, c_1) &:= \varepsilon(\mu, c_1, \zeta_{\text{ct}}(c_1); \bar{\xi}(\mu, c_1)) \\ &= -\frac{N_c^2}{4\pi^2} \mu^4 \left[\frac{4c_1^3 + 10c_1^2 - 50c_1 + 30}{30c_1^2(1-c_1)} - \frac{1-c_1}{c_1^2} \frac{\operatorname{arctanh} \sqrt{c_1}}{\sqrt{c_1}} \right. \\ &\quad \left. + \frac{\tilde{\nu}_2 - 2c_1\tilde{\nu}_3 + c_1^2\tilde{\nu}_4 + 2\gamma c_1(1-c_1)\tilde{\nu}_2(\tilde{j}_3 - 2c_1\tilde{j}_4 + c_1^2\tilde{j}_5)}{1-c_1} \right], \end{aligned} \quad (159)$$

where the integrals \tilde{i}_n, \tilde{j}_n are evaluated at $\bar{\xi}(\mu, c_1)$. For $c_1 \rightarrow 1$ several terms of the energy density (159) diverge and prevent the vacuum from encountering the limiting instability. For $|c_1| \ll 1$, on the other hand, the rather complex c_1 dependence of the full vacuum energy density (159) simplifies to

$$\bar{\varepsilon}(\mu, c_1) = \frac{N_c^2}{4\pi^2} \mu^4 \left\{ \frac{1}{5} - \tilde{i}_2(\bar{\xi}) - \left[\frac{1}{7} + \tilde{i}_4(\bar{\xi}) - 2\tilde{i}_3(\bar{\xi}) + 2\gamma\tilde{i}_2(\bar{\xi}) \tilde{j}_3(\bar{\xi}) \right] c_1 \right\} + O(c_1^2) \quad (160)$$

(where γ and the solution $\bar{\xi}$ of the gap equation are evaluated at $c_1 = 0$). For $c_1 = 0$ and $\zeta = 1$, finally, it reduces as expected to the energy density of Ref. [17],

$$\varepsilon(\mu, c_1 = 0, \zeta = 1; \bar{\xi}(\mu, c_1 = 0)) = \frac{N_c^2}{4\pi^2} \mu^4 \left[-\frac{2}{15} + \bar{\xi}^2 \left(1 - \bar{\xi} \arctan \frac{1}{\bar{\xi}} \right) \right]. \quad (161)$$

The full energy density (159) is plotted in Fig. 4 and will be discussed further in Sec. VIII A.

D. Energy density in the ordered phase (i.e. for $\mu \gg \Lambda_{\text{YM}}$)

The mean-field approximation (63) is reliable in the disordered phase, i.e. for those $\mu < \mu_c \leq 8.86\Lambda_{\text{YM}}$ (cf. Eq. 127) for which $\bar{\xi}$ is not too small. In order to get a more complete picture of the μ dependence of the vacuum energy density, however, one has to evaluate the soft-mode contributions in the ordered phase as well, i.e. for $\mu \gg \Lambda_{\text{YM}}$. While the mean-field approximation breaks down in this phase, the Yang-Mills coupling becomes small [69], i.e.

$$g^2(\mu \gg \Lambda_{\text{YM}}) \ll 1, \quad (162)$$

so that the soft-mode dynamics can instead be treated perturbatively. In accordance with our previous approximation scheme, we restrict ourselves further to the $2U$ contributions to Eqs. (42) and (44) with $c_{i \geq 2} = 0$, which yields the soft-mode action

$$\Gamma_{<}^{(2U)}[U_{<}] = -\frac{m_g}{2g^2} \int d^3z \text{tr} \left\{ U_{<}^\dagger \left(\partial^2 + \frac{c_1}{\mu^2} \partial^4 \right) U_{<} \right\}. \quad (163)$$

Since in the ordered phase fluctuations $\varphi_{<}^a$ around $U_{<} \sim 1$ are small, one can furthermore truncate the weak-coupling expansion of their exponential map, i.e.

$$U_{<} = \exp(ig\varphi_{<}^a \lambda^a) = 1 + ig\varphi_{<}^a \lambda^a + O(g^2), \quad (164)$$

which yields to $O(g^2)$ (with $\text{tr} \{ \lambda^a \lambda^b \} = 2\delta^{ab}$ and denoting the Fourier transform of φ as $\tilde{\varphi}$) the bilinear action

$$\Gamma_{<}^{(2U)}[\varphi_{<}] = \frac{1}{2} \int \frac{d^3k}{(2\pi)^3} \left[\tilde{\varphi}_{<}^a(-\vec{k}) 2m_g \left(k^2 - \frac{c_1}{\mu^2} k^4 \right) \tilde{\varphi}_{<}^a(\vec{k}) + \dots \right]. \quad (165)$$

From this ‘‘kinetic’’ term one reads off the $k < \mu$ propagator of the φ modes (which contains, in contrast to the soft-mode propagator (73), (74) in the disordered phase, no mass term) as

$$\langle \varphi_{<}^a(\vec{z}_1) \varphi_{<}^b(\vec{z}_2) \rangle = \frac{\delta^{ab}}{2m_g} \int \frac{d^3k}{(2\pi)^3} \theta(\mu^2 - k^2) \frac{e^{-i\vec{k}(\vec{z}_1 - \vec{z}_2)}}{k^2 - \frac{c_1}{\mu^2} k^4}. \quad (166)$$

Then the correlator (143), which determines the chromoelectric vacuum energy density due to the soft modes, becomes (with $\delta^{aa} = N_c^2 - 1$)

$$\langle L_{<,i}^a(\vec{z}_1) L_{<,i}^a(\vec{z}_2) \rangle \simeq 2 \left\langle \text{tr} \left\{ \partial_i U_{<}^\dagger(\vec{z}_1) \partial_i U_{<}(\vec{z}_2) \right\} \right\rangle \simeq 4g^2 \langle \partial_i \varphi_{<}^a(\vec{z}_1) \partial_i \varphi_{<}^a(\vec{z}_2) \rangle \quad (167)$$

$$= 2(N_c^2 - 1) \frac{g^2 \mu^2}{\zeta} \int \frac{d^3\kappa}{(2\pi)^3} \frac{\theta(1 - \kappa^2)}{1 - c_1 \kappa^2} e^{-i\mu\vec{\kappa}(\vec{z}_1 - \vec{z}_2)}. \quad (168)$$

After inserting this result into Eq. (148) one has

$$\langle E^2 \rangle_{U_{<}} = -(N_c^2 - 1) \frac{\zeta \mu^4}{2} \int \frac{d^3\kappa}{(2\pi)^3} \theta(1 - \kappa^2) (1 - c_1 \kappa^2) \quad (169)$$

$$= -\frac{N_c^2 - 1}{4\pi^2} \zeta \mu^4 \left(\frac{1}{3} - \frac{1}{5} c_1 \right) \quad (170)$$

and hence Eq. (157) yields the infrared contributions

$$\varepsilon_{<} = \frac{N_c^2 - 1}{4\pi^2} \frac{\mu^4}{\zeta c_1^2} \left(\frac{-3\zeta^2 c_1^3 + 5\zeta^2 c_1^2 - 5c_1 - 15}{15} + \frac{\operatorname{arctanh} \sqrt{c_1}}{\sqrt{c_1}} \right) \quad (171)$$

to the energy density which specialize with $\zeta_{\text{ct}}(c_1) = (1 - c_1)^{-1}$ to

$$\varepsilon_{<} = \frac{N_c^2 - 1}{4\pi^2} \mu^4 \frac{1 - c_1}{c_1^2} \left[\frac{-8c_1^3 + 25c_1 - 15}{15(1 - c_1)^2} + \frac{\operatorname{arctanh} \sqrt{c_1}}{\sqrt{c_1}} \right]. \quad (172)$$

Together with the hard-mode contribution (156) (which is identical in both vacuum phases) and after discarding the zero-point contribution, finally, the total vacuum energy density in the ordered phase becomes

$$\varepsilon(\mu, c_1) = \frac{N_c^2 - 1}{4\pi^2} \mu^4 \frac{1 - c_1}{c_1^2} \left[-\frac{c_1^3 + 15c_1^2 - 50c_1 + 30}{30(1 - c_1)^2} + \frac{\operatorname{arctanh} \sqrt{c_1}}{\sqrt{c_1}} \right] \quad (173)$$

$$= \frac{N_c^2 - 1}{4\pi^2} \mu^4 \left[\frac{1}{30} + \frac{8}{105} c_1 + \frac{32}{315} c_1^2 + O(c_1^3) \right]. \quad (174)$$

Several properties of Eq. (173) are noteworthy. First of all, in the $c_1 \rightarrow 0$ limit it reduces, as expected, to the result of Ref. [17] (cf. their Eq. (4.24)),

$$\varepsilon(\mu, c_1 = 0) = \frac{N_c^2 - 1}{120\pi^2} \mu^4. \quad (175)$$

Furthermore, the total energy density diverges for $c_1 \rightarrow 1$ where the vacuum wave functionals would become unnormalizable, thus preventing that c_1 grows to $c_1 \geq 1$ during energy minimization. Most importantly, however, for $\mu \gg \Lambda_{\text{YM}}$ the negative contribution (156) of the hard modes to the energy density is overcome by the positive one (172) from the soft modes. Indeed, the (large μ) vacuum energy density (173) is positive for all $c_1 < 1$ and thus a monotonically *increasing* function of μ . In addition, Eq. (173) increases monotonically with c_1 in the range $-2 < c_1 < 1$ which includes those $|c_1| \ll 1$ values for which our perturbative $O(c_1)$ treatment is reliable (and thus our result $c_1^* \simeq 0.15$ to be variationally determined in Sec. VIII A). Under these circumstances it is reasonable to expect that the perturbative result (173) remains at least qualitatively reliable for μ values down to the phase transition [17] at $\mu_c \lesssim 8.86\Lambda_{\text{YM}}$.

VIII. VARIATIONAL ANALYSIS

We are now prepared to variationally minimize the vacuum energy density in the trial-state family (1) according to the Rayleigh-Ritz procedure. Above we have found that (inside the validity range of our approximations) the energy density (159) in the strongly-coupled disordered phase monotonically decreases with increasing μ up to the phase transition, whereas its counterpart (173) in the ordered weak-coupling phase monotonically increases both with μ and c_1 . The combination of these results indicates that the vacuum energy density attains its minimum at the phase transition in the disordered phase, where the number of massless particles becomes maximal. Indeed, the number $N_c^2 - 1$ of massless Goldstone modes in the ordered phase (at very large μ all other modes have $m \sim \Lambda_{\text{UV}}$ and are too massive to contribute significantly) doubles at the transition where they are joined by degenerate parity partners. Hence the massless particles generate roughly twice the internal energy at the second-order transition, which therefore has a maximum at the critical μ_c^* [17]. (This argument is not affected by the higher-gradient interactions (43) since those share the symmetries of the leading term (42).)

Hence our program in the following subsections will be as follows: after finding the energy minimum at the transition in the disordered phase quantitatively in Sec. VIII A, we evaluate the associated, four-dimensional gluon condensate in Sec. VIII B. We then discuss the resulting vacuum field distribution and its physical interpretation in Sec. VIII C, and its impact on the phase structure of the soft-mode dynamics in Sec. VIII D. In Sec. VIII E we comment on the qualitative impact of the higher-gradient interactions in the soft-mode Lagrangian (43). Finally, in Sec. VIII F, we mention several options for improvements and further applications of the gauge-invariant variational framework.

A. Vacuum energy minimization

The energy density (159) in the disordered vacuum phase is plotted in Fig. 4 as a function of μ and c_1 (on the basis of the numerical solution of the gap equation, cf. Fig. 2). The plot range includes those regions in which (i) the

one-loop evaluation of the hard-mode contributions remains reasonably accurate (i.e. roughly for $\mu \geq 4\Lambda_{\text{YM}}$), (ii) the system stays in the disordered phase and (iii) the mean-field approximation remains approximately valid, i.e. where nontrivial solutions $\bar{\xi}$ of the gap equation exist. Together with Eq. (127) this implies

$$4\Lambda_{\text{YM}} \lesssim \mu \leq \mu_c^{(\text{max})} = \mu_c(c_1 = 0) \simeq 8.86\Lambda_{\text{YM}}. \quad (176)$$

For illustrative purposes the plot range of c_1 is chosen to cover almost the full existence range $-0.48 \lesssim c_1 \lesssim 0.95$ of gap-equation solutions, on the other hand, although our perturbative treatment of the $4U$ interactions becomes questionable close to the upper limit.

The arguably most prominent qualitative feature of the vacuum energy density $\bar{\varepsilon}(\mu, c_1)$ is its monotonic decrease with both μ and c_1 in the disordered phase, i.e. until the nontrivial solution of the gap equation ceases to exist at the second-order phase transition (cf. Fig. 4). This essential feature manifests itself already in the linearization (160) of the c_1 dependence around $c_1 = 0$. As a consequence, the energy of the disordered vacuum is minimized at $\bar{\xi} = 0_+$, i.e. at the disorder-order phase transition, for each admissible value of c_1 . In order to find the minimum of $\bar{\varepsilon}$ and the corresponding parameter values μ^* and c_1^* quantitatively, we plot the energy density along the critical line, i.e.

$$\bar{\varepsilon}(c_1) := \bar{\varepsilon}(\mu_c(c_1), c_1), \quad (177)$$

in the range $c_1 \in [-0.48, 1]$ where $\bar{\xi}(\mu_c(c_1), c_1) = 0$. As can be read off from Fig. 5, the minimum of $\bar{\varepsilon}$ in the disordered phase is attained at

$$c_1^* \simeq 0.15 \quad \text{with} \quad \mu^* = \mu_c(c_1^*) = 8.61\Lambda_{\text{YM}}. \quad (178)$$

Evaluating $\alpha_{\text{YM}}(\mu^*) = g_{\text{YM}}^2(\mu^*) / (4\pi) \simeq 0.27$ (to one loop) at this scale confirms that the running coupling is small enough to justify the perturbative treatment of the hard modes. (It exceeds the value $\alpha_{\text{YM}}(\mu_c(c_1 = 0)) \simeq 0.26$ by less than 2%.) Similarly, the resulting $c_1^* \ll 1$ justifies our perturbative treatment of the $4U$ contributions in Secs. VA and VII D. The rather small curvature of the critical line (126) around its maximum

$$\mu_c^{(\text{max})} = \mu_c(c_1 = 0) = \exp\left(\frac{24}{11}\right) \simeq 8.86\Lambda_{\text{YM}} \quad (179)$$

at $c_1 = 0$ furthermore causes our dynamical IR mass scale $\mu^* \simeq 8.6\Lambda_{\text{YM}}$ to be only about 3% smaller than $\mu_c^{(\text{max})}$. This has important consequences for the value of the gluon condensate to be discussed in Sec. VIII B and for other vacuum scales. The corresponding IR gluon mass, e.g., turns out to be

$$m_g^* = \frac{\mu_c(c_1^*)}{1 - c_1^*} \simeq 10.14\Lambda_{\text{YM}}. \quad (180)$$

(For $\Lambda_{\text{YM}} \simeq 0.15$ GeV [17] this value is somewhat larger than the potentially related mass $m_{\text{LG}} \sim 1.1$ GeV extracted from the intermediate-momentum behavior of the Landau-gauge gluon propagator on the lattice (second reference in [33]).)

The quantitative improvement of the vacuum description due to our generalized trial functional basis can be measured in terms of the achieved reduction of the variational bound on the Yang-Mills vacuum energy density. Comparing the minimum of our trial energy density (159),

$$\bar{\varepsilon}(c_1^*) \simeq -210.59\Lambda_{\text{YM}}^4, \quad (181)$$

to the value $\bar{\varepsilon}(c_1 = 0) \simeq -187.52\Lambda_{\text{YM}}^4$ (associated with the simplest IR covariance $G_{<}^{-1}(k) = \mu$) shows that the finite- c_1 correction lowers the vacuum energy density by about 11%. Hence the variational optimization in our extended trial space has produced a rather substantial improvement of the vacuum functional. (In contrast, the massive gluon propagator (24) is energetically disfavored: its IR behavior is approximately reproduced by $c_1 = -1/2$ and yields $\bar{\varepsilon}(c_1 = -1/2) \simeq 0$. We expect sizeable corrections to the $O(c_1)$ treatment of the $4U$ interactions for $c_1 = -1/2$, though, and further note that Eq. (24) does not match to the UV covariance (11) at $k = \mu$, in contrast to our IR covariance.)

B. Gluon condensate

Gluon condensates, i.e. the vacuum expectation values of gauge-invariant local operators composed of gluon fields, are among the key amplitudes which characterize the Yang-Mills ground state. The most important gluon condensate,

which dominates the operator product expansion e.g. of the glueball correlators [45], is the expectation value of the lowest-, i.e. four-dimensional operator $F^2 \equiv F_{\mu\nu}^a F^{a,\mu\nu} = -2(E_i^a E_i^a - B_i^a B_i^a)$. In our trial state, and to lowest order in the gauge coupling, this condensate becomes

$$\langle F^2 \rangle = 2 [\langle B^2 \rangle - \langle E^2 \rangle] \quad (182)$$

$$\begin{aligned} &= 2(N_c^2 - 1) \int \frac{d^3k}{(2\pi)^3} \theta(k^2 - \Lambda_{\text{UV}}^2) \left[k^2 G(k) - \frac{3}{2} G^{-1}(k) \right] \\ &+ (N_c^2 - 1) \int \frac{d^3k}{(2\pi)^3} [\theta(k^2 - \Lambda_{\text{UV}}^2) - \theta(k^2 - \mu^2)] G^{-1}(k) - 2 \langle E^2 \rangle_{U<} \end{aligned} \quad (183)$$

where we used Eqs. (137) – (139) and again performed the Σ integrals in the saddle-point approximation. As anticipated above, specializing to the asymptotically free UV covariance (11), i.e. $G_{>}^{-1}(k) = k$, results in the cancellation of the hard-mode contributions and indicates that the gluon condensate (183) is renormalized at μ . After inserting the IR covariance (20) and the propagator (21) (with $c_{n \geq 2} = 0$, as before) one further obtains

$$\langle F^2 \rangle = 2(N_c^2 - 1) \int \frac{d^3k}{(2\pi)^3} \theta(k^2 - \mu^2) \left[k^2 G_{<}(k) - \frac{3}{2} G_{<}^{-1}(k) \right] - 2 \langle E^2 \rangle_{U<} \quad (184)$$

$$= -\frac{N_c^2 - 1}{\pi^2} \frac{\mu^4}{\zeta c_1^2} \left[1 + \frac{c_1}{3} + \frac{1}{2} \zeta^2 c_1^2 \left(1 - \frac{3}{5} c_1 \right) - \frac{\text{arctanh} \sqrt{c_1}}{\sqrt{c_1}} \right] - 2 \langle E^2 \rangle_{U<}. \quad (185)$$

At the border of the disordered phase, where $\bar{\xi}(\mu_c(c_1), c_1) = 0$ and where the energy becomes minimal (cf. Sec. VIII A), we furthermore have from Eq. (149) in the $\xi \rightarrow 0$ limit, and with the expressions for the integrals $\tilde{i}_n(0, c_1)$ and $\tilde{j}_n(0, c_1)$ given in App. B 2,

$$\langle E^2 \rangle_{U<}(\mu_c(c_1), \bar{\xi}(\mu_c(c_1), c_1) = 0) = -\frac{(N_c^2 - 1)\zeta}{2\pi^2} \mu^4 \left[\frac{1}{3} - \frac{c_1}{5} - \frac{2\gamma}{3\zeta} \left(1 - \frac{\text{arctanh} \sqrt{c_1}}{\sqrt{c_1}} \right) \right]. \quad (186)$$

By combining the above results and specializing to $\zeta_{\text{ct}} = (1 - c_1)^{-1}$ and $\gamma^* = g^2(\mu^*) N_c / \pi^2 \simeq 1.012$ we obtain our final expression for the gluon condensate,

$$\langle F^2 \rangle = -\frac{N_c^2 - 1}{\pi^2} \mu^4 \left[\frac{7c_1^3 - 20\gamma^* c_1^3 + 15c_1^2 + 20\gamma^* c_1^2 - 50c_1 + 30}{30c_1^2(1 - c_1)} - \left(\frac{1 - c_1}{c_1^2} + \frac{2\gamma^*}{3} \right) \frac{\text{arctanh} \sqrt{c_1}}{\sqrt{c_1}} \right]. \quad (187)$$

For small c_1 Eq. (187) expands into powers of c_1 as

$$\langle F^2 \rangle = \frac{N_c^2 - 1}{\pi^2} \mu^4 \left[\frac{1}{30} - \left(\frac{13}{105} - \frac{2}{9} \gamma^* \right) c_1 + O(c_1^2) \right], \quad (188)$$

which shows that $\langle F^2 \rangle$ grows with c_1 when $c_1 \ll 1$. In the uncorrected case, with $c_1 = 0$ and the corresponding value $\alpha_{\text{YM}}(\mu_c(c_1 = 0)) / \pi = 1 / (4N_c)$ (cf. Eq. (101)) or $\gamma^*(\mu_c(c_c = 0)) = 1$ for the gauge coupling as well as Eq. (179) for the IR scale, and furthermore setting $N_c^2 - 1 \sim N_c^2$, $N_c = 3$, one finds [17]

$$\left\langle \frac{\alpha}{\pi} F^2 \right\rangle^{(\text{KK})} = \frac{N_c}{120\pi^2} \mu_c^4(c_c = 0) \simeq 15.62 \Lambda_{\text{YM}}^4. \quad (189)$$

Our improved value of the gluon condensate, on the other hand, is obtained by inserting the energy minimizing values $c_1^* \simeq 0.151$ and $\mu^* = 8.606 \Lambda_{\text{YM}}$ (cf. Eq. (178)) from the last section and the corresponding coupling $\gamma^* \simeq 1.012$. The result

$$\left\langle \frac{\alpha}{\pi} F^2 \right\rangle = 20.87 \Lambda_{\text{YM}}^4 \simeq 0.011 \text{ GeV}^4 \quad (190)$$

is about 25% larger than the uncorrected value (189). In the second equation above we have specialized to $\Lambda_{\text{YM}} \simeq 0.15$ GeV, which allows for comparison with the value range $\langle (\alpha/\pi) F^2 \rangle = 0.0080 - 0.024 \text{ GeV}^4$ for the gluon condensate obtained from QCD sum rules (for references see Ref. [45]). (We refrain from using the currently preferred value for Λ_{QCD} which contains quark contributions.) Our condensate value prediction (190) lies comfortably within this standard range.

C. Vacuum field distribution and quasigluon velocity

Our variationally optimized wave functional determines the distribution of the gauge-field modes $A_i(k)$ and thus contains new information about the field composition in the vacuum state. In our approximation, the IR covariance (20) with $c_{n \geq 2} = 0$ and Eq. (23) takes the form

$$G_{<}^{-1}(k) = \frac{\mu}{1-c_1} \left(1 - c_1 \frac{k^2}{\mu^2}\right) \theta(\mu^2 - k^2). \quad (191)$$

By construction, the covariance (191) is non-negative in the physical parameter range $\mu > 0$, $c_1 < 1$ and thus yields a normalizable wave functional. In addition, $G_{<}^{-1}(k)$ becomes larger (smaller) for positive (negative) values of c_1 . This holds for each $k < \mu$ independently, but becomes more pronounced for smaller k (cf. Fig. 1). Hence the Gaussian weight factors

$$\exp \left[- (2\pi)^{-3} d^3 k G_{<}^{-1}(k) A^2(k) / 2 \right], \quad (192)$$

which make up the IR part $\psi_{0,<}^{(G)}$ of the unprojected core functional (10) when multiplied for all $k < \mu$, become narrower (wider) in Fourier-mode space [70]. As a consequence, large $A_i^a(k)$ contributions to the IR part (10) of the unnormalized Gaussian vacuum wave functional, and thus to the functional integrands of any amplitude, are increasingly suppressed (enhanced) towards smaller $k \in [0, \mu]$.

Hence our positive variational result $c_1^* = 0.15$ indicates specifically how the vacuum field population is reshaped: relative to the uncorrected case $c_1 \equiv 0$ the attractive IR interactions generate a depletion of the ultralong-wavelength modes with $k \rightarrow 0$ and an enhancement of the $k \sim \mu$ modes. This effect helps to prevent the Savvidy instability which constant chromomagnetic fields experience in the Yang-Mills vacuum [46]. It also contributes to generating the expected average wavelength

$$\lambda \sim \Lambda_{\text{YM}}^{-1} \quad (193)$$

of the vacuum fields. In contrast, the massive vector covariance (24) with $c_1 = -1/2$ would populate the medium-soft modes with $k \lesssim \mu$ less (cf. Fig. 1), which is energetically disfavored. (When comparing the overall weight of the $k < \mu$ modes associated with different covariances, the G^{-1} dependent normalization factor \mathcal{N}_G has to be taken into account as well.) Since the higher-derivative interactions of the soft-mode dynamics (43) do not affect the $k = 0$ modes, the above findings underline the dominance of the finite-momentum IR modes in shaping the vacuum structure.

Regarding Eq. (191) as the dispersion relation $\omega(k)$ of “quasigluon” modes in the vacuum, furthermore, one may relate the parameter c_1 to the dimensionless quasigluon velocity

$$\vec{v}(\vec{k}) = \frac{\partial G_{<}^{-1}(\vec{k})}{\partial \vec{k}} = -2c_1 \frac{m_g}{\mu} \frac{\vec{k}}{\mu} \xrightarrow{m_g = \mu(1-c_1)^{-1}} -\frac{2c_1}{1-c_1} \frac{\vec{k}}{\mu}, \quad (194)$$

i.e. to the group velocity of wave packets which will generally broaden over time in the dispersive vacuum medium. Since our approximate dispersion relation (191) is quadratic in the momentum, one may further define a (momentum-independent) effective kinetic gluon mass

$$\overline{m}_g = -\frac{\mu^2}{2c_1 m_g} = -\frac{1-c_1}{2c_1} \mu. \quad (195)$$

which relates the velocity to the momentum as $\vec{k} = \overline{m}_g \vec{v}$. Note that \overline{m}_g is negative for $0 > c_1 > 1$. In any case, with $v(k) := \left| \vec{v}(\vec{k}) \right|$ one has

$$|c_1| = \frac{\mu}{2m_g} v(\mu) \quad (196)$$

which shows that c_1 is related to the quasigluon group velocity at the IR renormalization point $k = \mu$. Specializing to a continuous covariance by identifying $\mu/m_g = 1 - c_1$ then yields

$$|c_1| = \frac{v(\mu)}{v(\mu) + 2}. \quad (197)$$

This relation implies among other things that the velocity diverges toward the bound $c_1 \rightarrow 1$, and that the admissible velocity range is restricted to $\infty > v(\mu) = 2|c_1|/(1 - c_1) \geq -2$. For our result $c_1^* = 0.15$ one has $v^* := v(\mu^*) = 0.35$.

The positive sign of c_1^* further implies that the effective *kinetic* mass (195) is negative, i.e. that the quasigluon velocity is opposite to its momentum. Hence quasigluons in the vacuum decelerate when an external force is applied, in stark contrast to the behavior of free gluons. (An interesting and related issue is the vacuum response to external electric and magnetic background fields, cf. e.g. Ref. [26].) In this respect our IR dispersion relation is reminiscent of optical phonon branches in periodic structures over a Brillouin zone, or of the dispersion of electrons moving in such structures. In the latter case, for example, the effect is generated by the lattice exerting a large retarding force on the electron that counteracts and overcomes the applied force. Of course, in our aperiodic momentum space no Bloch-type oscillations are generated by color-electric external fields. However, quasigluons (with their small scattering amplitudes) or quarks could show a negative differential resistance. On a cautionary note, however, one should keep in mind that not all properties of the gauge-variant core wave functional (3) play a physical role (cf. Sec. IIB and Ref. [20]).

D. Phase structure and transition order

It is instructive to analyze some additional features of the $c_1 \neq 0$ interactions which have direct impact both on the phase structure of the soft-mode dynamics (42), (43) and on the vacuum energy minimum. To begin with, we recall that the vacuum instability for $c_1 \geq 1$ is encoded in $c_1 \rightarrow 1$ singularities of its energy density and in zeros of the amplitude entering the gap equation. Hence the constraint $c_1 < 1$ does not have to be imposed by hand but is automatically enforced by the diverging vacuum energy density and by the nontrivial saddle-point solution ceasing to exist. Since the energy density (159) decreases monotonically with μ , furthermore, its variational minimization could drive μ far below the validity range of the perturbative integration over the hard modes (cf. Sec. VII A), were it not stopped at μ^* by the vanishing of the gap-equation solution $\bar{\xi}(\mu, c_1)$, i.e. by the order-disorder phase transition. This behavior generalizes to the c_1 dependence. Indeed, although the energy density (159) monotonically decreases with c_1 as well (cf. Fig. 4), the eventual vanishing of $\bar{\xi}$ prevents the variational solution to attain c_1 values too close to unity where our $O(c_1)$ treatment of the $4U$ interactions would break down. Hence the bounded existence range of $\bar{\xi}(\mu, c_1) > 0$ solutions, inside the critical line of Fig. 3, is indispensable both for our approximations to remain valid and for the quantitatively reasonable size prediction (190) of the gluon condensate and other vacuum scales to emerge.

Another issue meriting discussion is the order of the transition between the strongly- and weakly-coupled vacuum phases. Above we found the (dis)order parameter $\bar{\xi}$ to vanish continuously at the phase boundary, which indicates a second-order transition. The same order was encountered in the Ref. [17], although lattice simulations predict a first-order transition [42]. In Ref. [17] this mismatch was argued to be a shortcoming of the mean-field approximation (which in any case breaks down close to the transition). Nevertheless, one may wonder whether the mean-field approximation could generate a first-order transition when the higher-derivative interactions corresponding to $c_n \neq 0$ are taken into account. One could imagine, for example, that the lowest-energy gap-equation solution $\bar{\xi} > 0$ may cease to exist for increasing μ and/or that a competing solution $\bar{\xi} \simeq 0$ may become energetically favorable before any of them vanishes. This raises the question whether more than one solution of the gap equation (119) could exist. In principle, this is indeed possible, and an example can be constructed by treating the dominant $2U$ part of the $c_1 \neq 0$ interactions perturbatively to $O(c_1)$, instead of resumming it as we did in Eq. (74). In this case two solution branches of the gap equation would indeed emerge. One of them is not continuous in the $c_1 = 0$ limit, though, and the energy competition with the other one turns out to be unable to generate a first-order transition. In our case such scenarios are excluded from the outset, furthermore, since the nontrivial solution of our gap-equation is unique.

E. Impact of the higher-gradient corrections

From Sec. V onward, we have restricted our practical calculations to contributions from the dominant higher-gradient interactions, associated with the low-momentum coupling c_1 . Hence a few comments on the impact of the subleading higher-gradient corrections (associated with the couplings $c_{n \geq 2}$ in the soft-mode Lagrangian (43)) may be useful. All c_n dependence originates from the expansion (13) of the infrared covariance. Through the generating functional (45), it then enters the soft-mode matrix elements (e.g. Eq. (103)) and thereby any amplitude, both in terms of the propagators Δ^{-1} and $\bar{\Delta}^{-1}$ (cf. Eqs. (73) and (100)) and by virtue of the factors which originate from the perturbative expansion (58) of the $4U$ contributions. In order to take the contributions from the $2(n+1)$ gradient interactions with $n \geq 2$ into account, one therefore has (i) to include the explicit c_n dependence from Eq. (20) in the expressions for the chromo-electric (137) and -magnetic (139) expectation values, (ii) to continue the expansion of the

$4U$ contributions (58) to higher c_n , and (iii) to generalize the integrals (B1) and (B2) in the soft-mode contributions to

$$\tilde{\eta}_n(\xi, c_1, c_2, c_3, \dots) := \int_0^1 \frac{\kappa^{2n}}{\kappa^2(1 - c_1\kappa^2 + c_2\kappa^4 - c_3\kappa^6 + \dots) + \xi^2} d\kappa \quad n \geq 1, \quad (198)$$

$$\tilde{j}_n(\xi, c_1, c_2, c_3, \dots) := \int_0^1 \frac{\kappa^{2n}}{[\kappa^2(1 - c_1\kappa^2 + c_2\kappa^4 - c_3\kappa^6 + \dots) + \xi^2]^2} d\kappa \quad n \geq 1, \quad (199)$$

which summarize the c_n contributions to the $2U$ interactions. (The monotonicity properties of the integrals (198), (199) are straightforward generalizations of those discussed in App. B.)

In Eqs. (198) and (199) the low-momentum constants c_n appear multiplied by $2n$ powers of the dimensionless momentum $\kappa \in [0, 1]$. This provides the basis for a consistent power counting. Indeed, the contributions from larger n are systematically suppressed and at least parametrically dominated by the four-derivative interactions associated with c_1 . Since the c_n are furthermore bounded by the normalizability constraints (22) and since our optimal value $c_1^* \simeq 0.15$ already keeps the dominant contribution rather small, one may expect that a variational treatment of the $c_{n \geq 2}$ contributions would result in even substantially smaller corrections. (Vacuum energy, gluon condensate and other matrix elements could then be estimated by expanding the integrals (198) and (199) around $c_{n \geq 2} = 0$, incidentally, with the expansion coefficients determined by the integrals of App. B.) With the above considerations in mind, we have not pursued the quantitative evaluation of $c_{n \geq 2}$ contributions in this paper, although our framework is fully equipped to take them into account. Another reason for neglecting these corrections was that their inclusion would reduce the transparency of our explorative study. (The full visualization of the vacuum energy density and its minimum in Fig. 4, e.g., is possible only for $c_{n \geq 2} = 0$.)

F. Further physical implications and applications

We conclude our analysis by briefly reviewing several additional features of the resulting vacuum description. To begin with the UV physics, we note that the one-loop Yang-Mills β function can be recovered almost completely from the dynamics implemented in the UV covariance (11) (up to a missing 6% correction due to color screening [34]). As already mentioned, the screening contribution may be accounted for as well, by generalizing the tensor structure of the UV covariance [18]. (Perturbation theory (even to higher orders of the gauge coupling) could be set up directly in the Rayleigh-Schrödinger representation (familiar from quantum mechanics), incidentally, since the wave-functional basis (1) renders Gauss' law manifest.

Turning to the IR physics content, we start by emphasizing that dimensional transmutation emerges naturally [18] from gauge-invariant wave functionals (1) with Gaussian cores (3), and that it generates both the infrared mass scale and the crucial mass gap dynamically [17]. In fact, since a Gaussian becomes the exact ground state of both massless and massive vector fields in the non-interacting limit, one may expect it to yield an adequate description whenever the main net effect of the interactions is to create a quasi-particle-like selfenergy. Similarly, it was argued in Ref. [17] that the Gaussian approximation should provide a reasonable description of Yang-Mills vacuum physics as long as the latter is dominated by a single gluon condensate (which QCD sum-rule analyses especially in the glueball sector suggest [45, 47]).

An important advantage of the gauge-projected wave functionals (1) is that they incorporate the nontrivial topology of the gauge group and thereby of the gauge fields. In particular, they contain instanton effects [21, 22] which play an especially important role in the spin-0 glueball sector [35, 45, 49] and emerge even in basic holographic duals for Yang-Mills theory [50]. Furthermore, the functional (1) comprises large classes of additional, gauge-invariant IR degrees of freedom which are often of topological origin as well [21]. Those are typically collective excitations gathered by gauge orbits of vacuum fields which were found to dominate the saddle-point expansion of the generating soft-mode functional (45) and to provide gauge-invariant physical interpretations e.g. for merons and Faddeev-Niemi knots [21, 23].

Another crucial consequence of the infrared field population in the Yang-Mills vacuum, confinement, is characterized by the emergence of a linear potential between sufficiently far separated, static quark sources. Despite the rather direct access to the interquark potential provided in the Schrödinger representation [18, 20] and heuristic arguments given in Refs. [17, 18, 20], however, it remains to be shown that gauge-averaged wave functionals (1) with a Gaussian core of the type (3) are capable of generating the confinement-induced area law for large, spacelike Wilson loops. (The behavior of the adjoint Wilson loop would be of interest as well.) Explorations of this crucial issue in Coulomb gauge encouragingly found a Gaussian wave functional, multiplied by the square root of the Faddeev-Popov determinant, to generate a linear heavy-quark potential [48].

In any case, one should emphasize that in our framework confinement (as well as other crucial vacuum features) is expected to emerge only after gauge projection. In fact, Feynman had argued almost three decades ago [11] that for a mass gap to be generated in a non-Abelian gauge theory, all field configurations with non-vanishing support at “large” A should either be gauge-equivalent to others with support only at “small” A or damped by their magnetic field energy. This argument is suggestive because then, in analogy with finite-dimensional quantum mechanics, the wave functionals of the ground and first-excited states cannot arbitrarily reduce their energy difference by favoring long-wavelength potentials A extending over all of space. As a consequence, the energy or (in the static case) mass gap cannot be closed. It would be interesting to check whether the gauge-projected Gaussian wave functional (1) can realize this mechanism.

In order to simplify the analysis and to focus on the still rather poorly understood infrared gluon sector of QCD, we have restricted our investigation to pure Yang-Mills theory without quarks. As the quenched approximation to lattice QCD, this provides stable and unmixed glueball states which set a benchmark for sorting out the QCD glueball spectrum. (For a first attempt to study glueball states on the basis of a gauge-invariant vacuum wave functional see Ref. [51].) However, static quark sources could be straightforwardly implemented into the gauge-invariant vacuum functional [20] and even the inclusion of light, dynamical quarks adds no conceptual problems, although a nonperturbative treatment of their interactions with the gluon sector appears challenging. (For a variational study of fermions in the 1+1 dimensional Abelian Schwinger model see Ref. [52])

We close this section by briefly discussing the improvement potential of our approach and by mentioning a few additional applications. The $O(g)$ treatment of the energy density and the $O(c_1)$ treatment of the $4U$ interactions could be systematically refined. In addition, one may evaluate the corrections due to higher-gradient contributions with couplings $c_{n \geq 2}$ in the effective soft-mode action (43). The mean-field analysis of the integral over the auxiliary field Σ could alternatively be performed in quaternionic variables for the gauge group $SU(2)$, as suggested in Ref. [18]. If this formulation, which keeps the fluctuations around the mean field under control, could be generalized to higher N_c , the corresponding saddle-point approximation may in fact become exact in the large- N_c limit [44]. One could further generalize the trial functional basis by including both longitudinal and transverse mode contributions to the covariance, or even allow for a non-diagonal color structure. Furthermore, one may consider non-analytic contributions to the IR covariance, and one could simulate the nonlinear soft-mode dynamics (41) and its phase structure numerically on a lattice.

A particularly interesting class of Yang-Mills amplitudes are the (equal-time) glueball correlation functions which contain information on the whole spectrum and the decay constants of glueballs. This information was variationally explored in Ref. [51] and is accessible in our framework as well. It could e.g. be analyzed by comparison with results from lattice simulations [53], the operator product expansion [45, 47] and holographic strong-coupling duals [50]. The pseudoscalar glueball correlator contains the topological susceptibility in its zero-momentum limit, furthermore, whose evaluation would complement the analysis of the topological vacuum structure mentioned above. Another interesting type of amplitude which may be at least approximately accessible are Bethe-Salpeter amplitudes of glueballs for which e.g. lattice [53] and instanton liquid model [49] results are available. Another natural and interesting extension of our analysis would be its generalization to finite temperature, as pioneered in Ref. [54] for the minimal trial-functional family of Ref. [17]. This opens up several important further application possibilities, including the study of the deconfinement phase transition [55] as well as of properties of the currently intensely debated and potentially strongly coupled gluon plasma at temperatures 2-3 times above the critical temperature [56]. In the longer run, the potential of our real-time Minkowski space formulation to describe quantum nonequilibrium physics should be exploited, too, e.g. by applying it to currently much discussed nonequilibrium processes in the early universe as well as in the aftermath of ultrahigh-energy nuclear collisions (for a brief introduction see Sec. V of Ref. [8]). Some of the above applications may even provide guidance for how to generalize the Gaussian approximation (3) to the core wave functional.

IX. SUMMARY AND CONCLUSIONS

We have implemented and studied a gauge-invariant variational approximation scheme for the Yang-Mills vacuum wave functional. Our approach is based on minimizing the Yang-Mills Hamiltonian in a gauge-projected Gaussian trial functional space which allows for an essentially general momentum distribution of the soft vacuum fields. This provides a substantial improvement upon previously used trial functionals which populated all infrared modes with identical, i.e. momentum-independent strength. Our extension of the trial basis rests on a controlled expansion of the infrared-mode dispersion relation (or “covariance”), which characterizes the vacuum wave functional, into powers of the soft momenta divided by the dynamically generated mass scale. The momentum dependence can therefore be systematically approximated by truncating the series, which allows us to restrict the quantitative part of our study to the leading-order corrections. (This truncation is conceptually helpful as well since the subleading corrections tend to reduce the transparency of the analysis.) After complementing the generalized soft vacuum-mode population by

the leading perturbative ultraviolet modes, finally, one ends up with the largest gauge-invariant trial space for the Yang-Mills vacuum wave functional which is currently available (in 3+1 dimensions) and which keeps the variational analysis analytically manageable.

The vacuum physics emerging from energy minimization in this extended trial space turns out to be multifaceted. To begin with, the momentum dependence of the infrared-mode distribution is to leading order characterized by just one variational parameter. After transforming the soft-mode dynamics of the wave functional into an effective Lagrangian for collective sets of gauge-field orbits, this parameter reappears as the coupling constant of the dominant higher-gradient interactions which modify the low-momentum dispersion relation of the soft modes. Moreover, it acquires an intuitive physical interpretation in terms of the group velocity of gauge-field quasiparticles in the vacuum. While this velocity vanishes in the unimproved ground state, it turns out to be finite in the improved one, which is one of our main results. Our new dispersion relation further reveals that infrared quasiglasons in the vacuum decelerate in the presence of an applied force. In other words, their “effective kinetic mass” is negative (analogous situations are encountered in several condensed matter systems) and their color conductivity can increase with increasing strength of an external color-electric field, implying a negative differential resistance of the vacuum.

The variationally optimized value of the higher-gradient coupling parameter turns out to be positive. This sign may at first appear surprising since it is opposite to the one induced by the massive vector propagator which was previously adopted as a model for the infrared covariance. Its physical role is quite instructive, however, since it implies that soft gauge-field modes with larger momenta populate the vacuum more strongly than their longer-wavelength counterparts. Vacuum fields with constant color-magnetic field strength are thus energetically disfavored, in particular, which prevents the onset of the Savvidy instability. The energy barrier against larger quasiglason velocities also preserves the normalizability of the vacuum wave functional and keeps the variationally determined value of the quasiglason velocity small. Another notable consequence is the existence of a saddle-point solution for the order-parameter field at a dynamically generated mass scale which is consistent with lattice results for the Yang-Mills scale. (As a practical side benefit, the relatively small optimized coupling parameter value also justifies a leading-order perturbative treatment of the four-soft-mode interactions.)

In addition, the above findings indicate that the dimensional transmutation mechanism is an almost quantitatively robust feature of gauge-projected Gaussian core functionals (instead of emerging accidentally from an oversimplified trial space). As a consequence, we obtain a finite gluon condensate of a magnitude well inside the range predicted by other sources, although it scales with the fourth power of the infrared mass scale. This supports the expectation that Gaussian trial functionals provide a reasonable vacuum description in dynamical situations where just one vacuum condensate dominates. While this holds e.g. for the Cooper-pair condensate in the BCS theory of superconductivity, it is less well established in Yang-Mills theory where the lowest-dimensional gluon condensate provides the natural candidate. The main reasons for the robustness of the vacuum scales turn out to be that the nontrivial solution of the gap equation is unique and that the corresponding disordered vacuum phase exists only in a limited domain of all variational parameters. Even the soft-mode dynamics’ order-disorder phase transition, at which the vacuum energy attains its minimum, remains squarely of second order. This is in contrast to the first order predicted by lattice simulations and probably a shortcoming of the mean-field approximation near the transition. In any case, the improved dispersion generates considerably more attraction among the variationally optimized vacuum fields and lowers the vacuum energy density by about 11%. This indicates that the nonvanishing quasi-gluon velocity provides a rather substantial overall improvement of the vacuum description.

Nevertheless, the gauge-invariant variational framework remains analytically tractable at a computational cost comparable to fully gauge-fixed approaches. The rather high degree of transparency owed to the explicit representation of the vacuum state is maintained as well. In combination, these qualities promise considerable further potential of our approach as a theoretical laboratory for gaining intuitive, structural and quantitative insights into the nonperturbative real-time physics of Yang-Mills theories. The established framework provides, in particular, a privileged testing ground for the impact of topological vacuum excitations and their interplay with the gauge symmetry (both are manifest in our effective soft-mode dynamics) which should be explored further. In addition, our approach is well suited to explore the maximal physics content which gauge-projected Gaussian core functionals can accommodate. In the longer run, this will allow to chart the principal limitations of the Gaussian approximation and may hopefully trigger new ideas for going beyond it in a both systematic and analytically manageable way.

Acknowledgments

Financial support from the Fundação de Amparo à Pesquisa do Estado de São Paulo (FAPESP) and from the Deutsche Forschungsgemeinschaft (DFG), as well as the hospitality of the Abdus Salam International Centre for Theoretical Physics (ICTP) in Trieste, Italy, are gratefully acknowledged.

Appendix A: Evaluation of vacuum expectation values

To establish our notation and to make the paper self-contained, we briefly review in this appendix how to calculate matrix elements in trial states given by a gauge-invariant vacuum wave functional of the type (1), following Ref. [17]. We recast this framework into the language of generating functionals and also derive several expressions which will be needed in the main text.

To begin with, consider multi-local, gauge-invariant operators $\mathcal{O}(A, E)$ composed of the static gauge fields $A_i^a(\vec{x})$ and their canonically conjugate momenta $-E_i^a(\vec{x})$ (where E is the chromoelectric field) in the Hamiltonian formulation of $SU(N_c)$ Yang-Mills theory in temporal (or Weyl) gauge. The canonical commutation relation $[E_i^a(\vec{x}), A_j^b(\vec{y})] = i\delta^{ab}\delta_{ij}\delta^3(\vec{x} - \vec{y})$ then implies that $E_i^a(\vec{x}) = i\delta/\delta A_i^a(\vec{x})$ in the Schrödinger coordinate representation. Our aim is to calculate the (trial) vacuum expectation value of \mathcal{O} , i.e. the matrix element

$$\langle \mathcal{O}(A, E) \rangle = \frac{\int D\vec{A} \Psi_0^*[\vec{A}] \mathcal{O}\left(\vec{A}^a, \frac{i\delta}{\delta \vec{A}^a}\right) \Psi_0[\vec{A}]}{\int D\vec{A} \Psi_0^*[\vec{A}] \Psi_0[\vec{A}]}, \quad (\text{A1})$$

where the unrestricted linear measure $D\vec{A}$ comprises all gauge orbits and topological charges. (Recall that Gauß' law must be enforced as a constraint on the physical states and in particular on the vacuum wave functional Ψ_0 , cf. Sec. II A.)

1. Exact integration over the gauge field

After inserting the (residual) gauge-invariant, unnormalized wave functional (1) (and interchanging the order of the A, \bar{U} and \tilde{U} integrations), the matrix element (A1) becomes

$$\langle \mathcal{O}(A, E) \rangle = \frac{\int D\bar{U} \int D\tilde{U} \int D\vec{A} \psi_0[\vec{A}^{\bar{U}}] \mathcal{O}\left(\vec{A}^a, \frac{i\delta}{\delta \vec{A}^a}\right) \psi_0[\vec{A}^{\tilde{U}}]}{\int D\bar{U} \int D\tilde{U} \int D\vec{A} \psi_0[\vec{A}^{\bar{U}}] \psi_0[\vec{A}^{\tilde{U}}]}. \quad (\text{A2})$$

Since \mathcal{O} is gauge-invariant, the integrand in the numerator can only depend on the relative transformation $U := \tilde{U}^{-1}\bar{U}$. Indeed, after changing the integration variable $A \rightarrow A' = A^{\tilde{U}}$ (for fixed \tilde{U}), one has

$$\int D\vec{A} \psi_0[\vec{A}^{\bar{U}}] \mathcal{O}\left(\vec{A}, \frac{i\delta}{\delta \vec{A}}\right) \psi_0[\vec{A}^{\tilde{U}}] = \int D\vec{A}' \psi_0[\vec{A}'^{\tilde{U}^{-1}\bar{U}}] \mathcal{O}\left(\vec{A}', \frac{i\delta}{\delta \vec{A}'}\right) \psi_0[A'] \quad (\text{A3})$$

and the analogous expression for the denominator. Using $\mathcal{O}(A) = \mathcal{O}(A')$ and $DA = DA'$, renaming A' to A and employing the translational invariance $D\bar{U} = DU$ of the Haar measure then yields

$$\int D\bar{U} \int D\vec{A} \psi_0[\vec{A}^{\bar{U}}] \mathcal{O}\left(\vec{A}, \frac{i\delta}{\delta \vec{A}}\right) \psi_0[\vec{A}^{\tilde{U}}] = \int DU \int D\vec{A} \psi_0[\vec{A}^U] \mathcal{O}\left(\vec{A}, \frac{i\delta}{\delta \vec{A}}\right) \psi_0[\vec{A}] \quad (\text{A4})$$

(and the analogous expression for the denominator) which does not depend on \tilde{U} since the latter was absorbed into the integration variable A . Hence the (infinite) gauge group volume $\int D\tilde{U}$ cancels between numerator and denominator, leaving us with

$$\langle \mathcal{O}(A, E) \rangle = \frac{\int DU \int D\vec{A} \psi_0[\vec{A}^U] \mathcal{O}\left(\vec{A}^a, \frac{i\delta}{\delta \vec{A}^a}\right) \psi_0[\vec{A}]}{\int DU \int D\vec{A} \psi_0[\vec{A}^U] \psi_0[\vec{A}]}. \quad (\text{A5})$$

Now it is useful to define an effective bare action $\Gamma_b[U]$ and the associated nonlocal gauge-field correlators by writing

$$\exp\{-\Gamma_b[U]\} := \int D\vec{A} \psi_0[\vec{A}^U] \psi_0[\vec{A}] =: \int D\vec{A} e^{-\gamma[A, U]}, \quad (\text{A6})$$

$$\langle \langle \langle \vec{A} \dots \vec{A} \dots \vec{E} \dots \vec{E} \rangle \rangle \rangle \exp\{-\Gamma_b[U]\} := \int D\vec{A} \psi_0[\vec{A}^U] \vec{A} \dots \vec{A} \dots \frac{i\delta}{\delta \vec{A}} \dots \frac{i\delta}{\delta \vec{A}} \psi_0[\vec{A}], \quad (\text{A7})$$

where the triple-brackets $\langle\langle\langle\dots\rangle\rangle\rangle$ denote (nondiagonal) matrix elements between U -rotated and unrotated core-functional states. (Note the symmetry $\Gamma_b[U] = \Gamma_b[g_L^\dagger U g_R]$ with $g_{L,R} \in \text{SU}(N_c)$ which originates from the translational invariance of the two group integrations in Eq. (A2).) With the relation

$$\mathcal{O}\left(\vec{A}^a, \frac{i\delta}{\delta\vec{A}^a(\vec{x})}\right) \psi_0[\vec{A}] \equiv \bar{\mathcal{O}}[A] \psi_0[\vec{A}], \quad (\text{A8})$$

which replaces the (quasi-) local, differential operator \mathcal{O} by a nonlocal functional $\bar{\mathcal{O}}$ of the A fields only, one then arrives at

$$\langle\mathcal{O}(A, E)\rangle = \frac{\int DU \int D\vec{A} \psi_0[\vec{A}^U] \bar{\mathcal{O}}[A] \psi_0[\vec{A}]}{\int DU \int D\vec{A} \psi_0[\vec{A}^U] \psi_0[\vec{A}]} = \frac{\int DU \langle\langle\langle\mathcal{O}(A, E)\rangle\rangle\rangle \exp\{-\Gamma_b[U]\}}{\int DU \exp\{-\Gamma_b[U]\}}. \quad (\text{A9})$$

Hence the calculation of the matrix element is reduced to evaluating the vacuum expectation value of the expressions (A7), specialized to contain A fields only, in the U field dynamics determined by Γ_b .

Owing to the Gaussian nature of the wave functional (3), the effective bare action defined in Eq. (A6) and hence the matrix elements (A7) can be calculated analytically. In order to render its U dependence explicit, we write

$$\gamma[A, U] := -\ln \psi_0^*[\vec{A}^U] \psi_0[\vec{A}] = \frac{1}{2} \left[(A^U)^T G^{-1} A^U + A^T G^{-1} A \right] \quad (\text{A10})$$

(in a triple matrix notation for the color, vector and spacial “indices”) where the rotated gauge field

$$\left(\vec{A}^U\right)^a = S^{ab}(\vec{x}) \vec{A}^b + g^{-1} \vec{L}^a(\vec{x}) \quad (\text{A11})$$

is expressed in terms of the homogeneous and inhomogeneous transformation functions

$$S^{ab}(\vec{x}) = \frac{1}{2} \text{tr} \left\{ \tau^a U^\dagger(\vec{x}) \tau^b U(\vec{x}) \right\}, \quad \vec{L}^a(\vec{x}) = i \text{tr} \left\{ \tau^a U^\dagger(\vec{x}) \vec{\partial} U(\vec{x}) \right\}. \quad (\text{A12})$$

After inserting the representation (A11) into Eq. (A10), one finds that γ contains an A independent piece and a term which is bilinear in A ,

$$\gamma[A, U] = \frac{1}{2} (A + a)^T \mathcal{M} (A + a) + \frac{1}{2g_b^2} L^T \mathcal{D} L, \quad (\text{A13})$$

where we defined [17]

$$\mathcal{M} := S^T G^{-1} S + G^{-1} = \mathcal{M}^T, \quad \vec{a} := g^{-1} \mathcal{M}^{-1} S^T G^{-1} \vec{L}, \quad (\text{A14})$$

$$\mathcal{D} := G^{-1} - G^{-1} S \mathcal{M}^{-1} S^T G^{-1} = (G + S G S^{-1})^{-1}. \quad (\text{A15})$$

(G^{-1} and \mathcal{M} are symmetric in a, b, i, j and \vec{x}, \vec{y} , and transposition of \vec{a} is also implied to invert the direction of the derivatives in G^{-1} .) After performing the Gaussian integration over A , we arrive at the explicit form

$$\begin{aligned} \Gamma_b[U] &= \int d^3x \int d^3y \mathcal{L}_b(\vec{x}, \vec{y}) \\ &= -\ln \int D\vec{A} \exp\{-\gamma[A, U]\} = \frac{1}{2} \text{Tr} \ln(\mathcal{M}) + \frac{1}{2g_b^2} L^T \mathcal{D} L \end{aligned} \quad (\text{A16})$$

of the *bare* action which is a nonlocal, nonlinear σ -model, regularized by the ultraviolet cutoff Λ_{UV} which is implicit in the definition of the wave functional. This dynamics sums up the interactions of the gauge fields with a “background” field U through the vector $\vec{a}[U]$ and the propagator $\mathcal{M}^{-1}[U]$ which arise from enforcing the gauge invariance of the functional (1). In the following we will omit the first term $\propto \text{Tr} \ln(\mathcal{M})$ in Eq. (A16) since it is of $O(g^2)$ relative to the second one and does not contain U derivatives [17, 34].

The connected (equal-time) n -point functions at fixed U ,

$$\langle\langle\langle A_{i_1}^{a_1}(\vec{z}_1) A_{i_2}^{a_2}(\vec{z}_2) \dots A_{i_n}^{a_n}(\vec{z}_n) \rangle\rangle\rangle = \frac{\int D\vec{A} \psi_0[\vec{A}^U] A_{i_1}^{a_1}(\vec{z}_1) A_{i_2}^{a_2}(\vec{z}_2) \dots A_{i_n}^{a_n}(\vec{z}_n) \psi_0[\vec{A}]}{\int D\vec{A} \psi_0[\vec{A}^U] \psi_0[\vec{A}]}, \quad (\text{A17})$$

are specializations of the definition (A7) to A fields only and can now be calculated by means of the generating functional

$$\int D\vec{A}\psi_0[\vec{A}^{U'}] \psi_0[\vec{A}] \exp(-\vec{J}\vec{A}) = \int D\vec{A} \exp(-\gamma[\vec{A}, U] - \vec{J}\vec{A}) \quad (\text{A18})$$

$$= \exp\left(\frac{1}{2}\vec{J}\mathcal{M}^{-1}\vec{J} + \vec{J}\vec{a}\right) \exp(-\Gamma_b[U]) \quad (\text{A19})$$

as

$$\langle\langle\langle A_{i_1}^{a_1}(\vec{z}_1) A_{i_2}^{a_2}(\vec{z}_2) \dots A_{i_n}^{a_n}(\vec{z}_n) \rangle\rangle\rangle = \frac{(-1)^n \delta^n \exp\left(\frac{1}{2}\vec{J}\mathcal{M}^{-1}\vec{J} + \vec{J}\vec{a}\right)}{\delta J_{i_1}^{a_1}(\vec{z}_1) \dots \delta J_{i_n}^{a_n}(\vec{z}_n)} \Bigg|_{\vec{J}=0}. \quad (\text{A20})$$

This expression reproduces the Wick expansion for correlators of a vector field \vec{A} with nontrivial propagator \mathcal{M}^{-1} in the background of the U and \vec{a} fields. (In contrast to free or mean-field correlators, it also generates finite $(2n+1)$ -functions and does not factorize $2n$ -point functions into products of n 2-point functions.) Explicit expressions for the 2, 3 and 4-point functions needed in the main text are

$$\langle\langle\langle A_{i_1}^{a_1}(\vec{z}_1) A_{i_2}^{a_2}(\vec{z}_2) \rangle\rangle\rangle = \mathcal{M}_{i_1 i_2}^{-1 a_1 a_2}(\vec{z}_1, \vec{z}_2) + a_{i_1}^{a_1}(\vec{z}_1) a_{i_2}^{a_2}(\vec{z}_2) \quad (\text{A21})$$

and (in shorthand notation for arguments and indices)

$$\langle\langle\langle A(1) A(2) A(3) \rangle\rangle\rangle = -[\mathcal{M}^{-1}(2, 3) a(1) + \mathcal{M}^{-1}(1, 3) a(2) + \mathcal{M}^{-1}(1, 2) a(3) + a(1) a(2) a(3)] \quad (\text{A22})$$

as well as

$$\begin{aligned} \langle\langle\langle A(1) A(2) A(3) A(4) \rangle\rangle\rangle &= \mathcal{M}^{-1}(1, 2) \mathcal{M}^{-1}(3, 4) + \mathcal{M}^{-1}(1, 3) \mathcal{M}^{-1}(2, 4) + \mathcal{M}^{-1}(1, 4) \mathcal{M}^{-1}(2, 3) \\ &+ \mathcal{M}^{-1}(1, 2) a(3) a(4) + \mathcal{M}^{-1}(2, 3) a(1) a(4) + \mathcal{M}^{-1}(3, 4) a(1) a(2) \\ &+ \mathcal{M}^{-1}(1, 4) a(2) a(3) + \mathcal{M}^{-1}(1, 3) a(2) a(4) + \mathcal{M}^{-1}(2, 4) a(1) a(3) \\ &+ a(1) a(2) a(3) a(4). \end{aligned} \quad (\text{A23})$$

Hence the above results reduce the calculation of the matrix element (A2) to performing the integral over the nonlocally interacting $U(\vec{x})$ fields according to Eq. (A9). The latter will be the subject of the next two sections.

2. Perturbative integration over the hard U modes

Since we are interested in amplitudes with external momenta $|\vec{p}_i| \ll \mu$ (where μ is a typical hadronic scale, e.g. the lowest glueball mass), the integral over U in Eq. (A9) can be approximately done in a two-step procedure [17]: one first integrates out the hard $U_>$ modes (with momenta $k \geq \mu$) perturbatively and then performs the integral over the remaining $U_<$ modes (with momenta $k < \mu$) in the saddle-point approximation. In preparation for this procedure, we factor the integration variable U in a group-structure preserving manner as

$$U(\vec{x}) = U_<(\vec{x}) U_>(\vec{x}), \quad U_>(\vec{x}) = \exp(-ig\phi^a(\vec{x}) \lambda^a/2), \quad (\text{A24})$$

where $U_<$ contains only soft (hard) modes with momenta $k^2 \lesssim \mu^2$. Since asymptotic freedom is implemented in the high-momentum covariance (11), the bare coupling g_b is small at the large cutoff scale Λ_{UV} where the theory is defined. Hence the hard modes can be integrated out perturbatively, e.g. by Wilson's momentum-shell technique [57], down to the infrared scale μ chosen such that the renormalized coupling $g(\mu)$ remains sufficiently small. The functional measure factorizes according to Eq. (A24) as

$$DU = DU_< DU_> \propto DU_< D\phi^a. \quad (\text{A25})$$

The hard modes ϕ carry momenta $\mu \in [k, \Lambda_{UV}]$ while the momenta of the soft modes $U_<$ stay in the range $0 > k > \mu$. The latter restriction implies a weak variation $U_<(\vec{x}) \simeq U_<(\vec{y})$ over distances $|\vec{x} - \vec{y}| < \mu^{-1}$. The bare action then becomes a functional of the fields $\phi, U_<$,

$$\Gamma_b[\phi, U_<] = \Gamma_{b,>}[\phi] + \Gamma_{b,<>}[\phi, U_<] + \Gamma_{b,<}[U_<], \quad (\text{A26})$$

and Eq. (A9) for the matrix element turns into

$$\langle \mathcal{O}(A, E) \rangle = \frac{\int DU_{<} \int D\phi \langle \langle \mathcal{O}(A, E) \rangle \rangle \exp\{-\Gamma_{\text{b}}[\phi, U_{<}] \}}{\int DU_{<} \int D\phi \exp\{-\Gamma_{\text{b}}[\phi, U_{<}] \}}. \quad (\text{A27})$$

As long as $g^2(\mu) \ll 1$ the ϕ field can be integrated out perturbatively to one loop in the bare coupling (where the loop momentum integrals are regularized by the cutoff Λ_{UV}). The result has the form

$$\langle \langle \mathcal{O}(A, E) \rangle \rangle \exp\{-\Gamma_{<}[U_{<}] \} := \int D\phi \langle \langle \mathcal{O}(A, E) \rangle \rangle \exp\{-\Gamma_{\text{b}}[\phi, U_{<}] \} \quad (\text{A28})$$

where we defined the soft-mode action $\Gamma_{<}[U_{<}]$ as

$$\exp\{-\Gamma_{<}[U_{<}] \} := \int D\phi \exp\{-\Gamma_{\text{b}}[\phi, U_{<}] \}, \quad (\text{A29})$$

made use of $\Gamma_{\text{b}, <}[U_{<}, \phi] = 0$ to leading order in the coupling, and implied that the (one-loop) anomalous dimension of the considered operator vanishes. (This is particularly appropriate for the conserved Yang-Mills Hamiltonian density (131) under consideration in the bulk of the paper.) The evaluation of the matrix element (A2) is then further reduced to calculating the soft-mode integral

$$\langle \mathcal{O}(A, E) \rangle = \frac{\int DU_{<} \langle \langle \mathcal{O}(A, E) \rangle \rangle \exp\{-\Gamma_{<}[U_{<}] \}}{\int DU_{<} \exp\{-\Gamma_{<}[U_{<}] \}}. \quad (\text{A30})$$

In order to exhibit the (approximate) $U_{<}$ dependence of $\Gamma_{<}[U_{<}]$ and $\langle \langle \mathcal{O}(A, E) \rangle \rangle$ explicitly, we now exploit the smallness of the bare coupling to truncate the expansion of $U_{>}$ in powers of g . Up to corrections of $O(g^3)$ one finds

$$U_{>} = \exp\left(-ig\phi^a \frac{\tau^a}{2}\right) = 1 - ig\phi^a \frac{\tau^a}{2} - \frac{g^2}{8} (\phi^a \tau^a)^2 + O(g^3), \quad (\text{A31})$$

$$\lambda_{>, i}^a = \partial_i \phi^a + O(g^3), \quad S_{>}^{ab} = \delta^{ab} + g f^{abc} \phi^c - \frac{g^2}{2} f^{ace} f^{bde} \phi^c \phi^d + O(g^3) \quad (\text{A32})$$

$$\lambda_i^a = S_{>}^{ab} \lambda_{<, i}^b + \lambda_{>, i}^a = \lambda_{<, i}^a + \partial_i \phi^a + g f^{abc} \lambda_{<, i}^b \phi^c - \frac{g^2}{2} f^{ace} f^{bde} \lambda_{<, i}^b \phi^c \phi^d + O(g^3) \quad (\text{A33})$$

(Above we have rescaled the Cartan-Maurer form (35) as $\lambda_i^a := L_i^a/g$ in order to facilitate explicit power counting in g . The spacial index should help to avoid confusion with the $\text{SU}(N_c)$ generators.) To the same order, the operator (A15) expands as

$$\mathcal{D}^{ab}(\vec{x}, \vec{y}) = \frac{G^{-1}(\vec{x} - \vec{y})}{2} \delta^{ab} \left\{ 1 + \frac{g^2}{N^2 - 1} [\phi^a(\vec{x}) \phi^a(\vec{x}) - 2\phi^a(\vec{x}) \phi^a(\vec{y}) + \phi^a(\vec{y}) \phi^a(\vec{y})] \right\} + O(g^3). \quad (\text{A34})$$

(Note that \mathcal{D} is independent of $U_{<}$, as a consequence of $S_{<} G S_{<}^{-1} \simeq G$ which holds because $S_{<}$ varies slowly over the distances $|\vec{x} - \vec{y}| \lesssim \mu^{-1}$ over which the decaying G remains non-negligible.) Inserting the above expansions into the bare action (A16), one finds the associated Lagrangian

$$\mathcal{L}_{\text{b}}(\vec{x}, \vec{y}) = \mathcal{L}_{\text{b}, >}(\vec{x}, \vec{y}) + \mathcal{L}_{\text{b}, <}(\vec{x}, \vec{y}) + \mathcal{L}_{\text{b}, < >}(\vec{x}, \vec{y}) + O(g^3) \quad (\text{A35})$$

with the bilinear parts

$$\mathcal{L}_{\text{b}, >}(\vec{x}, \vec{y}) = \frac{1}{4} \partial_i \phi^a(\vec{x}) G^{-1}(\vec{x} - \vec{y}) \partial_i \phi^a(\vec{y}), \quad (\text{A36})$$

$$\mathcal{L}_{\text{b}, <}(\vec{x}, \vec{y}) = \frac{1}{4} \lambda_{<, i}^a(\vec{x}) G^{-1}(\vec{x} - \vec{y}) \lambda_{<, i}^a(\vec{y}) \quad (\text{A37})$$

and the hard-soft-mode interactions (rewritten with $G^{-1}(\vec{x} - \vec{y}) = G^{-1}(\vec{y} - \vec{x})$ and anticipating the exchange symmetry $\vec{x} \leftrightarrow \vec{y}$ after integration over \vec{x} and \vec{y})

$$\begin{aligned} \mathcal{L}_{\text{b}, < >}(\vec{x}, \vec{y}) &= \frac{g}{2} f^{abc} \lambda_{<, i}^b(\vec{x}) G^{-1}(\vec{x} - \vec{y}) \phi^c(\vec{x}) \partial_i \phi^a(\vec{y}) \\ &+ \frac{g^2}{8} \left(\frac{N_c \delta^{ab} \delta^{cd}}{N^2 - 1} - 2 f^{ace} f^{bde} \right) \\ &\times \lambda_{<, i}^b(\vec{x}) G^{-1}(\vec{x} - \vec{y}) \lambda_{<, i}^a(\vec{y}) [\phi^c(\vec{x}) \phi^d(\vec{x}) - \phi^c(\vec{x}) \phi^d(\vec{y})] \end{aligned} \quad (\text{A38})$$

(which are invariant under $\phi \rightarrow -\phi$). To leading order in g the hard and soft modes decouple, and the higher-order interactions $\mathcal{L}_{b,<}$ can be treated perturbatively. (The $O(g)$ term in $\mathcal{L}_{b,<}$ contributes neither to the β -function nor to the soft-mode action.) Writing further

$$\Gamma_b[U] = \Gamma_{b,<}[U_{<}] + \Gamma_{b,>}[\phi] + g\Gamma_1[\phi, U_{<}] + g^2\Gamma_2[\phi, U_{<}] + O(g^3) \quad (\text{A39})$$

renders the bare-coupling dependence of the action explicit. In terms of the kinetic operator

$$K^{ab}(\vec{x} - \vec{y}) \equiv \frac{1}{2}\delta^{ab} [\partial_{yi}\partial_{xi}G^{-1}(\vec{x} - \vec{y})]_{p^2 > \mu^2} \quad (\text{A40})$$

of the Lagrangian (A36), furthermore, the hard-mode action becomes

$$\Gamma_{b,>}[\phi] = \int d^3x \int d^3y \mathcal{L}_{>,b}(\vec{x}, \vec{y}) = \frac{1}{2} \int d^3x \int d^3y \phi^a(\vec{x}) K^{ab}(\vec{x} - \vec{y}) \phi^b(\vec{y}) + O(g) \quad (\text{A41})$$

$$= \frac{1}{4} \frac{d^3k}{(2\pi)^3} [\theta(\Lambda_{UV}^2 - k^2) - \theta(\mu^2 - k^2)] \tilde{\phi}^a(\vec{k}) G^{-1}(k) k^2 \tilde{\phi}^a(-\vec{k}) \quad (\text{A42})$$

from which one reads off the ϕ^a propagator

$$\langle \phi^a(\vec{x}) \phi^b(\vec{y}) \rangle \equiv \frac{\int D\phi_{\mu < k < \Lambda_{UV}} \phi^a(\vec{x}) \phi^b(\vec{y}) \exp\{-\Gamma_{b,>}[\phi]\}}{\int D\phi \exp\{-\Gamma_{b,>}[\phi]\}} = K^{-1ab}(\vec{x} - \vec{y}) \quad (\text{A43})$$

$$= \int \frac{d^3k}{(2\pi)^3} [\theta(\Lambda_{UV}^2 - k^2) - \theta(\mu^2 - k^2)] e^{i\vec{k}(\vec{x}-\vec{y})} \frac{2G_{>}(k)}{k^2} \delta^{ab}. \quad (\text{A44})$$

The nonstandard kinetic term of the high-momentum σ model (A42) thus generates a propagator with large- k asymptotics $K^{-1}(k) \propto G_{>}(k)/k^2 \sim 1/k^3$ (instead of the standard $1/k^2$ behavior which impedes perturbative renormalizability in three dimensions). Hence this high-momentum σ model is renormalizable (the tadpole diagram diverges only logarithmically) and asymptotically free, with a perturbative β function very similar to that of Yang-Mills theory [34].

Then one has from the definition (A29) and the decomposition (A35) of the bare action

$$\exp\{-\Gamma_{<}[U_{<}]\} = \exp\{-\Gamma_{b,<}[U_{<}] \int D\phi \exp\{-\Gamma_{b,>}[\phi] - \Gamma_{b,<,>}[U_{<}, \phi]\}\} \quad (\text{A45})$$

$$= \exp\left\{-\Gamma_{b,<}[U_{<}] - \langle \Gamma_{b,<,>}[U_{<}, \phi] \rangle_{\Gamma_{b,>}} + O(g^2)\right\} \quad (\text{A46})$$

(where the average $\langle \dots \rangle_{\Gamma_{b,>}}$ over ϕ is weighted by $\exp(-\Gamma_{b,>}[\phi])$) which yields the renormalized soft-mode action

$$\Gamma_{<}[U_{<}] = -\Gamma_{b,<}[U_{<}] - \langle \Gamma_{b,<,>}[\phi, U_{<}] \rangle_{\Gamma_{b,>}} + O(g^2) \quad (\text{A47})$$

$$= \frac{1}{4g^2(\mu)} \int d^3x \int d^3y L_{<,i}^a(\vec{x}) G_{<}^{-1}(\vec{x} - \vec{y}) L_{<,i}^a(\vec{y}) + O(g^2). \quad (\text{A48})$$

To the considered order (and for $G_{>}(k) = k^{-1}$), $\Gamma_{<}$ has therefore the same form as the bare soft-mode action $\Gamma_{b,<}$, but with the bare coupling replaced by the renormalized one,

$$g(\mu) = g_b + \frac{g_b^3 N_c}{(2\pi)^2} \ln \frac{\Lambda_{UV}}{\mu} + O(g_b^5), \quad (\text{A49})$$

which was calculated in Ref. [34]. This renormalization of the soft-mode interactions compensates for the removal of the hard (i.e. $k^2 > \mu^2$) U modes from amplitudes with external momenta $p^2 \ll \mu^2$. Analogously, the ϕ mode contributions to the amplitude

$$\langle\langle \mathcal{O}(A, E) \rangle\rangle = \frac{\int D\phi \langle\langle \mathcal{O}(A, E) \rangle\rangle \exp\{-\Gamma_b[U_{<}, \phi]\}}{\int D\phi \exp\{-\Gamma_b[U_{<}, \phi]\}} \quad (\text{A50})$$

can be integrated out perturbatively by rewriting

$$\langle\langle \mathcal{O}(A, E) \rangle\rangle = \frac{\exp\{-\Gamma_{b,<}[U_{<}]\}}{\exp\{-\Gamma_{<}[U_{<}]\}} \int D\phi \langle\langle \mathcal{O}(A, E) \rangle\rangle \exp\{-\Gamma_{b,<,>}[U_{<}, \phi]\} \exp\{-\Gamma_{b,>}[\phi]\} \quad (\text{A51})$$

$$\simeq \frac{\int D\phi \langle\langle \mathcal{O}(A, E) \rangle\rangle \exp\{-\Gamma_{b,>}[\phi]\}}{\int D\phi \exp\{-\Gamma_{b,>}[\phi]\}} \quad (\text{A52})$$

where to the considered order the anomalous dimension of $\mathcal{O}(A, E)$ arising from the perturbative interactions $\Gamma_{b, <} [U_<, \phi]$ can be neglected. (This approximation becomes exact for the operator considered in the main text, i.e. the Yang-Mills Hamiltonian density (131) in temporal gauge.) After introducing another generating functional

$$z_> [j] := \int D\phi \exp \left[-\Gamma_{b, >} [\phi] - \int d^3x j^a(\vec{x}) \phi^a(\vec{x}) \right] \quad (\text{A53})$$

$$= z_> [0] \exp \left[\frac{1}{2} \int d^3x \int d^3y j^a(\vec{x}) K^{-1ab}(\vec{x} - \vec{y}) j^b(\vec{y}) \right], \quad (\text{A54})$$

the ϕ^a fields in $\langle\langle\langle\mathcal{O}(A, E)\rangle\rangle\rangle$ can be replaced by derivatives $-\delta/\delta j^a$ with respect to the source j^a , which yields

$$\langle\langle\langle\mathcal{O}(A, E)\rangle\rangle\rangle \simeq \frac{1}{z_> [0]} \left\langle \left\langle \left\langle \mathcal{O} \left(U_<, \frac{-\delta}{\delta j} \right) \right\rangle \right\rangle \right\rangle z_> [j] \Big|_{j=0} \quad (\text{A55})$$

and shows explicitly that this intermediate matrix element is a functional of G^{-1} and $U_<$ only.

3. Saddle-point integration over the soft U modes

With the result (A55) for the intermediary matrix element $\langle\langle\langle\mathcal{O}(A, E)\rangle\rangle\rangle$ at hand, it remains to perform the functional integral

$$\langle\mathcal{O}(A, E)\rangle = \frac{\int DU_< \langle\langle\langle\mathcal{O}(A, E)\rangle\rangle\rangle \exp \{-\Gamma_< [U_<]\}}{\int DU_< \exp \{-\Gamma_< [U_<]\}} \quad (\text{A56})$$

over the soft modes $U_<$. In order to prepare for this last step, we integrate instead over a complex matrix field V and represent the unitarity constraint $U_< U_<^\dagger = 1$ by inserting a delta functional. The latter is rendered explicit by additionally integrating over an auxiliary Hermitian field $\Sigma(\vec{x})$ which acts as a Lagrange multiplier, as explained in Sec. IV A. The result is

$$\langle\mathcal{O}(A, E)\rangle = \frac{\int D\Sigma \int DV \langle\langle\langle\mathcal{O}(A, E)\rangle\rangle\rangle \exp \{-\Gamma_< [V] - \Gamma_\Sigma [V, \Sigma]\}}{\int D\Sigma \int DV \exp \{-\Gamma_< [V, \Sigma]\}} \quad (\text{A57})$$

where the integration contour for $\Sigma(\vec{x})$ runs parallel to the imaginary axis and where

$$\Gamma_\Sigma [V, \Sigma] \equiv \frac{m_g}{2g^2} \int d^3x \text{tr} \{ \Sigma (V^\dagger V - 1) \}. \quad (\text{A58})$$

(Note that Σ is Hermitian since VV^\dagger is. The unimodularity constraint $\det U_< = 1$ could additionally be implemented by integrating over a minimally coupled $U(1)$ gauge field [17]. We refrain from doing so because the impact of the difference between $SU(N_c)$ and $U(N_c)$ is of order $1/N_c^2$.) The matrix element (A57) can therefore be obtained from the soft-mode generating functional (47), i.e.

$$Z [j, j^\dagger] = \int D\Sigma \int DV \exp \left[-\Gamma_< [V] - \Gamma_\Sigma [V, \Sigma] - \int d^3x \text{tr} \{ j V^\dagger + j^\dagger V \} \right], \quad (\text{A59})$$

after replacing the $U_<$ and $U_<^\dagger$ fields in $\langle\langle\langle\mathcal{O}(A, E)\rangle\rangle\rangle$ by derivatives with respect to the matrix sources j^\dagger and j , i.e.

$$\langle\langle\langle\mathcal{O}(A, E)\rangle\rangle\rangle \simeq \frac{1}{Z [0, 0]} \left\langle \left\langle \left\langle \mathcal{O} \left(\frac{-\delta}{\delta j}, \frac{-\delta}{\delta j^\dagger} \right) \right\rangle \right\rangle \right\rangle Z [j, j^\dagger] \Big|_{j, j^\dagger=0}. \quad (\text{A60})$$

The unconstrained integral over V in Eq. (A59) is Gaussian and can be done exactly (cf. Sec. IV A), and the remaining integral over Σ can be performed in the saddle-point (or mean-field) approximation, as detailed in Sec. IV B. To leading order, this amounts to substituting the solution $\bar{\Sigma}$ of the gap equation (62) into the integrand of Eq. (A59).

Given an explicit expressions for the soft-mode action $\Gamma_< [U_<]$, as in our case Eq. (41) which originates from the generalized infrared covariance (13), the amplitude (A57) is thus uniquely represented as a functional of $G_<^{-1}$. In the (trial) vacuum expectation value $\langle\mathcal{H}_{\text{YM}}\rangle$ of the Yang-Mills Hamiltonian, in particular, $G_<^{-1}$ plays the role of a variational trial function. By means of our parametrization (20), the (trial) vacuum energy density then becomes a function of the variational parameters μ , m_g , and $\{c_i\}$ with respect to which it has to be minimized according to the Rayleigh-Ritz procedure. (The bare cutoff $\Lambda_{\text{UV}} \gg \Lambda_{\text{YM}}$ can be traded for Λ_{YM} , on the other hand, which will be obtained from lattice results, cf. Sec. VIII.)

Appendix B: Coincidence limit integrals

The coincidence limit of the soft-mode correlators calculated in Secs. IV and V is (for $c_{n \geq 2} = 0$) determined by integrals of the type

$$\tilde{i}_n(\xi, c_1) := \int_0^1 \frac{\kappa^{2n}}{\kappa^2(1 - c_1\kappa^2) + \xi^2} d\kappa \quad n \geq 1, \quad (\text{B1})$$

$$\tilde{j}_n(\xi, c_1) := \int_0^1 \frac{\kappa^{2n}}{[\kappa^2(1 - c_1\kappa^2) + \xi^2]^2} d\kappa \quad n \geq 1 \quad (\text{B2})$$

with $c_1 < 1$ (which ensures normalizability of the vacuum wave functional). In the following we list pertinent properties of these integrals and derive analytic expressions to be used e.g. for the numerical solution of the gap equation and for the evaluation of the vacuum energy. To start with, we note the obvious relations

$$\tilde{i}_n(\xi, c_1) > \tilde{i}_{n+1}(\xi, c_1), \quad (\text{B3})$$

$$\tilde{j}_n(\xi, c_1) > \tilde{j}_{n+1}(\xi, c_1) \quad (\text{B4})$$

which hold point by point. Furthermore, for the physically required $c_1 < 1$ all integrals (B1), (B2) are non-negative. They decrease monotonically with increasing $\xi \geq 0$ and increase monotonically with increasing c_1 in the allowed range $-\infty < c_1 < 1$ (where $1 - c_1\kappa^2 \geq 0$ decreases with increasing c_1 for fixed $\kappa \in [0, 1]$). All integrals are regular at $c_1 = 0$ and at $\xi = 0$, with the exception of \tilde{j}_1 which contains a single pole at $\xi = 0$ (see below). Due to the factors of κ^2 in the numerator, all integrands have most of their support close to $\kappa \rightarrow 1$, i.e. at momenta $k \sim \mu$.

1. Analytical expressions

An efficient strategy for analytically evaluating the integrals $\tilde{i}_n(\xi, c_1)$ starts from the identity

$$\frac{1}{\kappa^2(1 - c_1\kappa^2) + \xi^2} = \frac{1}{\sqrt{1 + 4c_1\xi^2}} \left(\frac{1}{\kappa^2 - \kappa_2^2} - \frac{1}{\kappa^2 - \kappa_1^2} \right) \quad (\text{B5})$$

which exhibits poles at the positions

$$\kappa_{1,2}^2(\xi, c_1) = \frac{1}{2c_1} \left(1 \pm \sqrt{1 + 4c_1\xi^2} \right). \quad (\text{B6})$$

Hence the evaluation of

$$\tilde{i}_n(\xi, c_1) = \frac{1}{\sqrt{1 + 4c_1\xi^2}} \int_0^1 \kappa^{2n} \left(\frac{1}{\kappa^2 - \kappa_2^2} - \frac{1}{\kappa^2 - \kappa_1^2} \right) d\kappa \quad (\text{B7})$$

is reduced to the calculation of one-pole integrals. The simple identity

$$\frac{\kappa^{2n}}{\kappa^2 - x^2} = x^2 \frac{\kappa^{2(n-1)}}{\kappa^2 - x^2} + \kappa^{2(n-1)} \quad (\text{B8})$$

implies the recursion relation

$$\int_0^1 \frac{\kappa^{2n}}{\kappa^2 - x^2} d\kappa = \frac{1}{2n-1} + x^2 \int_0^1 \frac{\kappa^{2(n-1)}}{\kappa^2 - x^2} d\kappa \quad (\text{B9})$$

and allows to reduce the $\tilde{i}_n(\xi, c_1)$ to analytic expressions involving only the simplest integral

$$\int_0^1 \frac{1}{\kappa^2 - x^2} d\kappa = -\frac{1}{2x} \ln \frac{x+1}{x-1} = -\frac{1}{x} \operatorname{arctanh} \left(\frac{1}{x} \right) \quad (\text{for } x^2 \notin]0, 1[). \quad (\text{B10})$$

(Note that our $\kappa_{1,2}^2$ ensure $x^2 \notin]0, 1[$ inside the κ integration range (except at $\xi = 0$.) From the recursion relation one then finds (for $x^2 \notin]0, 1[$)

$$\int_0^1 \frac{\kappa^2}{\kappa^2 - x^2} d\kappa = 1 - x \operatorname{arctanh} \left(\frac{1}{x} \right), \quad (\text{B11})$$

$$\int_0^1 \frac{\kappa^4}{\kappa^2 - x^2} d\kappa = \frac{1}{3} + x^2 - x^3 \operatorname{arctanh} \left(\frac{1}{x} \right), \quad (\text{B12})$$

$$\int_0^1 \frac{\kappa^6}{\kappa^2 - x^2} d\kappa = \frac{1}{5} + \frac{1}{3}x^2 + x^4 - x^5 \operatorname{arctanh} \left(\frac{1}{x} \right), \dots \quad (\text{B13})$$

and so on. Combining the above results one obtains the following expressions for the first four \tilde{i}_n which are needed in the main text:

$$\tilde{i}_1(\xi, c_1) = \frac{\kappa_1 \operatorname{arctanh} \left(\frac{1}{\kappa_1} \right) - \kappa_2 \operatorname{arctanh} \left(\frac{1}{\kappa_2} \right)}{\sqrt{1 + 4c_1\xi^2}}, \quad (\text{B14})$$

$$\tilde{i}_2(\xi, c_1) = \frac{\kappa_2^2 \left[1 - \kappa_2 \operatorname{arctanh} \left(\frac{1}{\kappa_2} \right) \right] - \kappa_1^2 \left[1 - \kappa_1 \operatorname{arctanh} \left(\frac{1}{\kappa_1} \right) \right]}{\sqrt{1 + 4c_1\xi^2}}, \quad (\text{B15})$$

$$\tilde{i}_3(\xi, c_1) = \frac{\kappa_2^2 \left[\frac{1}{3} + \kappa_2^2 - \kappa_2^3 \operatorname{arctanh} \left(\frac{1}{\kappa_2} \right) \right] - \kappa_1^2 \left[\frac{1}{3} + \kappa_1^2 - \kappa_1^3 \operatorname{arctanh} \left(\frac{1}{\kappa_1} \right) \right]}{\sqrt{1 + 4c_1\xi^2}} \quad (\text{B16})$$

$$\tilde{i}_4(\xi, c_1) = \frac{\kappa_2^2 \left[\frac{1}{5} + \frac{\kappa_2^2}{3} + \kappa_2^4 - \kappa_2^5 \operatorname{arctanh} \left(\frac{1}{\kappa_2} \right) \right] - \kappa_1^2 \left[\frac{1}{5} + \frac{\kappa_1^2}{3} + \kappa_1^4 - \kappa_1^5 \operatorname{arctanh} \left(\frac{1}{\kappa_1} \right) \right]}{\sqrt{1 + 4c_1\xi^2}}. \quad (\text{B17})$$

(Note that all ξ and c_1 dependence of these expressions originates from the pole positions $\kappa_{1,2}(\xi, c_1)$, cf. Eq. (B6).)

Analytical solutions for the integrals $\tilde{j}_n(\xi, c_1)$ can either be derived from those for the $\tilde{i}_n(\xi, c_1)$ obtained above, by using the identity

$$\tilde{j}_n(\xi, c_1) = -\frac{1}{2\xi} \frac{\partial}{\partial \xi} \tilde{i}_n(\xi, c_1), \quad (\text{B18})$$

or again by direct integration of the pole decomposition. Following the latter path, we have from the square of relation (B5)

$$\tilde{j}_n(\xi, c_1) = \frac{1}{1 + 4c_1\xi^2} \int_0^1 \left(\frac{\kappa^{2n}}{(\kappa^2 - \kappa_1^2)^2} - \frac{2\kappa^{2n}}{(\kappa^2 - \kappa_1^2)(\kappa^2 - \kappa_2^2)} + \frac{\kappa^{2n}}{(\kappa^2 - \kappa_2^2)^2} \right) d\kappa \quad (\text{B19})$$

which can be evaluated further with

$$\int_0^1 \frac{\kappa^2}{(\kappa^2 - x^2)^2} d\kappa = \frac{1}{2} \frac{1}{x^2 - 1} - \frac{1}{2x} \operatorname{arctanh} \frac{1}{x}, \quad (\text{B20})$$

$$\int_0^1 \frac{\kappa^2}{(\kappa^2 - x_1^2)(\kappa^2 - x_2^2)} d\kappa = \frac{x_2 \operatorname{arctanh} \frac{1}{x_2} - x_1 \operatorname{arctanh} \frac{1}{x_1}}{x_1^2 - x_2^2} \quad (\text{B21})$$

and

$$\int_0^1 \frac{\kappa^4}{(\kappa^2 - x^2)^2} d\kappa = \frac{1}{2} \frac{3x^2 - 2}{x^2 - 1} - \frac{3}{2}x \operatorname{arctanh} \frac{1}{x}, \quad (\text{B22})$$

$$\int_0^1 \frac{\kappa^4}{(\kappa^2 - x_1^2)(\kappa^2 - x_2^2)} d\kappa = 1 - \frac{x_1^3 \operatorname{arctanh} \frac{1}{x_1} - x_2^3 \operatorname{arctanh} \frac{1}{x_2}}{x_1^2 - x_2^2} \quad (\text{B23})$$

as well as

$$\int_0^1 \frac{\kappa^6}{(\kappa^2 - x^2)^2} d\kappa = \frac{2 + 10x^2 - 15x^4}{6(1 - x^2)} - \frac{5}{2}x^3 \operatorname{arctanh} \frac{1}{x}, \quad (\text{B24})$$

$$\int_0^1 \frac{\kappa^6}{(\kappa^2 - x_1^2)(\kappa^2 - x_2^2)} d\kappa = \frac{1}{3} + (x_1^2 + x_2^2) - \frac{x_1^5 \operatorname{arctanh} \frac{1}{x_1} - x_2^5 \operatorname{arctanh} \frac{1}{x_2}}{x_1^2 - x_2^2} \quad (\text{B25})$$

(all for $x^2 \notin]0, 1[$), and so on.

This yield, in particular, the expressions

$$\begin{aligned} \tilde{j}_1(\xi, c_1) = & \frac{1}{1+4c_1\xi^2} \left[\frac{1}{2} \frac{1}{\kappa_1^2-1} + \frac{1}{2} \frac{1}{\kappa_2^2-1} + \left(\frac{2\kappa_1}{\kappa_1^2-\kappa_2^2} - \frac{1}{2\kappa_1} \right) \operatorname{arctanh} \frac{1}{\kappa_1} \right. \\ & \left. - \left(\frac{2\kappa_2}{\kappa_1^2-\kappa_2^2} + \frac{1}{2\kappa_2} \right) \operatorname{arctanh} \frac{1}{\kappa_2} \right] \end{aligned} \quad (\text{B26})$$

and

$$\begin{aligned} \tilde{j}_2(\xi, c_1) = & \frac{1}{1+4c_1\xi^2} \left[\frac{1}{2} \frac{3\kappa_1^2-2}{\kappa_1^2-1} + \frac{1}{2} \frac{3\kappa_2^2-2}{\kappa_2^2-1} - 2 \right. \\ & \left. - \left(\frac{3}{2}\kappa_1 - \frac{2\kappa_1^3}{\kappa_1^2-\kappa_2^2} \right) \operatorname{arctanh} \frac{1}{\kappa_1} - \left(\frac{3}{2}\kappa_2 + \frac{2\kappa_2^3}{\kappa_1^2-\kappa_2^2} \right) \operatorname{arctanh} \frac{1}{\kappa_2} \right] \end{aligned} \quad (\text{B27})$$

and

$$\begin{aligned} \tilde{j}_3(\xi, c_1) = & \frac{1}{1+4c_1\xi^2} \left[\frac{1}{6} \frac{15\kappa_1^4-10\kappa_1^2-2}{\kappa_1^2-1} + \frac{1}{6} \frac{15\kappa_2^4-10\kappa_2^2-2}{\kappa_2^2-1} - \frac{2}{3} \frac{\kappa_1^2+3\kappa_1^4-\kappa_2^2-3\kappa_2^4}{\kappa_1^2-\kappa_2^2} \right. \\ & \left. - \left(\frac{5}{2}\kappa_1^3 - \frac{2\kappa_1^5}{\kappa_1^2-\kappa_2^2} \right) \operatorname{arctanh} \frac{1}{\kappa_1} - \left(\frac{5}{2}\kappa_2^3 + \frac{2\kappa_2^5}{\kappa_1^2-\kappa_2^2} \right) \operatorname{arctanh} \frac{1}{\kappa_2} \right] \end{aligned} \quad (\text{B28})$$

and

$$\begin{aligned} \tilde{j}_4(\xi, c_1) = & \frac{1}{1+4c_1\xi^2} \left[\frac{1}{30} \frac{6+14\kappa_1^2+70\kappa_1^4-105\kappa_1^6}{1-\kappa_1^2} + \frac{1}{30} \frac{6+14\kappa_2^2+70\kappa_2^4-105\kappa_2^6}{1-\kappa_2^2} \right. \\ & - \frac{2}{15} \frac{3\kappa_1^2+5\kappa_1^4+15\kappa_1^6-3\kappa_2^2-5\kappa_2^4-15\kappa_2^6}{\kappa_1^2-\kappa_2^2} \\ & \left. - \left(\frac{7}{2}\kappa_1^5 - \frac{2\kappa_1^7}{\kappa_1^2-\kappa_2^2} \right) \operatorname{arctanh} \frac{1}{\kappa_1} - \left(\frac{7}{2}\kappa_2^5 + \frac{2\kappa_2^7}{\kappa_1^2-\kappa_2^2} \right) \operatorname{arctanh} \frac{1}{\kappa_2} \right] \end{aligned} \quad (\text{B29})$$

and finally

$$\begin{aligned} \tilde{j}_5(\xi, c_1) = & \frac{1}{1+4c_1\xi^2} \left[\frac{1}{70} \frac{10+18\kappa_1^2+42\kappa_1^4+210\kappa_1^6-315\kappa_1^8}{1-\kappa_1^2} + \frac{1}{70} \frac{10+18\kappa_2^2+42\kappa_2^4+210\kappa_2^6-315\kappa_2^8}{1-\kappa_2^2} \right. \\ & - \frac{2}{105} \frac{15\kappa_1^2+21\kappa_1^4+35\kappa_1^6+105\kappa_1^8-15\kappa_2^2-21\kappa_2^4-35\kappa_2^6-105\kappa_2^8}{\kappa_1^2-\kappa_2^2} \\ & \left. - \left(\frac{9}{2}\kappa_1^7 - \frac{2\kappa_1^9}{\kappa_1^2-\kappa_2^2} \right) \operatorname{arctanh} \frac{1}{\kappa_1} - \left(\frac{9}{2}\kappa_2^7 + \frac{2\kappa_2^9}{\kappa_1^2-\kappa_2^2} \right) \operatorname{arctanh} \frac{1}{\kappa_2} \right] \end{aligned} \quad (\text{B30})$$

(the $\kappa_{1,2}(\xi, c_1)$ are defined in Eq. (B6)) which are needed to evaluate the matrix elements derived in the main text.

2. Limits

When analyzing the soft-mode contributions to gap equation and energy density, it is useful to evaluate the $\xi \rightarrow 0$ and $c_1 \rightarrow 0$ limits. This boils down to finding the limits of the $\tilde{\gamma}_n$ and \tilde{j}_n integrals which we provide in the present section. The $\xi \rightarrow 0$ limits are (for $c_1 \leq 1$, as before)

$$\tilde{\gamma}_n(\xi=0, c_1) = \int_0^1 \frac{\kappa^{2n-2}}{1-c_1\kappa^2} d\kappa = \frac{1}{2n-1} {}_2F_1\left(1, n-\frac{1}{2}, n+\frac{1}{2}, c_1\right) \quad (\text{B31})$$

$$\xrightarrow{c_1 \rightarrow 0} \frac{1}{2n-1} \quad (\text{B32})$$

for $n > 1/2$ and

$$\tilde{j}_n(\xi=0, c_1) = \int_0^1 \frac{\kappa^{2n-4}}{(1-c_1\kappa^2)^2} d\kappa = \frac{1}{2n-3} {}_2F_1\left(2, n-\frac{3}{2}, n-\frac{1}{2}, c_1\right) \quad (\text{B33})$$

$$\xrightarrow{c_1 \rightarrow 0} \frac{1}{2n-3} \quad (\text{B34})$$

for $n > 3/2$. (The hypergeometric functions ${}_2F_1(a, b, c, z)$ are defined e.g. in Ref. [58].) Note that only \tilde{j}_1 , which does not appear in the coincidence limit of the soft-mode correlation functions, contains a $\xi \rightarrow 0$ divergence (cf. Eq. (B38)). The $\xi \rightarrow 0$ limit of the \tilde{i}_n integrals can be reexpressed via continued partial integration as

$$\tilde{i}_n(\xi = 0, c_1) = -\frac{1}{c_1^{n-1}} \left(\sum_{k=0}^{n-2} \frac{c_1^k}{2k+1} - \frac{\operatorname{arctanh} \sqrt{c_1}}{\sqrt{c_1}} \right) \quad (\text{B35})$$

which yields

$$\tilde{i}_1(\xi = 0, c_1) = \frac{\operatorname{arctanh} \sqrt{c_1}}{\sqrt{c_1}} \xrightarrow{c \rightarrow 0} 1, \quad (\text{B36})$$

$$\tilde{i}_2(\xi = 0, c_1) = -\frac{1}{c_1} \left(1 - \frac{\operatorname{arctanh} \sqrt{c_1}}{\sqrt{c_1}} \right), \quad (\text{B37})$$

etc.. Furthermore,

$$\tilde{j}_1(\xi, c_1) \xrightarrow{\xi \rightarrow 0} \frac{\pi}{4} \frac{1}{\xi} - \frac{1}{2} \left(\frac{2-3c_1}{1-c_1} - 3\sqrt{c_1} \operatorname{arctanh} \sqrt{c_1} \right) - \frac{15\pi}{8} c_1 \xi + O(\xi^2) \quad (\text{B38})$$

as well as

$$\tilde{j}_2(\xi = 0, c_1) = \frac{1}{2} \left(\frac{1}{1-c_1} + \frac{\operatorname{arctanh} \sqrt{c_1}}{\sqrt{c_1}} \right), \quad (\text{B39})$$

$$\tilde{j}_3(\xi = 0, c_1) = \frac{1}{2c_1} \left(\frac{1}{1-c_1} - \frac{\operatorname{arctanh} \sqrt{c_1}}{\sqrt{c_1}} \right), \quad (\text{B40})$$

$$\tilde{j}_4(\xi = 0, c_1) = \frac{1}{2c_1^2} \left(\frac{3-2c_1}{1-c_1} - 3 \frac{\operatorname{arctanh} \sqrt{c_1}}{\sqrt{c_1}} \right), \quad (\text{B41})$$

$$\tilde{j}_5(\xi = 0, c_1) = \frac{1}{6c_1^3} \left(\frac{15-10c_1-2c_1^2}{1-c_1} - 15 \frac{\operatorname{arctanh} \sqrt{c_1}}{\sqrt{c_1}} \right). \quad (\text{B42})$$

This implies, in particular,

$$e(\xi, c_1) := \tilde{i}_2 - 2c_1 \tilde{i}_3 + c_1^2 \tilde{i}_4 + 2c_1 \frac{\gamma}{\zeta} \tilde{i}_2 (\tilde{j}_3 - 2c_1 \tilde{j}_4 + c_1^2 \tilde{j}_5) \quad (\text{B43})$$

$$\stackrel{\xi \rightarrow 0}{=} \frac{1}{3} - \frac{c_1}{5} - \frac{2\gamma}{3\zeta} \left(1 - \frac{\operatorname{arctanh} \sqrt{c_1}}{\sqrt{c_1}} \right) \quad (\text{B44})$$

for the combination of integrals which appears in the electric soft-mode contribution (149) to the vacuum energy density (159).

Furthermore, we have the $c_1 \rightarrow 0$ limits

$$\tilde{i}_n(\xi) := \tilde{i}_n(\xi, c_1 = 0) = \int_0^1 \frac{\kappa^{2n}}{\kappa^2 + \xi^2} d\kappa, \quad n \geq 1, \quad (\text{B45})$$

$$\tilde{j}_n(\xi) := \tilde{j}_n(\xi, c_1 = 0) = \int_0^1 \frac{\kappa^{2n}}{(\kappa^2 + \xi^2)^2} d\kappa, \quad n \geq 1 \quad (\text{B46})$$

which we distinguish from the general integrals (B1), (B2) only by their arguments. Both $\tilde{i}_n(\xi)$ and $\tilde{j}_n(\xi)$ decay monotonically in $\xi \in [0, \infty]$, starting from the finite values

$$\tilde{i}_n(0) = \frac{1}{2n-1}, \quad n \geq 1, \quad (\text{B47})$$

$$\tilde{j}_n(0) = \frac{1}{2n-3}, \quad n \geq 2, \quad (\text{B48})$$

except for the special case

$$\tilde{j}_1(\xi) \xrightarrow{\xi \rightarrow 0} \frac{\pi}{4} \frac{1}{\xi} - 1 + \frac{2}{3} \xi^2 - \frac{3}{5} \xi^4 + O(\xi^6) \quad (\text{B49})$$

which exhibits, as already mentioned, a pole divergence at $\xi \rightarrow 0$. The $\tilde{i}_n(\xi)$, $\tilde{j}_n(\xi)$ further satisfy the recursion relations

$$\tilde{i}'_n(\xi) \equiv \frac{d\tilde{i}_n(\xi)}{d\xi} = -2\xi\tilde{j}_n(\xi) \leq 0, \quad (\text{B50})$$

$$\tilde{j}'_n(\xi) \equiv \frac{d\tilde{j}_n(\xi)}{d\xi} = -4\xi\tilde{k}_n(\xi) \leq 0, \quad (\text{B51})$$

and

$$\tilde{i}_n(\xi) = \frac{1}{2n-1} - \xi^2\tilde{i}_{n-1}(\xi), \quad (\text{B52})$$

$$\tilde{j}_n(\xi) = \frac{1}{2n-3} \left[\frac{1}{1+\xi^2} - (2n-1)\xi^2\tilde{j}_{n-1} \right] \quad (n > 1) \quad (\text{B53})$$

which may be summed up into a finite power series and a transcendental piece,

$$\tilde{i}_n(\xi) = \sum_{k=0}^{n-2} \frac{(-1)^k \xi^{2k}}{2n-2k-1} + (-1)^{n+1} (1 - \xi \arctan \xi^{-1}) \xi^{2n-2}. \quad (\text{B54})$$

Explicit expressions for the first few $\tilde{i}_n(\xi)$ and $\tilde{j}_n(\xi)$, which are needed in the main text, are thus

$$\tilde{i}_1(\xi) = 1 - \xi \arctan \frac{1}{\xi}, \quad (\text{B55})$$

$$\tilde{i}_2(\xi) = \frac{1}{3} - \xi^2 + \xi^3 \arctan \frac{1}{\xi}, \quad (\text{B56})$$

$$\tilde{i}_3(\xi) = \frac{1}{5} - \frac{1}{3}\xi^2 + \xi^4 - \xi^5 \arctan \frac{1}{\xi}, \quad (\text{B57})$$

$$\tilde{i}_4(\xi) = \frac{1}{7} - \frac{1}{5}\xi^2 + \frac{1}{3}\xi^4 - \xi^6 + \xi^7 \arctan \frac{1}{\xi} \quad (\text{B58})$$

as well as

$$\tilde{j}_1(\xi) = \frac{1}{2} \left(-\frac{1}{1+\xi^2} + \frac{1}{\xi} \arctan \frac{1}{\xi} \right), \quad (\text{B59})$$

$$\tilde{j}_2(\xi) = \frac{1}{2} \left(3 - \frac{1}{1+\xi^2} - 3\xi \arctan \frac{1}{\xi} \right), \quad (\text{B60})$$

$$\tilde{j}_3(\xi) = \frac{1}{2} \left(\frac{5}{3} - 5\xi^2 - \frac{1}{1+\xi^2} + 5\xi^3 \arctan \frac{1}{\xi} \right), \quad (\text{B61})$$

$$\tilde{j}_4(\xi) = \frac{1}{2} \left(\frac{7}{5} - \frac{7}{3}\xi^2 + 7\xi^4 - \frac{1}{1+\xi^2} - 7\xi^5 \arctan \frac{1}{\xi} \right), \quad (\text{B62})$$

$$\tilde{j}_5(\xi) = \frac{1}{2} \left(\frac{9}{7} - \frac{3}{5} (3 - 5\xi^2 + 15\xi^4) \xi^2 - \frac{1}{1+\xi^2} + 9\xi^7 \arctan \frac{1}{\xi} \right). \quad (\text{B63})$$

Finally, we note that the $\tilde{i}_n(\xi)$, $\tilde{j}_n(\xi)$ (and their analogs with increasing powers of the integrand's denominator) determine the coefficients of the expansion of the integrals $\tilde{i}_n(\xi; c_1)$ and $\tilde{j}_n(\xi; c_1)$ in powers of c_1 . Indeed, from

$$\frac{1}{\kappa^2(1-c_1\kappa^2) + \xi^2} = \frac{1}{\kappa^2 + \xi^2} + \frac{\kappa^4}{(\kappa^2 + \xi^2)^2} c_1 + \frac{\kappa^8}{(\kappa^2 + \xi^2)^3} c_1^2 + O(c_1^3), \quad (\text{B64})$$

$$\frac{1}{(\kappa^2(1-c_1\kappa^2) + \xi^2)^2} = \frac{1}{(\kappa^2 + \xi^2)^2} + \frac{2\kappa^4}{(\kappa^2 + \xi^2)^3} c_1 + \frac{3\kappa^8}{(\kappa^2 + \xi^2)^4} c_1^2 + O(c_1^3) \quad (\text{B65})$$

one has (with $\tilde{k}_n(\xi) := \int_0^1 \kappa^{2n} / (\kappa^2 + \xi^2)^3 d\kappa$)

$$\tilde{i}_n(\xi; c_1) = \tilde{i}_n(\xi) + \tilde{j}_{n+2}(\xi) c_1 + \tilde{k}_{n+4}(\xi) c_1^2 + O(c_1^3), \quad (\text{B66})$$

$$\tilde{j}_n(\xi; c_1) = \tilde{j}_n(\xi) + 2\tilde{k}_{n+2}(\xi) c_1 + O(c_1^2). \quad (\text{B67})$$

- [1] E. Schrödinger, *Ann. d. Phys.* **79**, 361 (1926); *ibid.* **79**, 489 (1926); *ibid.* **80**, 437 (1926); *ibid.* **81**, 8 (1926).
- [2] See e.g. Proceedings of the Intl. Workshop *Variational Calculations in Quantum Field Theory*, Wangerooge, Germany, Eds. L. Polley and D.E.L. Pottinger, World Scientific, Singapore (1988). See also J.O. Akeyo, H.F. Jones and C.S. Parker, *Phys. Rev. D* **51**, 1298 (1995) for a corresponding lattice ansatz of the trial action.
- [3] J. Greensite, *Nucl. Phys.* **B 158**, 469 (1979).
- [4] J. Cornwall, *Phys. Rev. D* **38**, 656 (1988).
- [5] A.K. Kerman and D. Vautherin, *Ann. Phys. (N.Y.)* **192**, 408 (1989).
- [6] R. Jackiw, *Analysis on Infinite-Dimensional Manifolds – Schroedinger Representation for Quantized Fields*, in *Field theory and particle physics*, Proceedings of the 5th Jorge Andre Swieca Summer School, Campos do Jordao, Brazil, Eds. O.J.P. Eboli, M. Gomes, A. Santoro, World Scientific, Singapore 1990, p. 731.
- [7] O. Eboli, R. Jackiw and S.-Y. Pi, *Phys. Rev. D* **37**, 3557 (1988).
- [8] R. Fariello and H. Forkel, *Phys. Rev. D* **80**, 025021 (2009).
- [9] See, for example, A. Kerman and R. Jackiw, *Phys. Lett. A* **71**, 158 (1979); Y. Tsue and Y. Fujiwara, *Prog. Theor. Phys.* **86**, 443 (1991); *ibid.* **86**, 469 (1991).
- [10] R.P. Feynman, in the Proceedings of the workshop *Variational Calculations in Quantum Field Theory*, Wangerooge, Germany, 1987, edited by L. Polley and D. Pottinger (World Scientific, Singapore, 1988).
- [11] R.P. Feynman, *Nucl. Phys.* **B 188**, 479 (1981).
- [12] K. Symanzik, *Nucl. Phys.* **B 190**, 1 (1981).
- [13] M. Lüscher, *Nucl. Phys.* **B 254**, 52 (1985).
- [14] A.P. Szczepaniak, *Phys. Rev. D* **69**, 074031 (2004).
- [15] C. Feuchter and H. Reinhardt, *Phys. Rev. D* **70**, 105021 (2004).
- [16] N. H. Christ and T. D. Lee, *Phys. Rev. D* **22**, 939 (1980) [*Phys. Scripta* 23, 970 (1981)].
- [17] I.I. Kogan and A. Kovner, *Phys. Rev. D* **52**, 3719 (1995).
- [18] D.I. Diakonov, lectures given at the 4th St. Petersburg Winter School in Theoretical Physics (1998), arXiv:hep-th/9805137.
- [19] A. Jaffe and E. Witten, [http://www.claymath.org/Millennium Prize Problems/Yang-Mills Theory/objects/Official Problem Description](http://www.claymath.org/Millennium_Prize_Problems/Yang-Mills_Theory/objects/Official_Problem_Description).
- [20] K. Zarembo, *Phys. Lett. B* **421**, 325 (1998).
- [21] H. Forkel, *Phys. Rev. D* **73**, 105002 (2006).
- [22] W.E. Brown, J.P. Garrahan, I.I. Kogan and A. Kovner, *Phys. Rev. D* **59**, 34015 (1999).
- [23] H. Forkel, *Int. J. Mod. Phys. E* **16**, 2789 (2007).
- [24] G.C. Rossi and M. Testa, *Nucl. Phys.* **B 163**, 109 (1980); *ibid.* **176**, 477 (1980); *ibid.* **237**, 442 (1984).
- [25] A.M. Polyakov, *Phys. Lett. B* **72**, 477 (1978); L. Susskind, *Phys. Rev. D* **20**, 2610 (1979); B. Svetitsky, *Phys. Rep.* 132, 1 (1986), M. Lüscher, R. Narayanan, P. Weisz and U. Wolff, *Nucl. Phys.* **B 384**, 168 (1992).
- [26] C. Heinemann, E. Iancu, C. Martin and D. Vautherin, *Phys. Rev. D* **61**, 116008 (2000).
- [27] H. Leutwyler, *Phys. Lett. B* **179**, 129 (1981).
- [28] I.I. Kogan and A. Kovner, *Phys. Rev. D* **51**, 1948 (1995); D. Nolland, arXiv:hep-th/0408075.
- [29] M. Consoli and G. Preparata, *Phys. Lett. B* **154**, 411 (1985).
- [30] T.H. Hansson, K. Johnson, and C. Peterson, *Phys. Rev. D* **26**, 2069 (1982).
- [31] W.E. Brown, *Int. J. Mod. Phys. A* **13**, 5219 (1998).
- [32] A. Cucchieri and T. Mendes, PoS(Confinement8)040 (2008); I.L. Bogolubsky, E.-M. Ilgenfritz, M. Müller-Preussker and A. Sternbeck, *Phys. Lett. B* **676**, 69 (2009); O. Oliveira and P.J. Silva, arXiv:0911.1643; see also A.C. Aguilar, A.A. Natale and P.S. Rodrigues da Silva, *Phys. Rev. Lett.* **90**, 152001 (2003); D. Dudal, J.A. Gracey, S.P. Sorella, N. Vandersickel and H. Verschelde, *Phys. Rev. D* **78**, 065047 (2008); A.C. Aguilar, D. Binosi and J. Papavassiliou, *Phys. Rev. D* **78**, 025010 (2008).
- [33] T. Iritani, H. Suganuma and H. Iida, arXiv:0908.1311v2; P. J. Silva, O. Oliveira, *Nucl. Phys.* **B 690**, 177 (2004).
- [34] W.E. Brown and I.I. Kogan, *Int. J. Mod. Phys. A* **14**, 799 (1999).
- [35] T. Schaefer and E.V. Shuryak, *Rev. Mod. Phys.* **70**, 323 (1998); D.I. Diakonov, *Prog. Part. Nucl. Phys.* **51**, 173 (2003). For an elementary introduction to instantons see H. Forkel, *A Primer on Instantons in QCD*, hep-ph/0009136.
- [36] M.F. Atiyah and N.S. Manton, *Phys. Lett. B* **222**, 438 (1989).
- [37] V. de Alfaro, S. Fubini and G. Furlan, *Phys. Lett. B* **65**, 163 (1976); *Phys. Lett. B* **72**, 203 (1977); C.G. Callan, R.G. Dashen and D.J. Gross, *Phys. Lett.* **66B**, 375 (1977); *Phys. Rev. D* **17**, 2717 (1978); **19**, 1826 (1979); F. Lenz, J.W. Negele and M. Thies, *Phys. Rev. D* **69**, 074009 (2004); hep-lat/0409083.
- [38] G. 't Hooft, in *High Energy Physics*, edited by A. Zichichi, Editrice Compositori, Bologna, (1976); S. Mandelstam, *Phys. Reports* **23C**, 245 (1976); G. 't Hooft, *Nucl. Phys.* **B190**, 455 (1981); A. Kronfeld, G. Schierholz and U. J. Wiese, *Nucl. Phys.* **B293**, 461 (1987); G. Ripka, *Lecture Notes in Physics* 639, Springer, Berlin (2004).
- [39] L.D. Faddeev, *Quantization of Solitons*, Institute for Advanced Study preprint IAS-75-QS70; in *Einstein and Several Contemporary Tendencies in the Field Theory of Elementary Particles, Relativity, Quanta and Cosmology*, Vol. 1 (Eds. M. Pantaleo and F. De Finis), 185 (Johnson Reprint, 1979).
- [40] L.D. Faddeev and A.J. Niemi, *Nature* **387**, 58 (1997); *Phys. Rev. Lett.* **82**, 1624 (1999).
- [41] F.R. Brown et al., *Phys. Rev. Lett.* **65**, 2491 (1990); *Phys. Lett. B* **251**, 181 (1990).
- [42] J.B. Kogut, M. Snow and M. Stone, *Nucl. Phys.* **B 200** (1982) 211.
- [43] R. Pisarski and F. Wilczek, *Phys. Rev. D* **29**, 338 (1984).
- [44] A.M. Polyakov, *Gauge fields and strings*, Harwood Academic, Chur, Switzerland (1987).
- [45] H. Forkel, *Phys. Rev. D* **71**, 054008 (2005); Proceedings of “Continuous advances in QCD,” Minneapolis, 2006, p. 283

[arXiv:hep-ph/0608071].

- [46] G. K. Savvidy, Phys. Lett. **B 71**, 133 (1977).
- [47] S. Narison, Nucl. Phys. **B 509**, 312 (1998).
- [48] H. Reinhardt and D. Epple, Phys. Rev. D **76**, 065015 (2007); M. Pak and H. Reinhardt, arXiv:0910.2916; D. Campagnari, A. Weber, H. Reinhardt, F. Astorga and W. Schleifenbaum, arXiv:0910.4548.
- [49] T. Schaefer and E.V. Shuryak, Phys. Rev. Lett. **75**, 1707 (1995).
- [50] H. Forkel, Phys. Rev. D **78**, 025001 (2008); *Glueball correlators as holograms*, arXiv:0808.0304 [hep-ph]; PoS (CONFINEMENT8) 184 (2008).
- [51] B.M. Gripaos, Int. J. Mod. Phys. A **18**, 85 (2003).
- [52] W.E. Brown, J.P. Garrahan, I.I. Kogan, and A. Kovner, Phys. Rev. D **62**, 016004 (2000).
- [53] R. Gupta et al., Phys. Rev. D **43**, 2301 (1991); P. de Forcrand and K.-F. Liu, Phys. Rev. Lett. **69**, 245 (1992); C. Morningstar and M. Peardon, Phys. Rev. D **60**, 034509 (1999); W. Lee and D. Weingarten, Phys. Rev. D **61**, 014015 (2000); SESAM and TxL Collaborations, G. Bali et al., Phys. Rev. D **62**, 054503 (2000); A. Hart and M. Teper, Phys. Rev. D **65**, 034502 (2002); N. Ishii, H. Suganuma and H. Matsufuru, Phys. Rev. D **66**, 94506 (2002); B. Lucini, M.J. Teper and U. Wenger, JHEP **06**, 012 (2004); H.B. Meyer and M.J. Teper, Phys. Lett. **B 605**, 344 (2005); M. Loan and Y. Ying, arXiv:hep-lat/0603030; Y. Chen et al., Phys. Rev. D **73**, 014516 (2006); H.B. Meyer, arXiv:0808.3151.
- [54] I. Kogan, A. Kovner and J.G. Milhano, JHEP **12**, 017 (2002).
- [55] B.M. Gripaos and J.G. Milhano, Phys. Lett. **B 564**, 104 (2003).
- [56] E. Shuryak, J. Phys. G **30**, S1221 (2004).
- [57] K.G. Wilson and J.B. Kogut, Phys. Rep. **12**, 75 (1974); for a textbook exposition see M. E. Peskin and D.V. Schroeder, *An Introduction to Quantum Field Theory*, Addison-Wesley, Reading, MA, USA (1995).
- [58] M. Abramowitz and I.A. Stegun, *Handbook of Mathematical Functions*, National Bureau of Standards Applied Mathematics Series 55, (U.S. GPO, Washington, DC, 1972).
- [59] Non-equilibrium processes of particular current interest in high-energy physics are those in the early universe and in the aftermath of ultrarelativistic nuclear collisions at the RHIC and the CERN LHC (for a brief discussion see e.g. Sec. V of Ref. [8]).
- [60] It may, for example, shed new light on the interplay between gauge symmetry and topological vacuum properties, which emerge transparently in the Schroedinger picture [6, 21], and on microscopic aspects of the confinement mechanism [10, 11].
- [61] On the other hand, perturbation theory becomes more complex in temporal gauge (or other axial gauges) [24].
- [62] The gauge transformations of Yang-Mills theory without matter span the coset $SU(N_c)/Z_{N_c}$ since center elements of $SU(N_c)$ act trivially on the gauge fields. Following Ref. [17], however, we will refrain from making the deviation of the gauge group from $SU(N_c)$ manifest, although it could be implemented in the action (34) and may become relevant, e.g., for the discussion of center vortices.
- [63] The dynamical mass gap and other nonperturbative features of 2+1 dimensional compact photodynamics are described exactly by a Gaussian vacuum wave functional as well [28].
- [64] As pointed out in Ref. [17], minimizing the mode energy by using the more general power ansatz $G_>(k) = \alpha k^\beta$ for the UV covariance results in $\alpha = 1, \beta = -1$, i.e. precisely the covariance (11) required by asymptotic freedom.
- [65] Adopting Eq. (11) for *all* momenta $0 \leq k \leq \Lambda_{UV}$, on the other hand, would turn the functional (1) into the exact ground state of $N_c^2 - 1$ copies of U(1) photodynamics (since averaging over the gauge group $[U(1)]^{N_c}$ removes the longitudinal gauge-field modes).
- [66] In the weakly-coupled phase (RG-improved) perturbation theory should work, while the mean-field approximation becomes increasingly reliable with growing coupling in the strongly coupled phase (at least as long as the mass gap is large enough to effectively suppress fluctuations). As is well known [44], however, the above saddle-point approximation does not become exact at large N_c . In principle, this could be corrected if a practicable analog of the quaternion representation for SU(2) could be found for $N_c \geq 3$ [18].
- [67] Alternatively, one could trade the $4U$ interactions for another composite field of the form $\chi_{ik} = (\partial_i \partial_k U_L^\dagger) U$ and treat its contributions at the mean-field level.
- [68] The first-order transition expected from the ϵ expansion and lattice simulations may not be reproduced due to limitations of the mean-field approximation [17].
- [69] Numerical studies [42] show that the phase transition in the nonlinear σ -model (42) (i.e. for $c_n = 0$) is strongly first order and occurs when $\langle U \rangle \gtrsim 0.5$, indicating that perturbation theory should remain qualitatively reliable down to the transition point.
- [70] The contributions of the Fourier modes to the VWF are of course also affected by the (c_1 dependent) normalization $Z^{-1/2} = \left(\int D\vec{A} \Psi[\vec{A}] \Psi[\vec{A}] \right)^{-1/2}$. This overall factor does not change the relative weight of the $A_i^a(k)$ for different k , however.

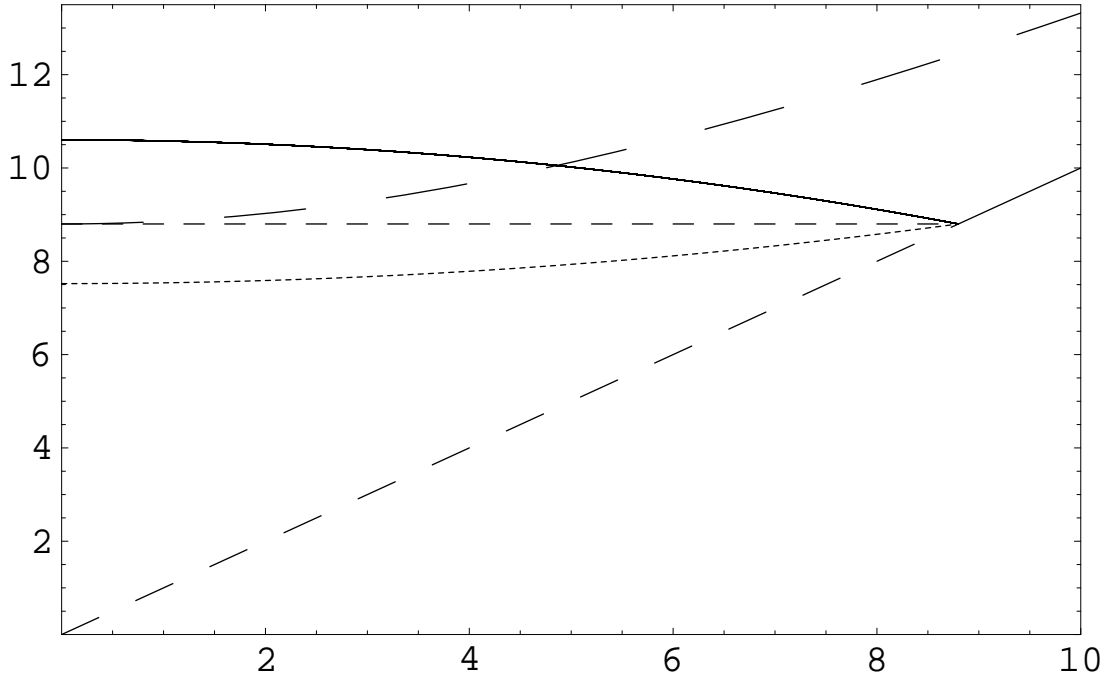


FIG. 1: The generalized IR covariance $G_{<}^{-1}(k) = \mu(1 - c_1 k^2 / \mu^2) / (1 - c_1)$ for $c_1 = 0.17$ (full line) and $c_1 = -0.17$ (dotted), together with the UV covariance $G_{>}^{-1}(k) = k$, and in comparison with $G_0^{-1}(k) = k$ (medium dashed), $G_{0,m_g=\mu}^{-1}(k) = \sqrt{k^2 + \mu^2}$ (long dashed) and $G_{\text{KK}}^{-1}(k) = \mu$ (short dashed) (all curves for $\mu = 8.8\Lambda_{\text{YM}}$).

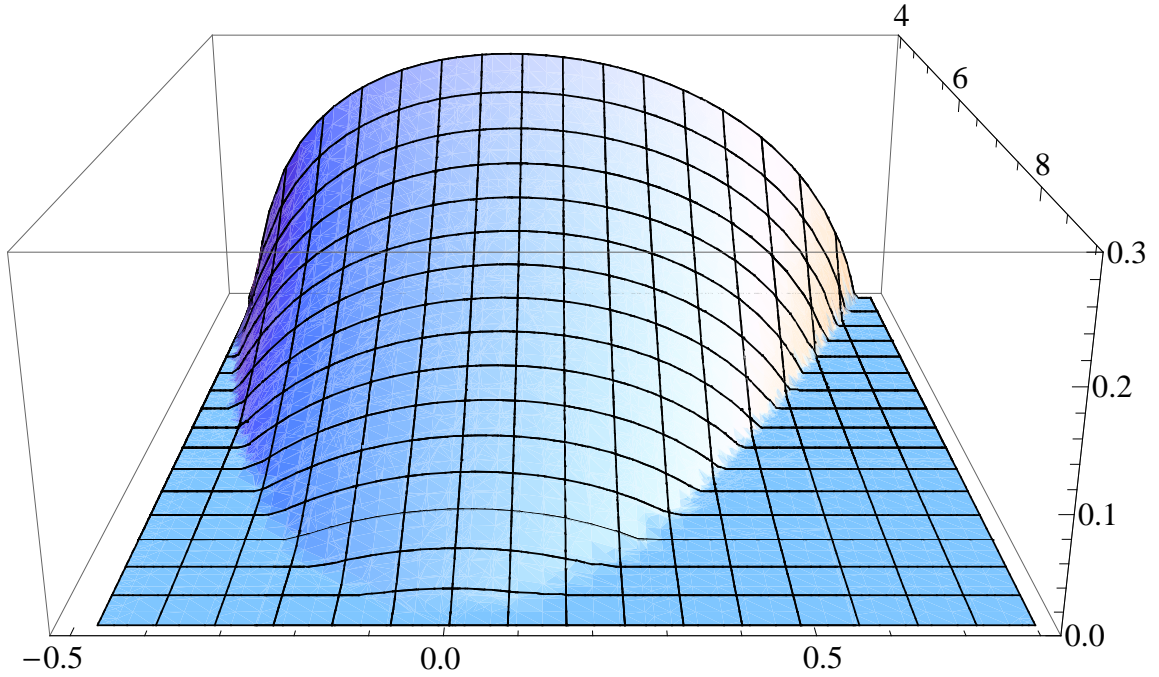


FIG. 2: The order-parameter solution $\bar{\xi}(\mu, c_1)$ of the gap equation in the variable ranges $\mu \in \{4, 9\} \Lambda_{\text{YM}}$ and $c_1 \in \{-0.5, 0.8\}$.

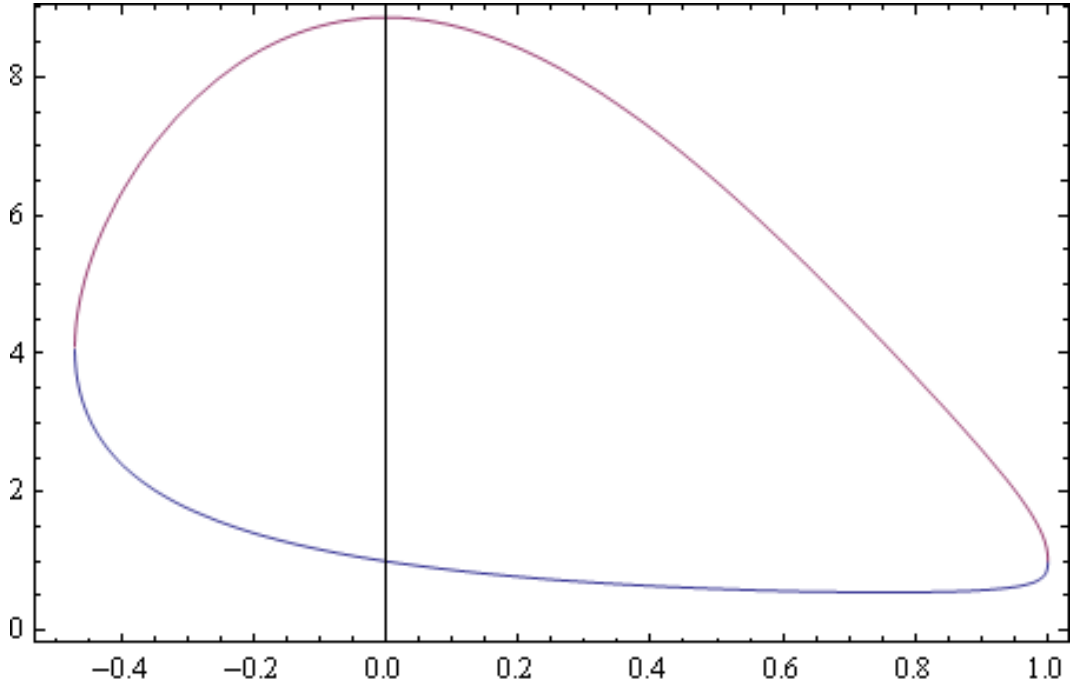


FIG. 3: Vacuum phase diagram: inside the plotted phase boundary $\mu_c(c_1)/\Lambda_{\text{YM}}$ the theory is in its strongly-coupled disordered phase. (Our treatment is approximately valid in the range $\mu \gtrsim 4\Lambda_{\text{YM}}$ and $c_1 \in \{-0.5, 0.5\}$).

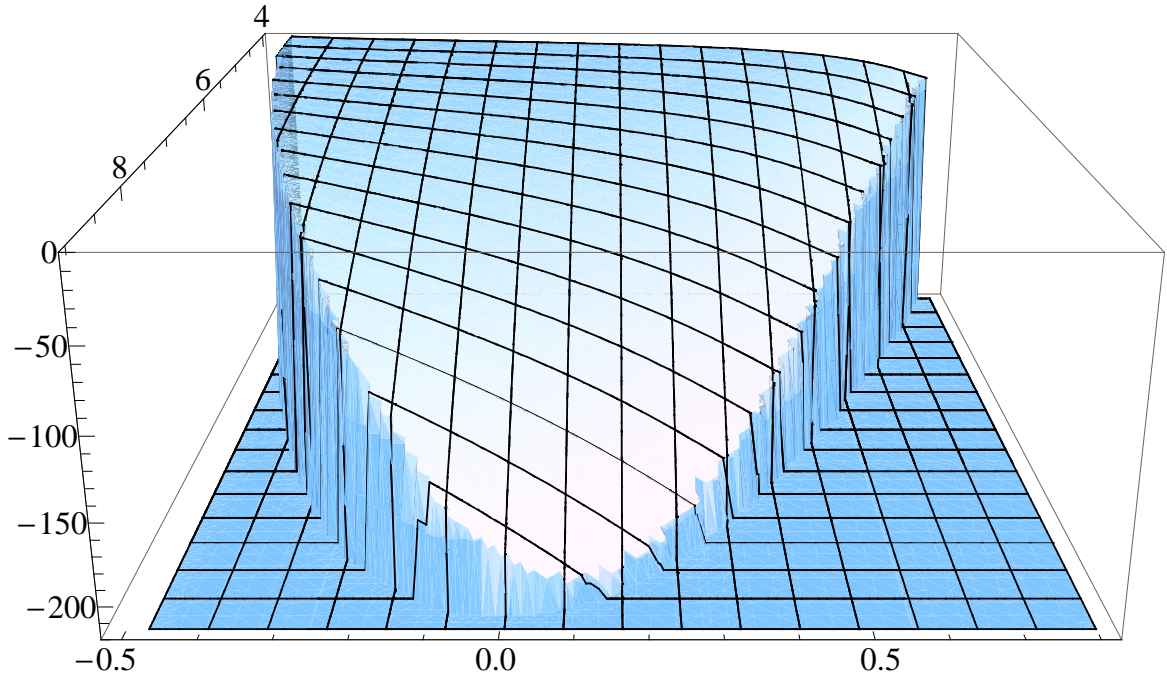


FIG. 4: The energy density $\bar{\varepsilon}(\mu, c_1)$ of the vacuum field solution $\bar{\xi}(\mu, c_1)$ in the parameter ranges $\mu \in \{4, 9\} \Lambda_{\text{YM}}$ and $c_1 \in \{-0.5, 0.8\}$. Note the minimum of the energy surface at $c_1 \simeq 0.15$.

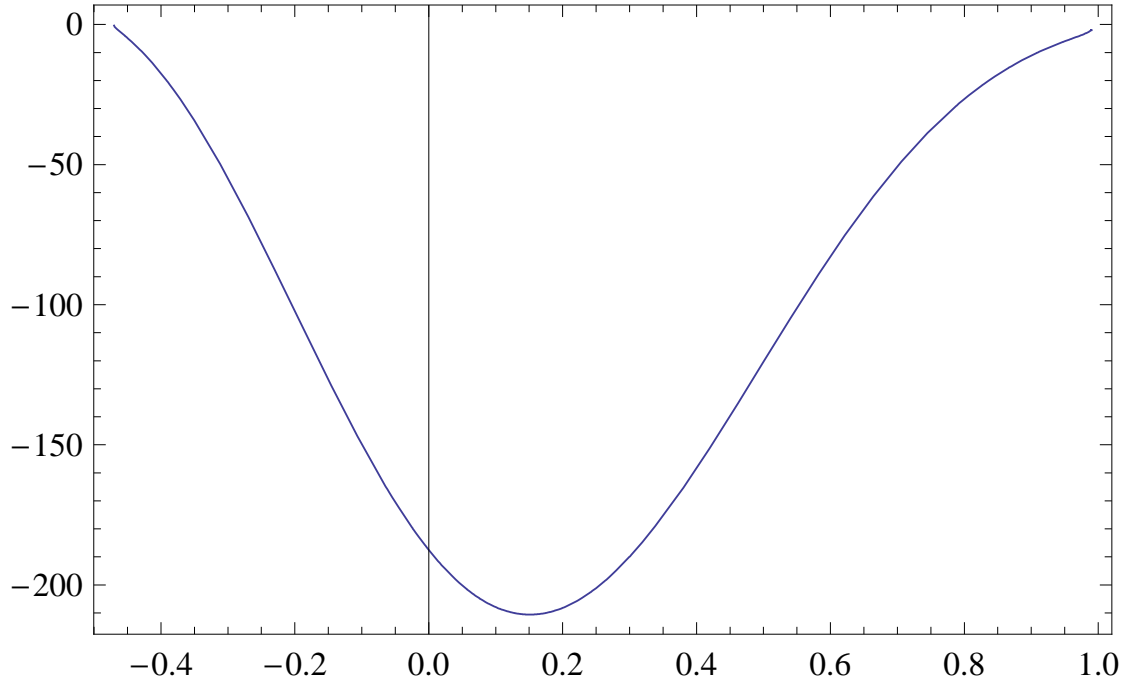


FIG. 5: The energy density $\bar{\varepsilon}(c_1) \equiv \bar{\varepsilon}(\mu_c(c_1), c_1)$ at the phase transition point μ_c in units of Λ_{YM} .